

MECHANISTIC STUDIES OF ENZYMATIC STEREO-SELECTIVITY IN AQUEOUS AND ORGANIC MEDIA

by

TAO KE

B.Sc., Chemistry
University of Science and Technology of China, 1993

Submitted to the Department of Chemistry
in Partial Fulfillment of the Requirements for the Degree of

DOCTOR OF PHILOSOPHY
IN CHEMISTRY

at the

MASSACHUSETTS INSTITUTE OF TECHNOLOGY

November, 1998

[February 1999]

© 1998 Massachusetts Institute of Technology. All rights reserved.

Signature of Author: _____
November 30, 1998

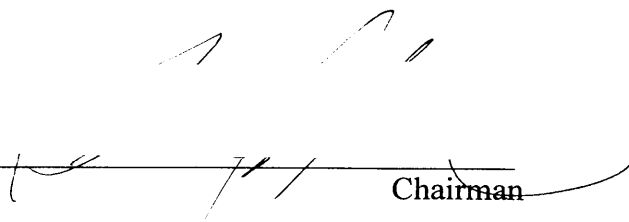
Certified by: _____
Professor Alexander M. Klibanov, Thesis Supervisor

Accepted by: _____
Professor Dietmar Seyferth, Chairman
Departmental Committee on Graduate Students

Science

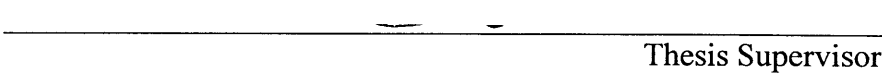
This doctoral thesis has been examined by a Committee of the Department of Chemistry as follows:

Prof. Lawrence J. Stern
Department of Chemistry



Chairman

Prof. Alexander M. Klibanov
Department of Chemistry



Thesis Supervisor

Prof. Bruce Tidor
Department of Chemistry



MECHANISTIC STUDIES OF ENZYMATIC STEREOSELECTIVITY IN AQUEOUS AND ORGANIC MEDIA

by TAO KE

Submitted to the Department of Chemistry on November 30th, 1998, in Partial Fulfillment of the Requirements for the Degree of Doctor of Philosophy in Chemistry

ABSTRACT

(i) A new, quantitative model has been elaborated to rationalize the solvent dependence of enzymatic selectivity solely on the basis of the thermodynamics of substrate desolvation in the enzyme-bound transition state. The model predicts that any type of the selectivity (defined as the ratio of $k_{\text{cat}}/K_{\text{M}}$ values) should be proportional to the ratio of the thermodynamic activity coefficients of the desolvated portions of the substrate(s) in the relevant transition state of the enzymatic reaction. The developed general model has been verified with prochiral selectivity of enzymes. Crystals (lightly cross-linked with glutaraldehyde) of the proteases γ -chymotrypsin and subtilisin Carlsberg, used as asymmetric catalysts in organic solvents, almost quantitatively adhere to the predictions of the model in the acetylation of 2-substituted 1,3-propanediols. The solvent dependence of this prochiral selectivity is dominated by that of $(k_{\text{cat}}/K_{\text{M}})_{\text{pro-R}}$, which has been explained on the basis of a computer modeling analysis of *pro-R* and *pro-S* transition-state structures. There is no correlation between the solvent-induced changes in $k_{\text{cat}}/K_{\text{M}}$ values and those of either k_{cat} or K_{M} individually, presumably reflecting the complex nature of the latter two parameters. Finally, the observed metamorphosis of chymotrypsin from a non-selective to a highly selective catalyst upon variation in the solvent is *not* attained at the expense of lowered enzymatic reactivity; in fact, prochiral selectivity and catalytic efficiency seem to rise concomitantly.

(ii) Enantioselectivity (E) of α -chymotrypsin in the hydrolysis of tropic (3-hydroxy-2-phenylpropionic) acid methyl ester in water has found to be 31 in favor of the *R* enantiomer, while for the corresponding transesterification with propanol in cyclohexane, E was found to be 12 in favor of *S* enantiomer. Importantly, using the developed thermodynamic substrate desolvation model, we can successfully explain this almost 400-fold change in enantioselectivity. This model has been tested further in concentrated aqueous salt solutions but failed to predict the sizable change in observed enantioselectivity, suggesting that enzyme conformation change in those solutions might be the key factor.

(iii) As the initial step toward predicting enzyme stereoselectivity in any medium, a new molecular-modeling methodology, which combines vacuum molecular mechanics and the continuum solvation method, has been developed and applied to explain α -chymotrypsin's enantioselectivity in the hydrolysis of four chiral substrates in water. The reasons why the vacuum molecular mechanics, although not taking hydration into account, still in most cases provide a satisfactory approximation of reality have been proposed.

(iv) Catalytic activities of α -chymotrypsin and subtilisin Carlsberg in various hydrous organic solvents have been measured as a function of how the enzyme suspension had been prepared. In one method, lyophilized enzyme is directly suspended in the solvent containing 1% water. In another, the enzyme is precipitated from its aqueous solution by a 100-fold dilution with an anhydrous solvent. In most cases, the reaction rate in a given nonaqueous enzymatic

system strongly (up to an order of magnitude) depends on the mode of enzyme preparation. The magnitude of this dependence is markedly affected by the nature of the solvent and enzyme. A mechanistic hypothesis proposed to explain the observed dependence has been verified in additional experiments in which the water contents and enzyme history have been further varied.

(v) A new methodology, based on modifying the substrate with Brønsted-Lowry acids or bases to form a salt, has been developed to markedly enhance enzymatic enantioselectivity in various organic solvents using both crystalline and lyophilized enzymes (*Pseudomonas cepacia* lipase and subtilisin Carlsberg). These enhancement effects have been rationalized using molecular modeling to derive enzyme-bound transition-state structures of *R* and *S* enantiomers of both free substrates and their salts. The calculated areas of substrate surfaces overlapping with enzyme's turn out to be a remarkably good predictor of enzymatic enantioselectivity E — the greater the difference in the area of surface overlap between the enantiomers, the higher the E value. The elaborated enantioselectivity enhancement strategy is effective in organic solvents, in which substrate salts are intact, but not in water, where the salts apparently dissociate to regenerate the free substrates.

Thesis Supervisor: Dr. Alexander M. Klivanov, Professor of Chemistry

ACKNOWLEDGMENTS

I wish to express my gratitude to my thesis advisor, Alexander Klibanov for both the guidance and financial support, which has allowed me to pursue this research.

I am also grateful to the past and present members of the Klibanov group, especially Charles Wescott, Jen Schmitke, Henry Costantino and Roman Rariy for helpful discussions and for their friendship.

Most importantly, I am thankful to my parents, Ke Yuanfa and Zhao Chunxian, and to my wife, Jing Li, for their support, guidance, and patience.

TABLE OF CONTENTS

| | |
|---|-----|
| Abstract | 3 |
| Acknowledgments..... | 5 |
| Introduction..... | 8 |
| | |
| I. Prediction of the Solvent Dependence of Enzymatic Prochiral Selectivity by Means of Structure-Based Thermodynamic Calculations | 12 |
| A. Introduction..... | 12 |
| B. Theory | 13 |
| C. Result and Discussion | 17 |
| D. Concluding Remarks..... | 29 |
| E. Materials and Methods | 30 |
| F. Reference | 40 |
| | |
| II. Insights into the Solvent Dependence of Chymotryptic Prochiral Selectivity..... | 46 |
| A. Introduction..... | 46 |
| B. Results and Discussion..... | 47 |
| C. Experimental Section | 58 |
| D. Reference | 60 |
| | |
| III. Computational and Experimental Examination of the Effect of Inorganic Salts on Chymotryptic Enantioselectivity in Water..... | 63 |
| A. Introduction..... | 63 |
| B. Materials and Methods | 64 |
| C. Results and Discussion..... | 68 |
| D. Reference | 77 |
| | |
| IV. Molecular-Modeling Calculations of Enzymatic Enantioselectivity Taking Hydration into Account..... | 81 |
| A. Introduction..... | 81 |
| B. Theory | 82 |
| C. Results and Discussion..... | 89 |
| D. Reference | 94 |
| | |
| V. On Enzymatic Activity in Organic Solvents as a Function of Enzyme History | 97 |
| A. Introduction..... | 97 |
| B. Materials and Methods | 98 |
| C. Results and Discussion..... | 100 |
| D. References | 108 |
| | |
| VI. Markedly Enhancing Enzymatic Enantioselectivity in Organic Solvents by Forming Substrate Salts..... | 110 |
| A. Introduction..... | 110 |
| B. Results and Discussion..... | 111 |

| | |
|-----------------------------------|-----|
| C. Materials and Methods | 127 |
| D. References and Footnotes | 133 |
| Biographical Note | 137 |

INTRODUCTION

Enzymatic catalysis has become a useful synthetic method during recent years.¹ Not only do enzymes remain catalytically active in organic solvents with little or no added water (instead of their natural aqueous milieu), but they also offer many significant advantages in those media as well. Many useful substrates are not soluble in water but readily soluble in organic solvents. In addition, some undesirable side reactions in water can be avoided in organic solvent. Because enzymes are usually insoluble in organic solvents, the enzyme can be recovered from the product solution by simple filtration. Also, enzyme suspensions in organic solvents are often more stable than their soluble counterparts in water. Furthermore, since the thermodynamic equilibrium of many reactions is markedly solvent-dependent, a solvent can be selected which favors the formation of the desired products. Importantly, it has become apparent recently that through prudent choice of the solvent,² one can profoundly manipulate, and in some cases reverse, the selectivity, such as stereoselectivity, of enzyme-catalyzed reactions.

Among these attractive properties of enzyme in organic solvents, the ability to control stereoselectivity (e.g., prochiral and enantiomeric selectivity) is the most valuable asset for synthetic chemists.¹ Unfortunately, the lack of mechanistic quantitative models is a major drawback hindering useful applications. Prior to this thesis work, some qualitative models have been proposed for correlating enzyme selectivity with physicochemical properties of the solvent such as $\log P$,³ dielectric constant,⁴ dipole moment,⁴ etc. Such models may work reasonably well under specific conditions, but once the enzyme or substrate system changes, they are likely to fail because: i) there is no theoretical foundation in terms of energetics; and ii) none of those

¹ Klibanov, A.M. *Trends Biochem. Sci.* **1989**, *14*, 141. Chen, C.-S.; Sih, C.J. *Angew. Chem., int. Ed. Engl.* **1989**, *28*, 695. Klibanov, A.M. *Acc. Chem. Res.* **1990**, *23*, 114. Dordick, J.S. *Biotechnol. Prog.* **1992**, *8*, 259.

² Wescott, C.R., Klibanov, A.M. *Biochim. Biophys. Acta* **1994**, *1206*, 1.

³ Terradas, F., Teston-Henry, M., Fitzpatrick, P.A. and Klibanov, A.M. *J. Am. Chem. Soc.* **1993**, *115*, 390.

models uses the structural information concerning the enzyme active site, thus failing to account for any specific enzyme-substrate interactions.

Recently, X-ray crystal structures of several enzymes in neat organic solvents have been solved. These include the structure of subtilisin Carlsberg in anhydrous acetonitrile and dioxane⁵ and the structure of γ -chymotrypsin in hexane⁶. In both cases, the enzyme structures in organic solvents have been found to be nearly indistinguishable from those in water. These discoveries enable me to utilize the structural information to investigate the solvent dependence of enzyme stereoselectivity in organic media.

In Chapter I, a thermodynamic model that takes into account the variations in substrate desolvation in the transition state is elaborated to explain solvent-dependent prochiral selectivity. Thermodynamic activity coefficients of the desolvated portions of the substrate, calculated using computer-generated, transition-state structures and UNIFAC⁷, correctly predict the solvent-dependence of prochiral selectivity of crystalline chymotrypsin and subtilisin.

Once the goal of predicting enzyme prochiral selectivity as a function of solvent has been achieved, there are still several important mechanistic issues unresolved, such as: a) which stereochemical route (*pro-S* or *pro-R*) is the major contributor to the solvent effect; b) are the solvent-dependent changes in k_{cat} or K_{M} the chief contributors to the observed solvent effects;

⁴ Fitzpatrick, P.A. and Klivanov, A.M. *J. Am. Chem. Soc.* **1991**, *113*, 3166.

⁵ Fitzpatrick, P.A., Steinmetz, A.C.U., Ringe, D. and Klivanov, A.M. *Proc. Natl. Acad. Sci. U.S.A.* **1993**, *90*, 8653.

Fitzpatrick, P.A.; Ringe, D.; Klivanov, A.M. *Biochem. Biophys. Res. Commun.* **1994**, *198*, 675-681. Schmitke, J.L.; Stern, L.J.; Klivanov, A.M. *Proc. Natl. Acad. Sci. USA* **1997**, *94*, 4250-4255. Schmitke, J.L.; Stern, L.J.; Klivanov, A.M. *Proc. Natl. Acad. Sci. USA* **1998**, *95*, 12918-12923.

⁶ (a) Yennawar, H.P., Yennawar, N.H., Farber, G.K. *Biochemistry* **1994**, *33*, 7326. (b) Yennawar H.P., Yennawar, N.H., Farber, G.K. *J. Am. Chem. Soc.* **1995**, *117*, 577.

⁷ UNIFAC is a computational method for the estimation of Rault's law activity coefficients. Being a group contribution method, it can calculate activity coefficients in systems for which there is no experimental data by assessing the individual contribution of each chemical group which makes up the system. Use of this method requires three types of parameters for each group in the system: the group's surface area, the volume of the group, and empirically determined parameters which reflect the free energy of interaction between a given group and every other group in the system. See Chapter I ref 4 for more details.

and c) does enzyme reactivity correlate with selectivity? Chapter II provides answers to these questions.

In the previous two studies as well as elsewhere,⁸ we have elaborated the thermodynamic desolvation model that almost quantitatively explains the solvent dependence of enzymatic stereoselectivity in organic media. Since the model is only based on the differential desolvation energetics, it should not be limited to organic media. Therefore, as a strategic expansion, in Chapter III we test it in aqueous solutions and particularly in those containing high salt concentrations.

Being able to predict enzyme stereoselectivity in any given medium has always been an important goal, which would ultimately enable chemists to tailor and design enzyme/solvent systems to catalyze any stereospecific chemical reaction at will. In Chapter IV, as a first step toward this ambitious goal, we propose a simplified computational model that combines vacuum molecular mechanics and continuum electrostatics and calculates the enantioselectivity of chymotrypsin for four chiral substrates in water instead of vacuum.

In order to expand the utility of enzymes in synthesis, we have elaborated two novel approaches other than "media engineering" advanced in the previous chapters. The first approach, involving enzyme "memory" with the preparation method, is presented in Chapter V. It has been found that in organic environments, due to the absence of the "molecular lubricant" water, enzymes are conformationally rigid and kinetically trapped in their previous conformations⁹, therefore enzymes "remember" their history in organic solvents. In this study, we examine how and why the extent of this kinetic trapping depends on solvents and preparation methods, which will provide insights into optimizing enzyme preparation in organic solvents.

⁸ Wescott, C.R., Noritomi, H., Klibanov, A.M. *J. Am. Chem. Soc.* **1996**, *118*, 10365.

⁹ (a) Klibanov, A.M. *Trends Biochem. Sci.* **1989**, *14*, 141. (b) Klibanov, A.M. *Nature* **1995**, *374*, 596.

In a second approach, in Chapter VI we propose a new strategy for increasing the enantioselectivity of enzymes in organic solvents. It is based on the idea that discrimination between the two substrate enantiomers by a given enzyme can be enhanced by temporarily enlarging the substrate via salt formation. A bulky counter-ion of the substrate will exacerbate the steric hindrance encountered by the less reactive (and hence more sterically constrained) enantiomer in the enzyme-bound transition state, thus increasing the enantioselectivity *E*. Following the enzymatic resolution and enzyme removal, the reaction mixture is simply treated with a strong acid or base to dissociate the salt and recover the free substrate and product.

For the convenience of the reader, each chapter contains its own introduction, results and discussion, methods, and reference sections. Note that each chapter has resulted in a publication: Chapter I in *J. Am. Chem. Soc.* **1996**, *118*, 3366; Chapter II in *J. Am. Chem. Soc.* **1998**, *120*, 4259; Chapter III in *Biocatalysis Biotransformation*, *in press*; Chapter IV in *Biotechnol. Bioeng.* **1998**, *57*, 741; Chapter V in *Biotechnol. Bioeng.* **1998**, *57*, 746; and Chapter VI submitted to *J. Am. Chem. Soc.*

CHAPTER I. PREDICTION OF THE SOLVENT DEPENDENCE OF ENZYMATIC PROCHIRAL SELECTIVITY BY MEANS OF STRUCTURE-BASED THERMODYNAMIC CALCULATIONS

A. INTRODUCTION

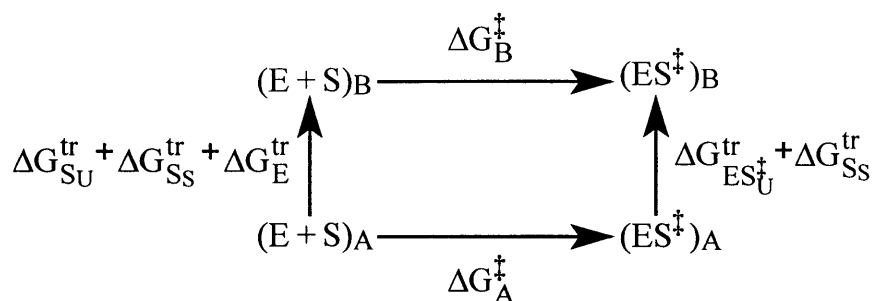
One of the most profound revelations arisen from nonaqueous enzymology¹ is the discovery that the specificity of an enzyme strongly depends on the solvent.² Of all the types of enzyme specificity found to be controlled by the solvent — enantioselectivity, prochiral selectivity, substrate specificity, regioselectivity, and chemoselectivity — the first two are particularly important for synthetic applications. Indeed, if generalized and understood, solvent control of enzymatic stereoselectivity should enhance the utility of biocatalysis in organic chemistry by allowing the rational manipulation of the stereochemical outcome of asymmetric transformations simply by altering the reaction medium. The ultimate challenge in this regard is to learn how to predict enzyme selectivity as a function of the solvent.

As a first step toward this goal, we have recently elaborated a thermodynamic model, which explains the substrate specificity of the protease subtilisin Carlsberg in organic solvents on the basis of solvent-to-water partition coefficients of the substrates.³ These partition coefficients can be either measured experimentally or calculated using the UNIFAC computer algorithm.⁴ An explicit assumption of our analysis is that the substrates are fully desolvated, i.e., inaccessible to the solvent, in the enzyme-bound transition state. This assumption precludes the extension of the proposed model to enantioselectivity, since the partition coefficients for different enantiomers of the same compound are identical. Likewise, prochiral, regio-, and chemoselectivities cannot be analyzed either, because in all these instances the same substrate molecule (just different parts of it) reacts with the enzyme.

In the present study, we further develop and broaden our thermodynamic treatment to eliminate the aforementioned limitations. The resultant model, tested herein with prochiral selectivity, takes into account variations in substrate desolvation in the transition states for *pro-R* and *pro-S* orientations. Thermodynamic activity coefficients of the desolvated portions of the substrate, calculated using computer-generated, transition-state structures and UNIFAC, correctly predict the solvent dependence of prochiral selectivity of crystalline chymotrypsin and subtilisin.

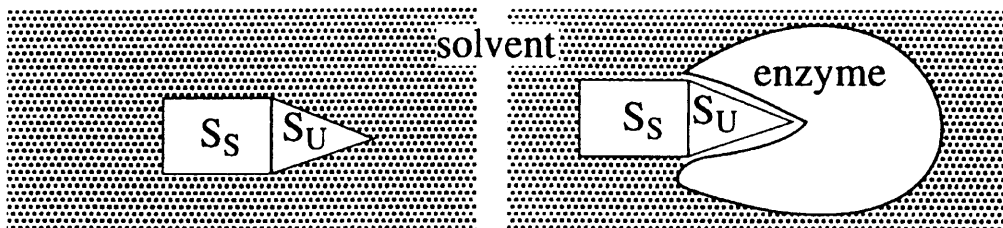
B. THEORY

Scheme 1



The solvent may influence enzymatic selectivity through several distinct mechanisms. For instance, it could change the enzyme conformation and thus affect the selectivity of the reaction by altering enzyme-substrate interactions.^{5,6} Alternatively, solvent molecules could bind within the enzyme active site and block the normal binding mode of the substrate.^{7,8} While these two possible mechanisms do not necessarily influence selectivity, a third, driven by the energetics of substrate solvation, must do so, regardless of the presence of other mechanisms. Indeed, it has been demonstrated that the energetics of substrate solvation is the dominant means by which the solvent influences the substrate specificity of subtilisin.

Scheme 2



The contribution of solvation energies to the solvent dependence of enzyme kinetics is demonstrated by the thermodynamic cycle in Scheme 1. The lower horizontal arrow represents the enzyme (E) and the substrate (S) reacting in solvent A to form the transition state $(ES^\ddagger)_A$ with an activation free energy of ΔG_A^\ddagger . This transition state spontaneously decomposes to ultimately form the free enzyme and products. An alternative, hypothetical path exists leading to the same transition state complex. In this path, the substrate and enzyme are separately transferred from solvent A to solvent B, where they react to form the transition state $(ES^\ddagger)_B$, which is subsequently transferred back to solvent A. For thermodynamic purposes, the substrate can be represented as the sum of two portions (see Scheme II), that which is solvated in the transition state (S_S) and that which is enveloped by the enzyme and is thus unsolvated in the transition state (S_U). Similarly, the transition state is regarded as the sum of S_S and another portion which includes only the enzyme and the unsolvated substrate moiety in the transition state (ES_U^\ddagger). ΔG_A^\ddagger can be expressed as the sum of the energetic terms of the alternative path:⁹

$$\Delta G_A^\ddagger = \Delta G_B^\ddagger + \Delta G_E^{\text{tr}} + \Delta G_{S_S}^{\text{tr}} + \Delta G_{S_U}^{\text{tr}} - \Delta G_{ES_U^\ddagger}^{\text{tr}} - \Delta G_{S_S}^{\text{tr}} \quad (1)$$

where ΔG_B^\ddagger is the activation free energy for the reaction in solvent B, and ΔG^{tr} is the free energy of transfer of the moiety indicated in the subscript from solvent A to B. Assuming that the

solvated surfaces of E and ES_U^\ddagger for low-molecular-weight substrates are identical,¹⁰

$\Delta G_E^{\text{tr}} = \Delta G_{ES_U^\ddagger}^{\text{tr}}$. Consequently, equation (1) can be simplified to:

$$\Delta G_A^\ddagger = \Delta G_B^\ddagger + \Delta G_{S_U}^{\text{tr}} \quad (2)$$

ΔG^\ddagger is related to k_{cat}/K_M as:¹¹

$$\Delta G^\ddagger = -RT \ln \left[\left(\frac{k_{\text{cat}}}{K_M} \right) \left(\frac{h}{\kappa T} \right) \right] \quad (3)$$

where h , κ , R , k_{cat} , K_M and T are the Planck, Boltzmann, gas, catalytic, and Michaelis constants and temperature, respectively. ΔG^{tr} can be expressed in terms of thermodynamic activity coefficients as $RT \ln (x_B \gamma_B / x_A \gamma_A)$, where γ and x are the activity coefficient and mole fraction, respectively, of the solute in the indicated solvent.¹² If γ' is defined as the activity coefficient of the *unsolvated* substrate moiety (S_U), then:

$$\Delta G_{S_U}^{\text{tr}} = RT \ln (x_B \gamma'_B / x_A \gamma'_A) \quad (4)$$

Substituting equations (3) and (4) into (2) yields:

$$(k_{\text{cat}}/K_M)_A = (\gamma'_A / \gamma'_B) (x_A / x_B) (k_{\text{cat}}/K_M)_B \quad (5)$$

Note that for dilute solutions x_A / x_B depends only on the molar volume of the solvents when the transfer is done at constant molar concentration.¹³ The mole fraction ratio is thus the same for any substrate and cancels out when equation (5) is expressed for two substrates, I and II, and solved for the logarithm of the selectivity in solvent A:

$$\log \left[\frac{(k_{\text{cat}}/K_M)_I}{(k_{\text{cat}}/K_M)_II} \right]_A = \log \left(\frac{\gamma'_I}{\gamma'_II} \right)_A + \log \left[\frac{\gamma'_II (k_{\text{cat}}/K_M)_I}{\gamma'_I (k_{\text{cat}}/K_M)_II} \right]_B \quad (6)$$

Equation (6) expresses the general relationship between enzymatic selectivity and solvent-transition-state interactions. In the present work, we specifically test equation (6) with respect to prochiral selectivity. While the same substrate leads to both the *R* and *S* products, the reaction proceeds through conformationally distinct transition states for the production of each enantiomer (a *pro-R* transition state results in the *R* product, while a *pro-S* transition state forms the *S* product). Thus, differences between γ'_{I} and γ'_{II} arise from variations in transition state solvation, not from chemical differences between two substrates. The parameters for substrates I and II in equation (6) can therefore be replaced with those for the *pro-R* and *pro-S* reaction pathways to describe prochiral selectivity. Also, if B is fixed as a reference solvent,¹⁴ the final term in equation (6) will be a constant. Consequently, one arrives at the following equation describing the solvent dependence of the prochiral selectivity of an enzyme in terms of a γ' ratio:

$$\log \left[\frac{(k_{\text{cat}}/K_{\text{M}})_{\text{pro-S}}}{(k_{\text{cat}}/K_{\text{M}})_{\text{pro-R}}} \right] = \log \left(\frac{\gamma'_{\text{pro-S}}}{\gamma'_{\text{pro-R}}} \right) + \text{const} \quad (7)$$

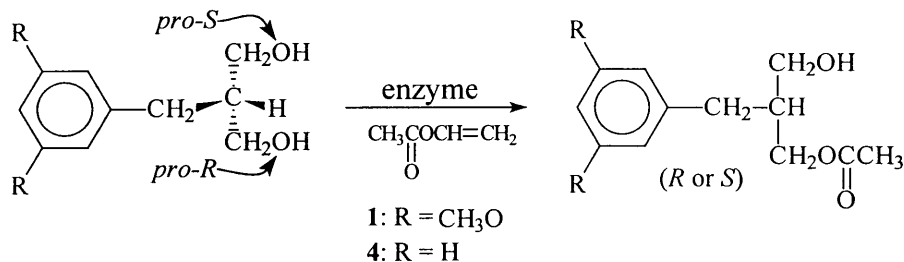
Unlike the situation for substrate specificity, where solvent-dependent variation in the activity coefficient ratio for the two substrates is primarily driven by chemical differences between the substrates, γ' for prochiral selectivity differs for each reaction pathway only due to differences in transition state solvation. In this work, we calculate γ' for both the *pro-R* and *pro-S* transition states using a three-step procedure. First, the desolvated portion of the substrate in the transition state is determined using molecular modeling based on the crystal structure of the enzyme. Second, this desolvated moiety is expressed in terms of distinct chemical groups to yield a model compound, which approximates the portion of the substrate removed from the

solvent in the transition state. Finally, the thermodynamic activity coefficient of this model compound is calculated using UNIFAC and then equated to γ' . According to equation (7), knowing only γ'_{pro-R} and γ'_{pro-S} for a series of solvents, it should be possible to predict the solvent dependence of prochiral selectivity.

C. RESULTS AND DISCUSSION

As an initial test of the ability of the model described above to predict the solvent dependence of prochiral selectivity, we have examined the enzymatic acylation of a designed prochiral diol, 2-(3,5-dimethoxybenzyl)-1,3-propanediol (**1**), by vinyl acetate to produce the chiral monoester 3-hydroxy-2-(3,5-dimethoxybenzyl)propyl acetate (**2**) (see Scheme III). The crystalline chymotrypsin, lightly cross-linked with glutaraldehyde, has been selected as a catalyst.¹⁵ Its structure in an organic solvent has been recently determined by X-ray crystallography¹⁶ and found to be nearly the same as in water, thus enabling structure-based computer modeling.

Scheme 3



The first step in the implementation of the model is the determination of the desolvated portions of **1** in the transition state for each product enantiomer. Since serine proteases suspended in organic solvents act via the ping-pong bi-bi mechanism,¹⁷ at least two transition states are involved in each enzyme turnover, one for the acylation by vinyl acetate to form the acyl-enzyme intermediate, and the other for the regeneration of the free enzyme by the nucleophile. The latter transition state leads to the production of the chiral product. Thus, two structural models were constructed (see Methods for details) of the transition state for the reaction of **1** with the acyl-chymotrypsin. In the first (Fig. 1A), **1** binds to the enzyme in such a way that the *S* product is formed. Due to steric constraints, the dimethoxyphenyl group in the *pro-S* transition state is unable to enter the S1 binding site of chymotrypsin and hence must extend away from the enzyme into the solvent. The second model (Fig. 1B) depicts the transition state which leads to the *R* product. Unlike in the *pro-S* situation, the *pro-R* transition state adopts a conformation in which the dimethoxyphenyl group is buried in the S1 binding site of the enzyme. The determination of the solvent-accessible surface areas of **1** in each of the transition state models (Fig. 2) reveals that the entire substrate is unsolvated in the *pro-R* transition state, while it is largely solvated in the *pro-S* transition state.

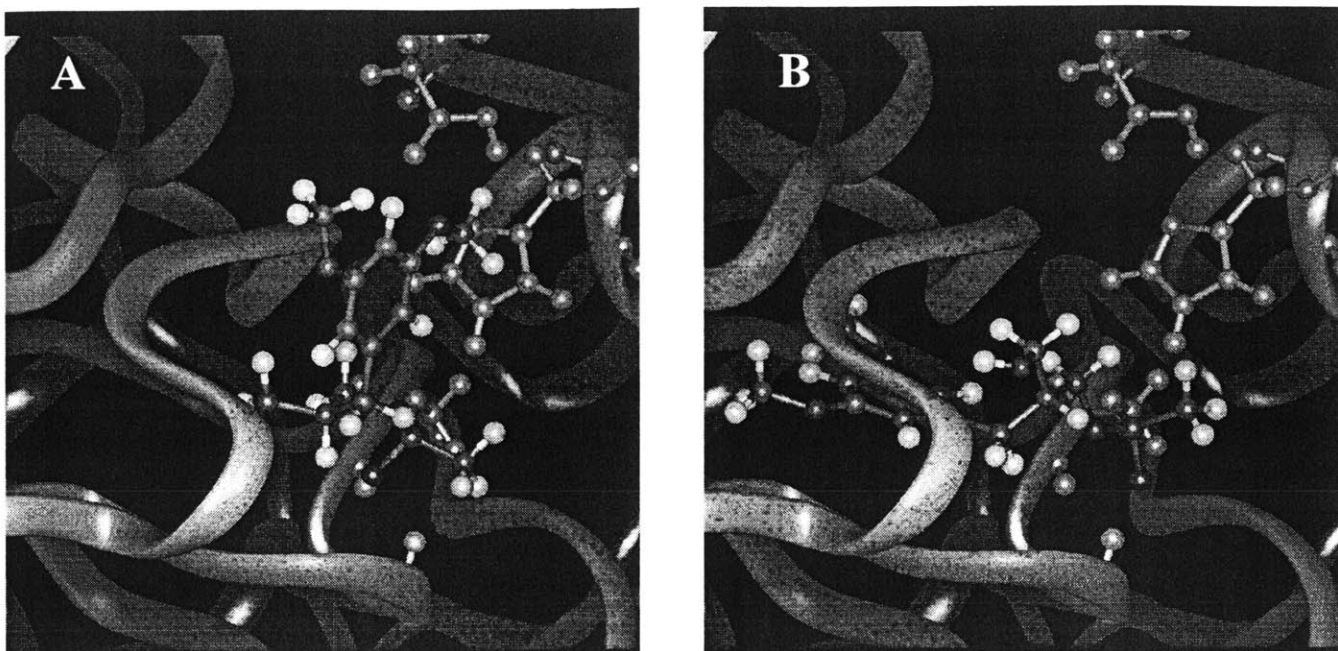


Figure 1. Conformation of substrate **1** in the *pro-S* (A) and *pro-R* (B) transition states with γ -chymotrypsin. See the Methods section for details on the construction of the molecular models

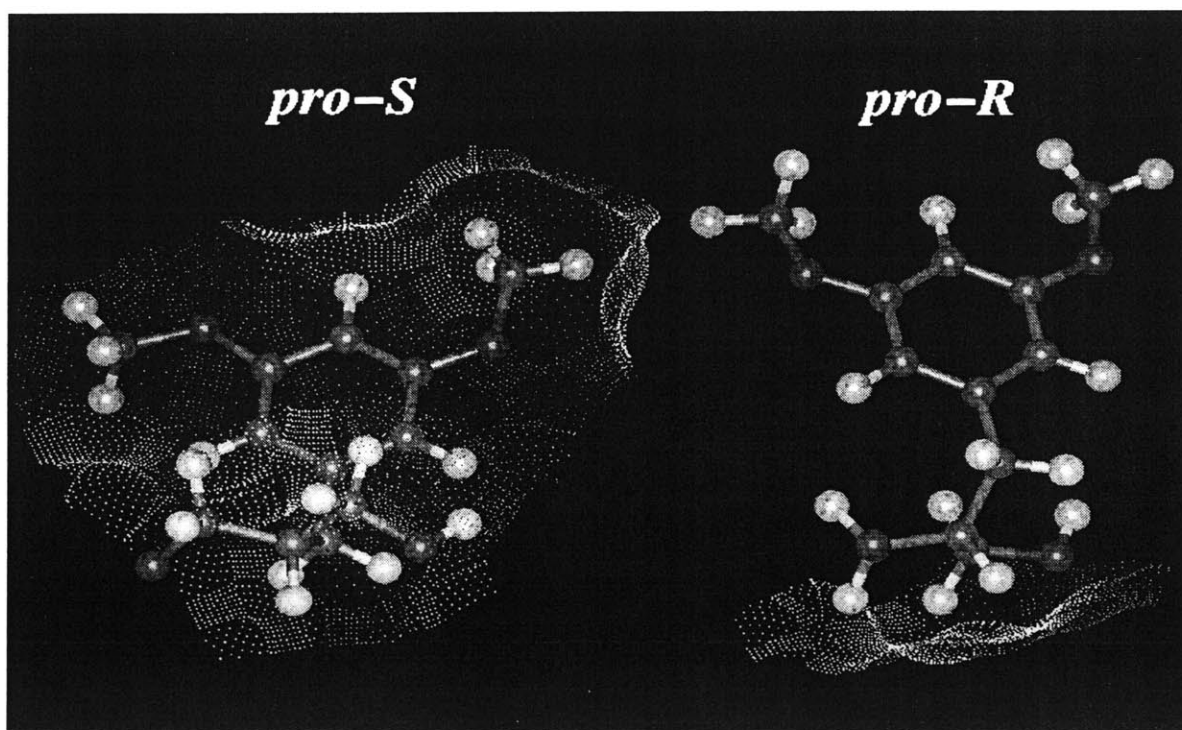
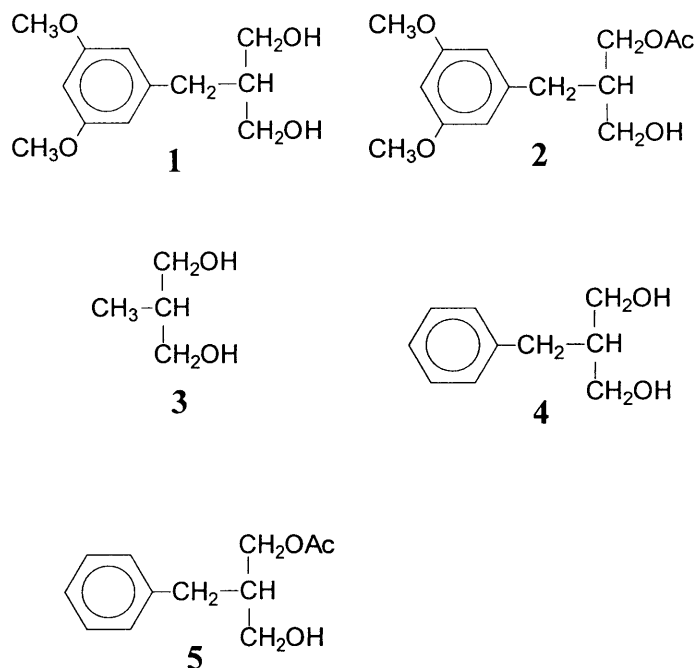
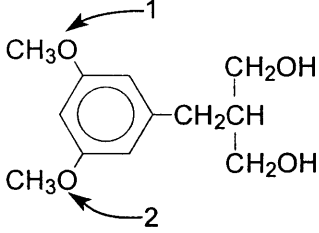


Figure 2. Solvent-accessible surface areas of substrate **1** in the *pro-S* (left) and *pro-R* (right) transition states with γ -chymotrypsin. The solvent-accessible surfaces (represented by dot surfaces) were calculated using the Connolly method (see the Methods section for details)



With the extent of solvation of the substrates elucidated, it is possible to proceed with the second phase of our strategy: the selection of model compounds that mimic the unsolvated portion of **1** in the *pro-S* and *pro-R* transition states. Table 1 quantitatively examines the extent to which each chemical group of the substrate is desolvated. The 2-methyl-1,3-propanediol (**3**) moiety is almost equally desolvated in the *pro-S* and *pro-R* transition states and consequently should be a constituent of both model compounds. The methoxy and phenyl groups are completely desolvated only in the *pro-R* transition state and are therefore only included in the *pro-R* model compound; their partial desolvation in the *pro-S* transition state is disregarded (see below). Thus analysis of the data in Table 1 leads to the choice of **3** and **1** as the *pro-S* and *pro-R* model compounds, respectively.

Table 1. Extent of desolvation of **1** in the transition state with γ -chymotrypsin

| compound | group | percentage of desolvation ^a | |
|---|--------------------------|--|--------------|
| | | <i>pro-S</i> | <i>pro-R</i> |
|  | methoxy 1 | 35% | 100% |
| | methoxy 2 | 49% | 100% |
| | phenyl | 14% | 100% |
| | 2-methyl-1,3-propanediol | 78% | 71% |

^a The desolvated surface area of each group of the substrate in the enzyme-bound transition state was determined using molecular models (see Figs. 1 and 2) and expressed as a percentage of the solvent-accessible surface area of the group in the unbound substrate.

The final phase in the prediction of the solvent dependence of enzymatic prochiral selectivity is the employment of the model compounds to calculate γ'_{pro-R} and γ'_{pro-S} for use in equation (7). Because γ' is defined as the activity coefficient of the unsolvated substrate moiety in the transition state, it is approximated by the activity coefficient of the appropriate model compound. Consequently, UNIFAC-calculated activity coefficients of **3** and **1** are reported in Table 2 as γ'_{pro-S} and γ'_{pro-R} , respectively.

Table 2. Thermodynamic activity coefficients of compounds modeling the desolvated fractions of substrates **1** and **4** in the transition states with γ -chymotrypsin calculated using UNIFAC

| solvent | substrate 1 | | | substrate 4 | | |
|-------------------|--------------------|-------------------|---|--------------------|-------------------|---|
| | γ'_{pro-S} | γ'_{pro-R} | $\frac{\gamma'_{pro-S}}{\gamma'_{pro-R}}$ | γ'_{pro-S} | γ'_{pro-R} | $\frac{\gamma'_{pro-S}}{\gamma'_{pro-R}}$ |
| diisopropyl ether | 73.5 | 99.6 | 0.738 | 73.8 | 36.2 | 2.04 |
| dibutyl ether | 51.4 | 69.4 | 0.741 | | | |

| | | | | | | |
|----------------------------|------|-------|------|------|------|------|
| cyclohexane | 480 | 266 | 1.80 | | | |
| dioxane | 5.09 | 2.37 | 2.15 | 5.09 | 3.36 | 1.51 |
| <i>tert</i> -butyl acetate | 13.5 | 4.59 | 2.94 | 13.5 | 5.16 | 2.62 |
| tetrahydrofuran | 8.13 | 2.65 | 3.07 | | | |
| <i>para</i> -xylene | 70.7 | 16.1 | 4.39 | | | |
| toluene | 66.9 | 11.9 | 5.62 | | | |
| methyl acetate | 7.25 | 0.986 | 7.35 | 7.25 | 2.14 | 3.39 |
| propionitrile | 3.10 | 0.401 | 7.73 | | | |
| benzene | 67.6 | 7.28 | 9.29 | 67.6 | 14.6 | 4.63 |
| acetonitrile | 2.71 | 0.278 | 9.75 | | | |

Table 3. Solvent dependence of the prochiral selectivity of γ -chymotrypsin, prepared by different methods, toward substrate **1**.

| solvent | $(k_{\text{cat}}/K_{\text{M}})_{\text{pro-S}}/(k_{\text{cat}}/K_{\text{M}})_{\text{pro-R}}$ ^a | | |
|----------------------------|--|--------------------------|---------------------------------------|
| | cross-linked crystalline ^b | lyophilized ^c | acetone- precipitated ^d |
| diisopropyl ether | 0.10 | 0.98 | 0.63 |
| dibutyl ether | 0.17 | 0.67 | 0.77 |
| cyclohexane | 0.28 | 0.91 | 0.67 |
| <i>tert</i> -butyl acetate | 0.32 | 1.7 | |
| dioxane | 0.38 | 2.3 | |
| tetrahydrofuran | 0.45 | 1.6 | |
| <i>para</i> -xylene | 1.0 | 1.3 | |
| toluene | 1.3 | 1.2 | 1.2 |
| propionitrile | 1.4 | 2.1 | |
| acetonitrile | 1.9 | 2.9 | 1.0 |
| methyl acetate | 2.2 | 1.2 | 1.5 |

^a $(k_{\text{cat}}/K_{\text{M}})_{\text{pro-S}}/(k_{\text{cat}}/K_{\text{M}})_{\text{pro-R}}$ values were determined from the ratio of initial velocities for the production of each enantiomer as described in the Methods section. ^b The initial velocities, v_S and v_R , respectively, observed for 5 mg/mL crystalline γ -chymotrypsin were (in $\mu\text{M/hr}$): diisopropyl ether — 0.52 and 5.2; dibutyl ether — 0.34 and 2.0; cyclohexane —

0.74 and 2.6; *tert*-butyl acetate — 0.068 and 0.21; dioxane — 0.63 and 1.6; tetrahydrofuran — 1.4 and 3.1; *para*-xylene — 5.6 and 5.6; toluene — 31 and 24; propionitrile — 4.7 and 3.3; acetonitrile — 2.5 and 1.3; methyl acetate — 1.8 and 0.82. ^c The initial velocities, v_S and v_R , respectively, observed for 15 mg/mL lyophilized γ -chymotrypsin were (in $\mu\text{M/hr}$): diisopropyl ether — 44 and 45; dibutyl ether — 15 and 23; cyclohexane — 4.7 and 5.4; *tert*-butyl acetate — 14 and 24; dioxane — 3.8 and 8.6; tetrahydrofuran — 11 and 18; *para*-xylene — 120 and 96; toluene — 53 and 45; propionitrile — 6.7 and 3.2; acetonitrile — 2.4 and 8.1; methyl acetate — 11 and 9.2. ^d The initial velocities, v_S and v_R , respectively, observed for 15 mg/mL acetone-precipitated γ -chymotrypsin were (in $\mu\text{M/hr}$): diisopropyl ether — 32 and 53; dibutyl ether — 19 and 24; cyclohexane — 7.9 and 12; toluene — 73 and 61; acetonitrile — 28 and 27; methyl acetate — 18 and 12.

A profound solvent effect on the activity coefficient ratio is evident in Table 2:

$\gamma'_{pro-S}/\gamma'_{pro-R}$ varies over an order of magnitude when the solvent is changed from diisopropyl ether to acetonitrile. Equation (7) predicts that this variation in the activity coefficient ratio will be reflected in the same change in prochiral selectivity. As a test of this prediction, the prochiral selectivity of cross-linked crystalline γ -chymotrypsin toward **1** was measured experimentally in a variety of solvents (Table 3, first data column). In such solvents as diisopropyl ether and cyclohexane, the enzyme strongly favors production of the *R*-product. As predicted by equation (7), switching to solvents with higher $\gamma'_{pro-S}/\gamma'_{pro-R}$ ratios, such as dioxane or tetrahydrofuran, brings about a concomitant change in prochiral selectivity, eventually resulting in the preferential formation of the *S*-product, e.g., in acetonitrile and methyl acetate (i.e., a solvent-induced *inversion* of chymotrypsin's prochiral selectivity is observed). Indeed, the prochiral selectivity as a function of the solvent varies over the order of magnitude range predicted by equation (7).

Equation (7) further predicts that a double-logarithmic plot of $(k_{cat}/K_M)_{pro-S}/(k_{cat}/K_M)_{pro-R}$ vs. $\gamma'_{pro-S}/\gamma'_{pro-R}$ will produce a linear correlation. Such a plot, presented in Figure 3A, does

indeed yield a reasonable linear dependence ($R^2 = 0.94$). The slope of the regression line of Fig. 3A is 1.1, close to the predicted value of 1.0.

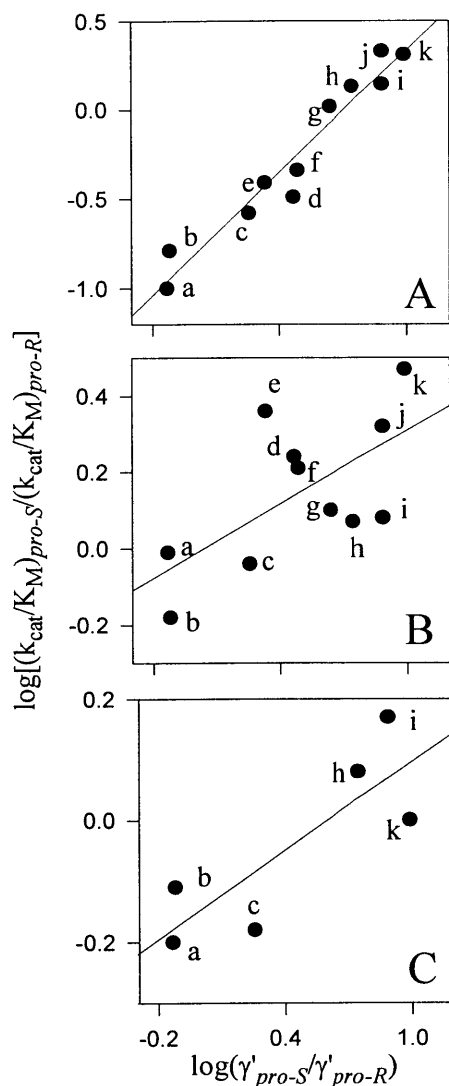


Figure 3. Dependence of the prochiral selectivity of different preparations of γ -chymotrypsin toward substrate **1** in various organic solvents on the ratio of the activity coefficients of the desolvated portions of the substrate in the *pro-S* and *pro-R* transition states (see equation (7)). A — cross-linked enzyme crystals; B — lyophilized enzyme powder; C — acetone-precipitated enzyme powder. Solvents: a - diisopropyl ether; b - dibutyl ether; c - cyclohexane; d - *tert*-butyl acetate; e - dioxane; f - tetrahydrofuran; g - *para*-xylene; h - toluene; i - propionitrile; j - methyl acetate; k - acetonitrile. The straight lines are drawn using linear regression; see text for discussion. For experimental details, see the Methods section.

Several sources of error are inherent to this treatment and may contribute to the 10% deviation of the slope from unity. First, the entire dimethoxyphenyl group of **1** in the *pro-S* transition state is treated as solvated. In reality, a fraction of its surface is partially desolvated (see Table 1), making it impossible to exactly represent the desolvated substrate moiety as a complete molecule. Second, there are unavoidable errors associated with UNIFAC, which produces a mere statistical estimate of the activity coefficient.

Because most enzymes used in organic solvents to date have been prepared in the form of lyophilized powders, it is important to ascertain whether the thermodynamic analytical methodology developed herein is applicable to such and other enzyme preparations besides cross-linked crystals. The determination of γ' is contingent on the ability to predict the specific interactions between the substrate and the enzyme. Hence, even a minor conformational perturbation of the enzyme active site could change the solvation of the transition state and thus invalidate the calculation of γ' . Recent hydrogen isotope exchange/NMR¹⁸ and FTIR¹⁹ experiments indicate that reversible conformational changes occur in proteins upon dehydration. Thus, we reasoned that lyophilized or precipitated (from water with cold acetone) chymotrypsin may not adhere to the solvent dependence of prochiral selectivity predicted on the basis of the enzyme crystal structure.

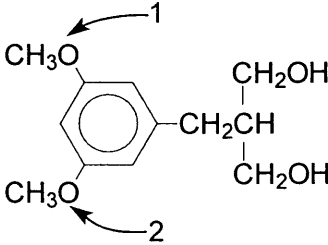
When the prochiral selectivity of lyophilized or acetone-precipitated chymotrypsin is measured for substrate **1** in several solvents (Table 3), the selectivity varies less than three fold, while the solvent effect predicted by equation (7) assuming an intact enzyme structure spans a factor of 13. Moreover, double-logarithmic plots of the prochiral selectivity of lyophilized (Fig. 3B) and acetone-precipitated (Fig. 3C) chymotrypsin vs. $\gamma'_{pro-S}/\gamma'_{pro-R}$ do not yield the correlations obtained for structurally intact chymotrypsin: while theory predicts that the slopes of

the aforementioned plots should be unity, those determined by linear regression are 0.32 and 0.24, respectively. Additionally, only a poor correlation between the prochiral selectivity of these enzyme powders and $\gamma'_{pro-S}/\gamma'_{pro-R}$ is reflected by R^2 values of 0.42 for lyophilized and 0.68 for acetone-precipitated chymotrypsin (as compared to 0.94 for the cross-linked crystals). These findings underscore the importance of dealing with structurally defined enzyme catalysts if a quantitative rationale involving stereoselectivity is sought after.

While our model requires the enzyme to be in a native (or at least a known) conformation in organic solvents, it places no further constraints on the catalyst. Therefore, the proposed analysis should be applicable to enzymes other than chymotrypsin. To test this prediction, the acylation of **1** by vinyl acetate, catalyzed by cross-linked crystalline subtilisin Carlsberg²⁰ (henceforth referred to as subtilisin), has been investigated using the same methodology as with the chymotrypsin-catalyzed reaction.

Because the S1 binding site of subtilisin is much more shallow than chymotrypsin's, no portion of substrate **1** in the either *pro-S* or *pro-R* transition state is fully shielded from the solvent. Furthermore, calculation of the unsolvated surfaces of the groups that make up the substrate reveals that there is little difference in the extent of desolvation of the two transition states (Table 4). Due to the analogous solvation patterns, the model compounds for the calculation of γ'_{pro-R} and γ'_{pro-S} , whatever they may be, should be identical, resulting in the prediction by equation (7) that the prochiral selectivity of subtilisin in the acetylation of **1** will be independent of the solvent. In support of this prediction, when $(k_{cat}/K_M)_{pro-S}/(k_{cat}/K_M)_{pro-R}$ for subtilisin is measured in a range of solvents which span a 19-fold change in the prochiral selectivity of chymotrypsin for the same substrate, less than a 2-fold variation is observed (Table 5).

Table 4. Extent of desolvation of **1** in the transition state with subtilisin Carlsberg

| compound | group | percentage of desolvation ^a | |
|---|---------------|--|--------------|
| | | <i>pro-S</i> | <i>pro-R</i> |
|  | methoxy 1 | 9% | 14% |
| | methoxy 2 | 54% | 60% |
| | phenyl | 55% | 52% |
| | 2-methyl-1,3- | 56% | 62% |
| | propanediol | | |

^a The desolvated surface area of each group of the substrate in the enzyme-bound transition state was determined using molecular models (similar to those in Figs. 1 and 2) and expressed as a percentage of the solvent-accessible surface area of the group in the unbound substrate.

Table 5. Solvent dependence of prochiral selectivity of cross-linked crystalline subtilisin Carlsberg for substrate **1**

| solvent | ^a |
|----------------------------|---|
| | $\frac{(k_{\text{cat}}/K_M)_{\text{pro-S}}}{(k_{\text{cat}}/K_M)_{\text{pro-R}}}$ |
| diisopropyl ether | 1.2 |
| cyclohexane | 1.2 |
| <i>tert</i> -butyl acetate | 1.6 |
| acetonitrile | 2.2 |
| toluene | 2.3 |

^a $(k_{\text{cat}}/K_M)_{\text{pro-S}}/(k_{\text{cat}}/K_M)_{\text{pro-R}}$ values were determined from the ratio of initial velocities for the production of each enantiomer as described in the Methods section. The initial velocities, v_S and v_R , respectively, observed for 2.5 mg/mL crystalline subtilisin Carlsberg were (in $\mu\text{M/hr}$): diisopropyl ether — 28 and 23; cyclohexane — 20 and 17; *tert*-butyl acetate — 4.3 and 2.7; acetonitrile — 3.1 and 1.4; toluene — 18 and 7.8.

In addition to being applicable to various enzymes, our treatment contains no restraints on the substrate. To verify its applicability to other substrates, we have examined the acylation of 2-benzyl-1,3-propanediol (**4**) (i.e., **1** devoid of both methoxy groups) by vinyl acetate catalyzed by cross-linked crystalline chymotrypsin. Modeling of the *pro-R* and *pro-S* transition states and subsequent calculation of the unsolvated areas of the substrates reveals that, as was the case with **1**, while the 2-methyl-1,3-propanediol fragment is unsolvated in both transition states,

the phenyl group is only protected from the solvent in the *pro-R*. Consequently, the model compounds representing the unsolvated portions of **4** in the *pro-S* and *pro-R* transition states are **3** and **4**, respectively.

Table 2 (last column) lists the γ' ratios for substrate **4** in some of the same solvents used for **1**. Using these γ' ratios, our model predicts that **4** will behave differently than substrate **1** in two respects. First, the γ' ratio varies only 3-fold for **4**, whereas it spans a 12-fold range for **1**. Thus the prochiral selectivity for substrate **4** should be similarly less solvent-sensitive. Second, the γ' ratio for **4** is lower in dioxane than in diisopropyl ether, while the opposite is true for **1**. An analogous inversion in the ranking of these solvents with respect to prochiral selectivity is predicted by equation (7) upon switching from substrate **1** to **4**.

The measured prochiral selectivities of chymotrypsin in the acetylation of **4** are presented in Table 6. As predicted, the solvent effect on selectivity is much smaller for substrate **4** than for **1**, spanning less than 3 fold vs. 22 fold. Also, the predicted inversion of the ranking of dioxane and diisopropyl ether with respect to prochiral selectivity is indeed observed. In further corroboration of equation (7), the double-logarithmic plot of prochiral selectivity vs. γ' ratio (Fig. 4) is linear (with a satisfactory correlation coefficient of 0.92) and has a slope of 0.82.

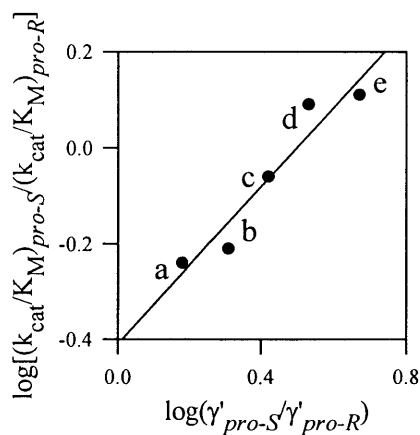


Figure 4. Dependence of the prochiral selectivity of γ -chymotrypsin toward substrate **4** in various organic solvents on the ratio of the activity coefficients of the desolvated portions of the substrate in the *pro-S* and *pro-R* transition states. Solvents: a - dioxane; b - diisopropyl ether; c - *tert*-butyl acetate; d - methyl acetate; e - benzene. See the legend to Fig. 3 for other details.

D. CONCLUDING REMARKS

When crystalline enzymes are used as asymmetric catalysts in anhydrous organic solvents, the solvent dependence of enzymatic prochiral selectivity can be attributed primarily to changes in the relative solvation energies for the *pro-R* and *pro-S* binding modes of the substrate in the transition state. This work presents a quantitative model which satisfactorily predicts the solvent effect on prochiral selectivity solely on the basis of these solvation energies. Thus other factors not considered by the model, e.g. the effect of the solvent on the enzyme or displacement of bound solvent molecules from the active site by the substrate, are deemed relatively unimportant. While this model performs reasonably well with crystalline enzymes, its implementation with respect to amorphous (lyophilized or acetone-precipitated) enzyme powders is not possible due to the ill-defined, reversibly denatured structure of proteins in such dehydrated states. Because no specific assumptions are made regarding the enzyme or the

substrate in the derivation of the equation, the model should be generally applicable. Moreover, our treatment should be similarly applicable to other types of enzymatic selectivity, such as enantioselectivity, chemoselectivity, regioselectivity, and substrate selectivity.

E. MATERIALS AND METHODS

Enzymes. *Rhizomucor miehei* lipase (EC 3.1.1.3) was obtained from Fluka. Subtilisin Carlsberg (alkaline protease from *Bacillus licheniformis*, EC 3.4.21.14) and bovine pancreatic γ - and α - chymotrypsins (EC 3.4.21.1) were purchased from Sigma Chemical Co. Note that the α - and γ - forms of chymotrypsin are covalently identical and interconvertible in a pH-dependent manner, differing primarily in their crystallization properties.²¹ γ -Chymotrypsin crystals were created from the α - form of the enzyme, following the method of Stoddard *et al.* (see the enzyme crystallization section for further details).

Chemicals and solvents. All chemicals and solvents were purchased from Aldrich Chemical Co. The organic solvents were of the highest purity available from that vendor (analytical grade or better) and were dried prior to use to a water content below 0.01% (as determined by the Karl Fischer titration²²) by shaking with Linde's 3-Å molecular sieves.

Dimethyl 2-(3,5-dimethoxybenzyl)malonate was prepared by dissolving 0.12 g (5 mmol) of metallic sodium in 20 mL of dry methanol, followed by addition of 0.6 g (5 mmol) of dimethyl malonate. The solution was cooled to 0 °C, and 0.76 g (4 mmol) of 3,5-dimethoxybenzyl chloride in 20 mL of dry THF was added dropwise over 30 min. The mixture was refluxed overnight under argon, cooled to room temperature, and then 20 mL of cold water was added to quench the reaction. The product was extracted with ethyl acetate and purified by

distillation. The yield of the product was 1.0 g (70% of theor.). $^1\text{H NMR}$ (CDCl_3) δ 6.2-6.3 (3 H, m), δ 3.71 (6 H, s), δ 3.67 (6 H, s), δ 3.64 (1 H, t, $J = 7.4$ Hz), δ 3.11 (2 H, d, $J = 7.4$ Hz).

1 was prepared by dissolving 0.56 g (2 mmol) of dimethyl 2-(3,5-dimethoxybenzyl)-malonate in 10 mL of dry THF, followed by a dropwise addition to 8 mL of a 1.0 M LiAlH_4 solution in ether at 0 °C. The mixture was stirred under argon overnight at room temperature, and then 0.5 mL of water was added to quench the reaction. The product was extracted using ether and, after rotary evaporation, purified by flash column chromatography (3:1 (v/v) ethyl acetate:hexane). The yield of **1** was 0.27 g (60% of theor.). $^1\text{H NMR}$ (CDCl_3) δ 6.2-6.4 (3 H, m), δ 3.76 (2 H, dd, $J = 10.2, 3.9$ Hz), δ 3.73 (6 H, s), δ 3.65 (2 H, dd, $J = 10.2, 6.9$ Hz), δ 2.55 (2 H, d, $J = 7.6$ Hz), δ 2.06 (1 H, m), δ 2.03 (2 H, s). Anal. Calcd for $\text{C}_{12}\text{H}_{18}\text{O}_4$: C, 63.70; H, 8.02; O, 28.28. Found: C, 62.60; H, 8.10; O, 29.63.

2 (a racemate used to calibrate the HPLC instrument) was prepared by dissolving 0.11 g (0.5 mmol) of **1** in 10 mL of dry ether, followed by addition of 0.05 mL of triethylamine at 0 °C and 0.05 mL of acetyl chloride dissolved in 5 mL of dry ether. The reaction was monitored by TLC and quenched by addition of 1 mL of water. The product was extracted with ethyl acetate and, after rotary evaporation, purified by flash column chromatography (1:1 (v/v) ethyl acetate:hexane). The yield was 54 mg (40% of theor.). $^1\text{H NMR}$ (CDCl_3) δ 6.2-6.3 (3 H, m), δ 4.15 (1 H, dd, $J = 12, 4.2$ Hz), δ 4.04 (1 H, dd, $J = 12, 6.4$ Hz), δ 3.73 (6 H, s), δ 3.56 (1 H, dd, $J = 12, 4.2$ Hz), δ 3.47 (1 H, dd, $J = 12, 6.6$ Hz), δ 2.57 (1 H, dd, $J = 13, 7.3$ Hz), δ 2.52 (1 H, dd, $J = 13, 6.6$ Hz), δ 2.1 (1 H, m), δ 2.05 (3 H, s), δ 1.66 (1 H, m). Anal. Calcd for $\text{C}_{14}\text{H}_{20}\text{O}_5$: C, 62.67; H, 7.51; O, 29.82. Found: C, 62.03; H, 7.62; O, 29.92.

4 was prepared by dissolving 0.50 g (2 mmol) of diethyl benzylmalonate in 10 mL of dry THF, and adding this solution dropwise to 8 mL of 1.0 M LiAlH_4 dissolved in ether at 0 °C.

The mixture was stirred under argon overnight at room temperature, and then 0.5 mL of water was added to quench the reaction. The product was extracted using ether and, after rotary evaporation, purified by flash column chromatography (3:1 (v/v) ethyl acetate:hexane). The yield was 0.20 g (60% of theor.). $^1\text{H NMR}$ (CDCl_3) δ 7.1-7.4 (5 H, m), δ 3.85 (2 H, dd, $J = 11$, 3.6 Hz), δ 3.72 (2 H, dd, $J = 11$, 6.7 Hz), δ 2.67 (2 H, d, $J = 7.6$ Hz), δ 2.1 (1 H, m), δ 2.08 (2 H, s). Anal. Calcd for $\text{C}_{10}\text{H}_{14}\text{O}_2$: C, 72.26; H, 8.49; O, 19.25. Found: C, 72.50; H, 8.85; O, 17.77.

5 (a racemate used to calibrate the HPLC instrument) was prepared by dissolving 83 mg (0.5 mmol) of **4** in 10 mL of dry ether, followed by addition of 0.05 mL of triethylamine at 0 °C and 0.05 mL of acetyl chloride dissolved in 5 mL of dry ether. The reaction was followed by TLC and quenched after 20 min with 1 mL of water. The product was extracted with ethyl acetate and purified by flash column chromatography (1:1 (v/v) ethyl acetate:hexane). The yield of **5** was 45 mg (43% of theor.). $^1\text{H NMR}$ (CDCl_3) δ 7.35 (5 H, m), δ 4.28 (1 H, dd, $J = 4.6$, 11.3 Hz), δ 4.18 (1 H, dd, $J = 6.4$, 11.2 Hz), δ 3.70 (1 H, dd, $J = 4.6$, 11.2 Hz), δ 3.60 Hz (1 H, dd, $J = 6.2$, 11.3 Hz), δ 2.77 (1H, dd, $J = 7.8$, 11.5 Hz), δ 2.73 (1 H, dd, $J = 7.8$, 11.5 Hz), δ 2.2 (1 H, m), δ 2.18 (3H, s), δ 1.94 (1H, m). Anal. Calcd for $\text{C}_{12}\text{H}_{16}\text{O}_3$: C, 69.21; H, 7.74; O, 23.05. Found: C, 68.21; H, 7.88; O, 24.01.

Enzymatically prepared (R)-2. In a 20-mL screw-cap scintillation vial, 45 mg (0.2 mmol) of **1** was dissolved in 10 mL of dried diisopropyl ether. Then, 20 mg of cross-linked γ -chymotrypsin crystals (see below) were added to the vial, followed by addition of 20 μl of deionized water and 0.4 mL (10 mmol) of vinyl acetate. The vial was shaken at 45 °C and 300 rpm for 12 hr. The mixture was filtered, and the crystalline enzyme was washed 3 times with 10 mL of diisopropyl ether. The washings were combined with the filtrate, and the subsequent workup of the mixture was the same as described above for the chemically synthesized racemic

2. The yield of **2** ($[\alpha]_D^{28} +20.3^\circ$ (CHCl₃), 82% ee by chiral HPLC) was 36 mg (71% of theor.); determination of its absolute configuration is described below. ¹H NMR (CDCl₃) δ 6.2-6.3 (3 H, m), δ 4.15 (1 H, dd, J = 12, 4.2 Hz), δ 4.04 (1 H, dd, J=12, 6.4 Hz), δ 3.73 (6 H, s), δ 3.56 (1 H, dd, J = 12, 4.2 Hz), δ 3.47 (1 H, dd, J = 12, 6.6 Hz), δ 2.57 (1 H, dd, J = 13, 7.3 Hz), δ 2.52 (1 H, dd, J = 13, 6.6 Hz), δ 2.1(1 H, m), δ 2.05 (3 H, s), δ 1.66 (1 H, m). Anal. Calcd for C₁₄H₂₀O₅: C, 62.67; H, 7.51; O, 29.82. Found: C, 62.03; H, 7.62; O, 29.92.

Enzymatically prepared (R)-5. In a 20-mL screw-cap scintillation vial, 62 mg (0.3 mol) of **4** was dissolved in 10 mL of dry diisopropyl ether. Then 30 mg of lyophilized *R. miehei* lipase powder was added, followed by 0.4 mL (4 mmol) of vinyl acetate. The vial was shaken at 45 °C and 300 rpm for 12 hr. The mixture was filtered, and the enzyme powder was washed 3 times with 10 mL of diisopropyl ether. The washings were combined with the filtrate, and the subsequent workup of the mixture was the same as described above for the chemically synthesized racemic **5**. The yield of (**R**)-**5** was 34 mg (55% of theor.). The observed $[\alpha]_D^{28} +24.4^\circ$ (CHCl₃) (83% ee by chiral HPLC) is in agreement with the value of $[\alpha]_D^{24} +24.2^\circ$ (86% ee) reported by Tsuji *et al.*²³ ¹H NMR (CDCl₃) δ 7.35 (5 H, m), δ 4.28 (1 H, dd, J = 4.6, 11.3 Hz), δ 4.18 (1 H, dd, J = 6.4, 11.2 Hz), δ 3.70 (1 H, dd, J = 4.6, 11.2 Hz), δ 3.60 Hz (1 H, dd, J = 6.2, 11.3 Hz), δ 2.77 (1H, dd, J = 7.8, 11.5 Hz), δ 2.73 (1 H, dd, J = 7.8, 11.5 Hz), δ 2.2 (1 H, m), δ 2.18 (3H, s), δ 1.94 (1H, m). Anal. Calcd for C₁₂H₁₆O₃: C, 69.21; H, 7.74; O, 23.05. Found: C, 68.71; H, 7.88; O, 23.51.

Anthroate derivatives of 2 and (R)-5 were prepared as described by Wiesler and Nakanishi.²⁴ The products were purified by flash column chromatography (1:3 (v/v) ethyl acetate:hexane) and characterized by ¹H NMR (CDCl₃). For the derivative of **2**: δ 8.55 (1 H, s),

δ 8.3 (2 H, m), δ 8.1 (2 H, m), δ 7.5 (4 H, m), δ 6.3 (3 H, m), δ 4.36 (1 H, dd, $J = 4.7, 11.2$ Hz), δ 4.29 (1 H, dd, $J = 6.5, 11.4$ Hz), δ 4.14 (1 H, dd, $J = 4.6, 11.3$ Hz), δ 4.06 (1 H, dd, $J = 6.4, 11.2$ Hz), δ 3.74 (6 H, s), δ 2.57 (1 H, dd, $J = 8.0, 11.6$ Hz), δ 2.54 (1 H, dd, $J = 7.8, 11.4$ Hz), δ 2.1 (1 H, m), δ 2.05 (3 H, s). For the derivative of (**R**)-**5**: δ 8.57 (1 H, s), δ 8.3 (2 H, m), δ 8.0 (2 H, m), δ 7.5 (4 H, m), δ 7.3 (5 H, m), δ 4.51 (1 H, dd, $J = 4.6, 11.3$ Hz), δ 4.40 (1 H, dd, $J = 6.2, 11.3$ Hz), δ 4.28 (1 H, d, $J = 4.6, 11.3$ Hz), δ 4.18 (1 H, dd, $J = 6.5$ Hz, 11.2 Hz), δ 2.78 (1 H, dd, $J = 7.8, 11.5$ Hz), δ 2.72 (1 H, dd, $J = 7.7, 11.5$ Hz), δ 2.2 (1 H, m), δ 2.18 (3 H, s). Both of the derivatives were further purified by HPLC prior to CD spectrum measurement.

Enzyme crystallization. Crystallization of γ -chymotrypsin followed the method described by Stoddard *et al.*²⁵ except that it was scaled up five fold. Crystals typically appeared within 1 week and were harvested after 2-3 weeks. The crystals were transferred from the mother liquor to 1.5-mL microcentrifuge tubes, with some 2 mg of crystals placed in each tube. One mL of cross-linking solution (1.5% (v/v) glutaraldehyde, 17% (w/v) Na₂SO₄, 30 mM sodium cacodylate adjusted to pH 7.5 by 1 M HCl) was added to each tube. After a brief shaking and a 20-min incubation at room temperature, each tube was centrifuged, and the supernate was discarded. The crystals were washed with deionized water (5 times), with 20 mM phosphate buffer, pH 7.8 (5 times), and stored in this buffer for 18 hr at 4 °C before use. Subtilisin Carlsberg was crystallized following the procedure of Niedhart and Petsko.²⁶ Cross-linking of subtilisin was accomplished in the same manner as described above for chymotrypsin. The cross-linked enzyme crystals were washed with water, which was subsequently removed by vacuum filtration prior to placement in organic solvents.

Enzyme lyophilization. γ -Chymotrypsin and *R. miehei* lipase were lyophilized from 5 mg/mL solutions in 20 mM sodium phosphate buffer (pH 7.8 for chymotrypsin, pH 7.0 for lipase). Both enzymes were freeze-dried for at least 24 hr.

Enzyme precipitation. One hundred mg of γ -chymotrypsin was dissolved in 1 mL of 20 mM Na₂HPO₄ solution at 4 °C. The pH was adjusted to 7.8, followed by addition of 10 mL of acetone at 0 °C to precipitate the enzyme. The precipitated protein was incubated at 4 °C for 20 min, centrifuged, washed 3 times with cold acetone, and dried in a vacuum desiccator at 4 °C before use.

Determination of the absolute configuration of 2. The CD chirality²⁷ method was used to determine the absolute configuration at C-2 in the enzymatically prepared **2**. Because **2** has a single chromophore, an additional one was added to facilitate the use of CD. To this end, the free hydroxyl group in **2** was acylated by 9-anthroyl chloride. The absolute configuration of the enzymatically prepared **5** was assigned to be *R* by comparison of optical rotation data with the literature value, and (*R*)-**5** was used as a reference compound for **2**. The CD spectrum of the anthroate derivative of (*R*)-**5** was measured in hexane to validate this method.

The molecular models of the anthroate derivatives²⁸ of (*R*)-**5** and **2** were constructed using the Insight II and Discover programs. The initial structures were energy-minimized using the steepest descent method for 100 iterations, followed by conjugate gradient minimization until the maximum derivative was less than 0.001 kcal/Å. In the low energy conformation of the derivative of (*R*)-**5**, the alignment of the electronic transitions in the two chromophores (¹B_b transition for the anthroate chromophore and CT transition for the benzyl group) shows positive chirality, which stands for positive first and negative second Cotton effects in the CD spectrum. The situation is the same for the derivative of (*R*)-**2** and the opposite for that of (*S*)-**2**.

The CD spectrum of the derivative of (*R*)-**5** features a positive first Cotton effect around 250 nm and a negative second Cotton effect around 210 nm, indicating positive chirality alignment of the two chromophores. This result is consistent with the known absolute configuration of (*R*)-**5**. In the CD spectrum of the derivative of **2**, there is a strong positive first Cotton effect at 252 nm and a negative second Cotton effect at 212 nm, indicating that the absolute configuration of enzymatically prepared **2** is *R*.

Structural modeling. The enzyme crystal structures used were those of γ -chymotrypsin in hexane (Brookhaven entry 1GMD) and subtilisin Carlsberg in acetonitrile²⁹ (Brookhaven entry 1SCB). Because the transition state for the acylation or deacylation of a serine protease is structurally similar to the corresponding tetrahedral intermediate for the reaction,³⁰ transition states were modeled as the tetrahedral intermediates for the reactions. Such models were produced using a two-step procedure. First, potential binding modes of the chiral products were generated by performing molecular dynamics simulations, followed by energy minimization. The carbonyl oxygen of the product was tethered to the oxyanion binding site using a harmonic potential with a force constant selected to allow widely different conformations to be explored, while preventing the product from diffusing too far from the enzyme. Second, each product binding mode thus identified was used as a template for creating an initial model of the tetrahedral intermediate. The low-energy conformation of each of these starting models was found using molecular dynamics simulations and energy minimizations. The lowest-energy conformer of the tetrahedral intermediate was selected as the model of the transition state.

The first step (the product binding mode search) is necessary because the covalently bound tetrahedral intermediate is sufficiently sterically constrained that molecular dynamics simulations do not sample highly different conformations separated by large energetic barriers.

For example, in the case of the *pro-R* transition state for the deacylation of acetyl-chymotrypsin by **1**, an initial tetrahedral intermediate model which starts with the dimethoxyphenyl group bound in the S1 pocket is unable to span the energetic barrier to sample conformations in the S1' binding pocket during molecular dynamics simulation. The product binding mode study identifies both these, as well as other potential starting structures, allowing each of these types of conformations to be examined in the modeling of the tetrahedral intermediate.

Molecular modeling and dynamics simulations were performed with the Insight II and Discover programs³¹ as follows: The initial structures were energy-minimized using the steepest descent method for 50 iterations, followed by conjugate gradient minimization until the maximum derivative was less than 0.001 kcal/Å. The minimized structure was then subjected to 40 ps of molecular dynamics at 900 K with steps of 1 fs. After each simulated ps, the atomic coordinates were saved, resulting in 40 independent structures with different conformations. The resulting structures were then minimized as outlined above, except the minimization proceeded until the maximum derivative was less than 0.0001 kcal/Å. During all minimizations and molecular dynamics simulations, only the atoms of the substrate and those of the catalytic triad's serine were allowed to move, and a cutoff distance of 11 Å was used with the CVFF force field provided with the Discover program. Because solvent molecules and counterions were not included in the simulations, all protein residues were modeled in their un-ionized forms. Of the 40 minimized structures, the lowest energy conformer was selected, and the solvent-accessible surface area was calculated using the Connolly algorithm, as implemented in the Insight software package.

In support of the validity of the structural modeling methods described above, we were able to use this procedure to correctly predict the conformation of *N*-acetyl-L-phenylalanine trifluoromethyl ketone in its hemiketal complex with chymotrypsin.³²

Activity coefficient calculation. All activity coefficients were calculated using the UNIFAC method. Because UNIFAC is a group contribution method, it allows the estimation of activity coefficients in systems for which there is no experimental data by assessing the individual contribution of each group which makes up the system. Use of this method requires three types of parameters for each group in the system: the group's surface area, the volume of the group, and empirically determined parameters which reflect the free energy of interaction between a given group and every other group in the system.

As a test of the accuracy of the UNIFAC calculations, we compared some activity coefficients derived from published vapor-liquid equilibrium (VLE) data to those calculated using UNIFAC. The types of systems for which such data are available are quite limited, but we were able to find VLE data for two compounds (3-methylphenol and 2-methyl-1-propanol) which represent some of the functional groups present in our model molecules in the most nonideal solvent observed in the present work, cyclohexane.³³ Interpreting the VLE data using the Wilson equation of state, for 298 K and a mole fraction of 0.001, the activity coefficients for 3-methylphenol and 2-methyl-1-propanol are 47 and 29, respectively. Under identical conditions, UNIFAC predicts an activity coefficient of 31 for 3-methylphenol, and 21 for 2-methyl-1-propanol. While the individual activity coefficients predicted by UNIFAC are underestimated by about 30%, the activity coefficient ratio (the quantity used in our work) is estimated to within 6%.

Activity coefficients reported in Table 2 include the effects of 100 mM vinyl acetate and 0.2% (v/v) water.

Kinetic measurements. One mL of solvent containing 100 mM vinyl acetate and 10 mM prochiral diol was added to 5 mg of crystals or 15 mg of acetone-precipitated or lyophilized enzyme. Then 0.2% (v/v) water was added to the system to enhance the rate of enzymatic transesterification. In the presence of the dissolved substrates, the amount of added water was soluble in each of the solvents used. The vinyl acetate hydrolysis product, acetic acid, was not detected during any of the reactions studied. Note that any competing hydrolysis would merely reduce the concentration of acetyl-enzyme available for reaction with the prochiral diol, equally reducing the rate of production of both enantiomers of the chiral monoester product, and thus leaving the prochiral selectivity unaffected. The suspensions were shaken at 45 °C and 300 rpm. Periodically, a 10- μ L sample was withdrawn and assayed by chiral HPLC. Because the reactions which lead to the *R* and *S* products take place in the same vial, and compete for the same population of free enzyme, the ratio of the initial velocities of the reactions is equal to $(k_{\text{cat}}/K_{\text{M}})_{\text{pro-S}}/(k_{\text{cat}}/K_{\text{M}})_{\text{pro-R}}$.^{2a,3a} Mass transfer constraints cannot alter the measured initial velocity ratio because both products are generated from the same substrate. Initial velocity ratios were measured two to four times to assure reproducibility. Standard deviations for the ratios were within 13% of the mean values.

Chiral HPLC separations were performed using a Chiralcel OD-H column and a mobile phase of 95:5 (v/v) hexane:2-propanol. A flow rate of 0.8 mL/min separated the enantiomers of **2** with retention times of 29 and 32 min for the *R* and *S* enantiomers, respectively. Chiral resolution of **5** was achieved with a flow rate of 0.5 mL/min, resulting in 30 and 32 min retention

times for the respective *R* and *S* enantiomers. The products were quantified using a UV absorbance detector tuned to 220 nm.

F. REFERENCES AND NOTES

1. (a) Klibanov, A.M. *Trends Biochem. Sci.* **1989**, *14*, 141. (b) Chen, C.-S.; Sih, C. J. *Angew. Chem., Int. Ed. Engl.* **1989**, *28*, 695. (c) Dordick, J.S. *Enzyme Microb. Technol.* **1989**, *11*, 194. (d) Klibanov, A.M. *Acc. Chem. Res.* **1990**, *23*, 114. (e) Gupta, M.N. *Eur. J. Biochem.* **1992**, *203*, 25. (f) Faber, K.; Riva, S. *Synthesis* **1992**, 895. (g) Halling, P.J. *Enzyme Microb. Technol.* **1994**, *16*, 178. (h) Koskinen, A.M.P.; Klibanov, A.M., Eds. *Enzymatic Reactions in Organic Media*; Blakie: London, 1996.
2. For a review, see (a) Wescott, C.R.; Klibanov, A.M. *Biochim. Biophys. Acta* **1994**, *1206*, 1. (b) Carrea, G.; Ottolina, G.; Riva, S. *Trends Biotechnol.* **1995**, *13*, 63.
3. (a) Wescott, C.R.; Klibanov, A.M. *J. Am. Chem. Soc.* **1993**, *115*, 1629. (b) Wescott, C.R.; Klibanov, A.M. *J. Am. Chem. Soc.* **1993**, *115*, 10362.
4. (a) Fredenslund, A.; Gmehling, J.; Rasmussen, P. *Vapor-Liquid Equilibria Using UNIFAC*; Elsevier: New York, 1977. (b) Steen, S.-J.; Bärbel, K.; Gmehling, J.; Rasmussen, P. *Ind. Eng. Chem. Process Des. Dev.* **1979**, *18*, 714. (c) Rasmussen, P.; Fredenslund, A. *Ind. Eng. Chem. Process Des. Dev.* **1982**, *21*, 118. (d) Macedo, E. A.; Weidlich, U.; Gmehling, J.; Rasmussen, P. *Ind. Eng. Chem. Process Des. Dev.* **1983**, *22*, 678. (e) Teigs, D.; Gmehling, J.; Rasmussen, P.; Fredenslund, A. *Ind. Eng. Chem. Res.* **1987**, *26*, 159. (f) Hansen, H. K.; Rasmussen, P.; Schiller, M.; Gmehling, J. *Ind. Eng. Chem. Res.* **1991**, *30*, 2355.

Recently, the use of UNIFAC for estimating thermodynamic activity coefficients has been called into question by van Tol *et al.* (van Tol, J.B.A.; Stevens, R.M.M.; Veldhuizen,

W.J.; Jongejan, J.A.; Duine, J.A. *Biotechnol. Bioeng.* **1995**, *47*, 71.) on the basis of a small number of experiments. However, references (a) through (f) above provide ample validation for UNIFAC for most solutes/solvents examined. Also, van Tol *et al.* used partition coefficients combined with solubility measurements (plagued with problems outlined in ref. 3a) to determine the activity coefficients, while a rigorous treatment requires the use of vapor-liquid equilibrium measurements.³³

5. This hypothesis has been proposed to explain solvent-induced variations in enzymatic selectivity: (a) Wu, H.-S.; Chu, F.-Y.; Wang, K.-T. *Bioorg. Med. Chem. Lett.* **1991**, *1*, 339. (b) Ueji, S.; Fujio, R.; Okubo, N.; Miyazawa, T.; Kurita, S.; Kitadani, M.; Muromatsu, A. *Biotechnol. Lett.* **1992**, *14*, 163.
6. In the present work, this mechanism is selected against through the use of crystalline chymotrypsin and crystalline subtilisin, whose conformations have been shown to be essentially unaffected by replacement of water by organic solvents as the medium. For example, it is reasoned that if the structure of chymotrypsin is nearly the same in water and in hexane, then it also should be the same in other organic solvents because the differences in physicochemical properties among them are less than those between water and hexane.
7. This hypothesis has been proposed to explain solvent-induced variations in enzymatic selectivity: (a) Nakamura, K.; Takebe, Y.; Kitayama, T.; Ohno, A. *Tetrahedron Lett.* **1991**, *32*, 4941. (b) Secundo, F.; Riva, S.; Carrea, G. *Tetrahedron: Asymmetry* **1992**, *3*, 267.
8. It is likely that the active center of the enzyme is occupied by at least a few solvent molecules when a substrate molecule is not bound. These bound solvent molecules would be in a dynamic equilibrium between the enzyme active center and the bulk solvent, described by a binding constant (effectively an inhibition constant, KI). If $1/(KI V_M) \ll [S]/K_M$ (where

VM is the molar volume of the solvent), the bound solvent would exert little effect on the catalytic properties of the system. If, on the other hand, the opposite were true, the solvent would act as an effective inhibitor. If such a tightly bound solvent molecule affects each substrate binding mode equally, it would not influence the prochiral selectivity. If the solvent molecule is tightly bound in such a way that it only hinders one substrate binding mode, the prochiral selectivity would be affected in a manner that could not be predicted by the treatment used in the present work.

9. Each of the steps of the cycle in Scheme 1 is reversible. Single, rather than double, arrows are used in the scheme solely to illustrate the directionality in the definition of the energetic terms.
10. Because the conformations of serine proteases (and most other enzymes) are not altered in the transition state, the solvent-accessible surface of the enzyme is assumed to be the same in ground and transition states. The only difference between E and ES_U^\ddagger is, apart from displacement of the solvent from the active site, the addition of SU, which is unsolvated and thus does not contribute to the solvated surface of the complex.
11. Fersht, A. *Enzyme Structure and Mechanism*, 2nd ed.; Freeman: New York, 1985.
12. The free energy of a solute dissolved in a solvent is described by $G = G^\circ + RT \ln(x\gamma)$.
Because the solvent is the primary variable in our work, the standard state is chosen as the pure liquid solute. Thus G° is independent of the solvent, and the free energy of transfer of the solute from solvent A to B (ΔG_{tr}) is $RT \ln(x_B \gamma_B / x_A \gamma_A)$.
- 13 For dilute solutions, $x_{solute} \approx n_{solute} / n_{solvent} = [solute] VM$, where VM is the molar volume of the solvent which is reciprocal to its molar concentration. For solvents A and B,

$x_A / x_B = [\text{solute}]_{\text{VMA}} / [\text{solute}]_{\text{VMB}}$. If the solute concentration is kept the same in both solvents (i.e., its transfer from A to B is done at constant molar concentration), [solute] cancels out, yielding: $x_A / x_B = V_{\text{MA}} / V_{\text{MB}}$, i.e., the ratio of the molar volumes of the solvents.

14. This reference solvent should not be confused with the standard state of the thermodynamic activity coefficients. It should further be noted that consideration of this constant in terms of a “corrected substrate specificity” will depend on the standard state chosen for the activity coefficients (Janssen, A.E.M.; Halling, P.J. *J. Am. Chem. Soc.* **1994**, *116*, 9827).
15. Such cross-linked enzyme crystals (CLECs) have been employed as robust catalysts in synthetic transformations. (a) St. Clair, N.L.; Navia, M.A. *J. Am. Chem. Soc.* **1992**, *114*, 7314. (b) Sobolov, S.B.; Bartoszko-Malik, A.; Oeschger, T.R.; Montalbano, M.M. *Tetrahedron Lett.* **1994**, *35*, 7751. (c) Persichetti, R.A.; St. Clair, N.L.; Griffith, J.P.; Navia, M.A.; Margolin, A.L. *J. Am. Chem. Soc.* **1995**, *117*, 2732. (d) Lalonde, J.J.; Govardhan, C.; Khalaf, N.; Martinez, A.G.; Visuri, K.; Margolin, A.L. *J. Am. Chem. Soc.* **1995**, *117*, 6845.
16. (a) Yennawar, N.H.; Yennawar, H.P.; Farber, G.K. *Biochemistry* **1994**, *33*, 7326. (b) Yennawar, H.P.; Yennawar, N.H.; Farber, G.K. *J. Am. Chem. Soc.* **1995**, *117*, 577.
17. (a) Zaks, A.; Klivanov, A.M. *J. Biol. Chem.* **1988**, *263*, 3194. (b) Chatterjee, S.; Russell, A. *J. Enzyme Microb. Technol.* **1993**, *15*, 1022.
18. (a) Desai, U.R.; Osterhout, J.J.; Klivanov, A.M. *J. Am. Chem. Soc.* **1994**, *116*, 9420. (b) Desai, U.R.; Klivanov, A.M. *J. Am. Chem. Soc.* **1995**, *117*, 3940.
19. (a) Prestrelski, S.J.; Tedeschi, N.; Arakawa, T.; Carpenter, J.F. *Biophys. J.* **1993**, *65*, 661. (b) Prestrelski, S.J.; Tedeschi, N.; Arakawa, T.; Carpenter, J.F. *Arch. Biochem. Biophys.* **1993**, *303*, 465. (c) Costantino, H.R.; Griebenow, K.; Mishra, P.; Langer, R.; Klivanov, A.M.

-
- Biochim. Biophys. Acta* **1995**, 1253, 69. (d) Griebenow, K.; Klibanov, A.M. *Proc. Natl. Acad. Sci. USA* **1995**, 92, 10969.
20. Whose X-ray crystal structure in an anhydrous solvent was found to be virtually indistinguishable from that in water.
21. Cohen, G.H.; Silverton, W.E.; Davies, D.R. *J. Mol. Biol.* **1981**, 148, 449.
22. Laitinen, H.A.; Harris, W.E. *Chemical Analysis*, 2nd ed.; McGraw-Hill: New York, 1975; pp. 361-363.
23. Tsuji, K.; Terao, Y.; Achiwa, K. *Tetrahedron Lett.* **1989**, 30, 6189.
24. Wiesler, W.T.; Nakanishi, K. *J. Am. Chem. Soc.* **1990**, 112, 5574.
25. Stoddard, B.L.; Bruhnke, J.; Porter, N.; Ringe, D.; Petsko, G.A. *Biochemistry* **1990**, 29, 4871.
26. Neidhart, D. J.; Petsko, G.A. *Protein Eng.* **1988**, 2, 271.
27. Harada, N.; Nakanishi, K. *Circular Dichroic Spectroscopy Excitation Coupling in Organic Stereochemistry*; University Science Books: Mill Valley, CA, 1983.
28. Harada, N.; Ono, H.; Uda, H.; Parveen, M.; Khan, N.U.-D.; Achari, B.; Dutta, K.P. *J. Am. Chem. Soc.* **1992**, 114, 7687.
- 29 (a) Fitzpatrick, P.A.; Steinmetz, A.C.U.; Ringe, D.; Klibanov, A.M. *Proc. Natl. Acad. Sci. USA* **1993**, 90, 8653. (b) Fitzpatrick, P.A.; Ringe, D.; Klibanov, A.M. *Biochem. Biophys. Res. Commun.* **1994**, 198, 675.
30. Warshel, A.; Naray-Szabo, G.; Sussman, F.; Hwang, J.-K. *Biochemistry* **1989**, 28, 3629.
31. Biosym Inc., San Diego, CA.
32. Brady, K.; Wei, A.; Ringe, D.; Abeles, R.H. *Biochemistry*, **1990**, 29, 7600.

-
33. Gmehling, J.; Onken, U.; Weidlich, U. *Vapor-Liquid Equilibrium Data Collection*,
Supplement 2d. DECHEMA: Frankfurt, 1982.

CHAPTER II. INSIGHT INTO THE SOLVENT DEPENDENCE OF CHYMOTRYPTIC PROCHIRAL SELECTIVITY

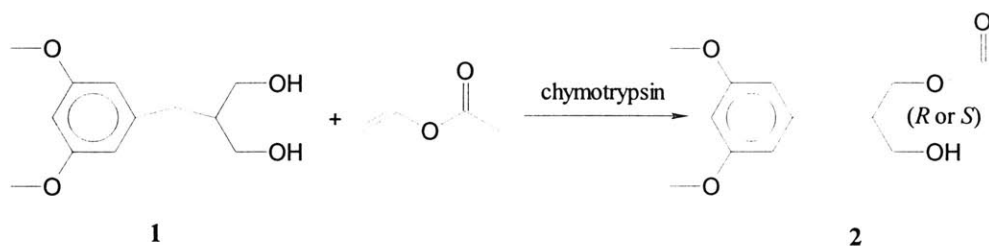
A. INTRODUCTION

Our discovery¹ that enzymatic stereoselectivity is a strong function of the reaction medium is the highlight of nonaqueous enzymology² which promises greater synthetic applications of enzymes³. In particular, prochiral selectivity of enzymes is markedly affected by the solvent.^{4,5} For example, prochiral selectivity of crystalline chymotrypsin in the acylation of 2-(3,5-dimethoxybenzyl)-1,3-propanediol (**1**) with vinyl acetate can be inverted and forced to change more than an order of magnitude merely by varying the solvent under otherwise identical conditions.⁵ We have been able to mechanistically and almost quantitatively account for this effect on the basis of the differential energetics of substrate desolvation in the *pro-R* and *pro-S* enzyme-bound transition states.⁵

That study⁵, however, left several important issues unresolved. Because of the experimental methodology employed, only the $(k_{\text{cat}}/K_{\text{M}})_{\text{pro-R}}/(k_{\text{cat}}/K_{\text{M}})_{\text{pro-S}}$ ratios (i.e., prochiral selectivities⁶), as opposed to the individual $k_{\text{cat}}/K_{\text{M}}$ values for each stereochemical route, were determined as a function of the solvent. Consequently, it is unknown whether the aforementioned solvent dependence of chymotrypsin's prochiral selectivity is mainly due to that of $(k_{\text{cat}}/K_{\text{M}})_{\text{pro-R}}$ or $(k_{\text{cat}}/K_{\text{M}})_{\text{pro-S}}$. Likewise, are the solvent-dependent changes in k_{cat} or in K_{M} the chief contributors to the observed solvent effects? Finally, while intuitively it seems plausible that a solvent-induced enhancement of enzymatic prochiral selectivity would be attained at the expense of lower absolute reactivity, is this really the case? The present study provides answers to all these questions.

B. RESULTS AND DISCUSSION

Scheme 1



The enzymatic transesterification reaction examined herein is depicted in Scheme 1. Crystalline chymotrypsin was selected as a catalyst because its X-ray structure is almost the same in aqueous and nonaqueous solvents⁷ thus allaying concerns about solvent-induced conformational changes and allowing structure-base computer modeling. The progress of the reaction was monitored by chiral HPLC that afforded a facile discrimination between the *R* and *S* monoacetyl products **2**. The initial rates of their formation in various organic solvents were measured as a function of the initial concentration of the prochiral nucleophile **1**, and the data obtained were plotted in double-reciprocal coordinates to determine k_{cat} and K_{M} values for both *pro-R* and *pro-S* reaction pathways. Table 1 lists these parameters, as well as the $k_{\text{cat}}/K_{\text{M}}$ values derived from them and the resultant $(k_{\text{cat}}/K_{\text{M}})_{\text{pro-R}}/(k_{\text{cat}}/K_{\text{M}})_{\text{pro-S}}$ ratios, in 11 organic solvents. Note that the prochiral selectivity values in Table 1 are overall similar to those⁵ obtained in a different way in our earlier study.

We demonstrated previously⁵ that the solvent dependence of prochiral (as well as of some other types, e.g. enantiomeric⁸) selectivity can be described by the following equation:

$$\log[(k_{\text{cat}}/K_{\text{M}})_{\text{pro-R}}/(k_{\text{cat}}/K_{\text{M}})_{\text{pro-S}}] = \log(\gamma'_{\text{pro-R}}/\gamma'_{\text{pro-S}}) + \text{constant} \quad (1)$$

where γ' is the thermodynamic activity coefficient of the desolvated portion of the substrate in

the corresponding enzyme-bound transition state. Figure 1 depicts the dependence of chymotrypsin's prochiral selectivity values from Table 1 on the γ' ratio (calculated by means of molecular modeling and the UNIFAC computer algorithm — see the Experimental Section); the expected linear correlation with a slope of unity is indeed observed. Therefore, having determined the individual kinetic parameters (Table 1), we were now in the position to address the questions outlined in the Introduction.

Even a cursory inspection of the Table 1 data reveals that $(k_{\text{cat}}/K_{\text{M}})_{\text{pro-R}}$ makes a much greater contribution to the solvent dependence of prochiral selectivity than $(k_{\text{cat}}/K_{\text{M}})_{\text{pro-S}}$. For example, upon transition from diisopropyl ether to the solvent on the other extreme in the table, acetonitrile, when prochiral selectivity slumps 32 fold, the enzymatic reactivity in the *pro-R* route also drops 20 fold, whereas that in the *pro-S* rises just 1.6 fold. Moreover, the entire body of the experimental data in Fig. 2 supports this conclusion, where $k_{\text{cat}}/K_{\text{M}}$ values for the *pro-R* and *pro-S* route are separately plotted against the prochiral selectivities in the corresponding solvents. One can see that the absolute value of the slope for the former exceeds that for the latter by a factor of three in double logarithmic coordinates.

These findings can be rationalized on the basis of the molecular modeling results depicted in Figures 3 and 4. Figs. 3A and 4A show **1** covalently bound to the active site of chymotrypsin in the *pro-R* and *pro-S* transition states, respectively. From these, one can identify the desolvated portions of the substrate in both transition states (non-dotted moieties in Figs. 3B and 4B). It is seen that, to the first approximation, what is desolvated in the *pro-S* transition state, is also desolvated in the *pro-R*. However, the 3,5-dimethoxyphenyl moiety, while solvated in the *pro-S* transition state, is desolvated in the *pro-R*. Since the contributions of the identical groups to the $\gamma'_{\text{pro-R}}$ and $\gamma'_{\text{pro-S}}$ in equation (1) approximately cancel out⁹, the solvent dependence

of prochiral selectivity should be dominated by that of the *pro-R* pathway, which is indeed the case (Fig. 2).

Table 1. Individual kinetic parameters for the acylation of **1** catalyzed by crystalline chymotrypsin in various organic solvents ^a

| solvent | stereochemical route | $k_{\text{cat}} \times 10^2$ (hr ⁻¹) | K_M (mM) | $(k_{\text{cat}}/K_M) \times 10^3$ (mM ⁻¹ hr ⁻¹) | $\frac{(k_{\text{cat}}/K_M)_{\text{pro-R}}}{(k_{\text{cat}}/K_M)_{\text{pro-S}}}$ |
|----------------------------|----------------------|---|-------------------|--|---|
| diisopropyl ether | <i>pro-R</i> | 8.1 ± 0.7 | 4.5 ± 1.2 | 18 ± 3 | 16 ± 4 |
| | <i>pro-S</i> | 1.3 ± 0.2 | 12 ± 4 | 1.1 ± 0.1 | |
| dibutyl ether | <i>pro-R</i> | 7.4 ± 0.7 | 7.7 ± 1.6 | 9.6 ± 1.2 | 8.0 ± 1.7 |
| | <i>pro-S</i> | 1.2 ± 0.2 | 9.9 ± 2.9 | 1.2 ± 0.2 | |
| <i>tert</i> -butyl acetate | <i>pro-R</i> | 3.2 ± 0.2 | 11 ± 2 | 2.9 ± 0.2 | 3.1 ± 0.7 |
| | <i>pro-S</i> | 0.97 ± 0.14 | 11 ± 4 | 0.92 ± 0.17 | |
| dioxane | <i>pro-R</i> | 4.1 ± 0.5 | 12 ± 3 | 3.4 ± 0.5 | 2.7 ± 0.7 |
| | <i>pro-S</i> | 1.6 ± 0.2 | 13 ± 3 | 1.3 ± 0.2 | |
| cyclohexane | <i>pro-R</i> | n.d. ^b | n.d. ^b | 5.0 ± 0.7 | 2.6 ± 0.8 |
| | <i>pro-S</i> | n.d. ^b | n.d. ^b | 1.9 ± 0.3 | |
| tetrahydrofuran | <i>pro-R</i> | 2.2 ± 0.3 | 12 ± 4 | 1.9 ± 0.3 | 2.1 ± 0.8 |
| | <i>pro-S</i> | 1.0 ± 0.2 | 11 ± 4 | 0.91 ± 0.19 | |
| <i>para</i> -xylene | <i>pro-R</i> | 1.4 ± 0.4 | 6.5 ± 2.3 | 2.1 ± 0.2 | 1.2 ± 0.3 |
| | <i>pro-S</i> | 1.4 ± 0.5 | 7.8 ± 3.5 | 1.8 ± 0.2 | |
| toluene | <i>pro-R</i> | 0.87 ± 0.07 | 3.7 ± 0.5 | 2.4 ± 0.2 | 1.1 ± 0.1 |
| | <i>pro-S</i> | 0.89 ± 0.10 | 4.1 ± 0.7 | 2.2 ± 0.1 | |

| | | | | | |
|----------------|--------------|-----------|---------|-------------|-------------|
| methyl acetate | <i>pro-R</i> | 15 ± 6 | 51 ± 24 | 2.9 ± 0.5 | 0.93 ± 0.25 |
| | <i>pro-S</i> | 27 ± 14 | 87 ± 52 | 3.1 ± 0.5 | |
| propionitrile | <i>pro-R</i> | 2.7 ± 0.7 | 24 ± 9 | 1.1 ± 0.2 | 0.55 ± 0.17 |
| | <i>pro-S</i> | 3.9 ± 1.0 | 20 ± 7 | 2.0 ± 0.3 | |
| acetonitrile | <i>pro-R</i> | 3.2 ± 0.7 | 35 ± 8 | 0.91 ± 0.07 | 0.50 ± 0.08 |
| | <i>pro-S</i> | 6.0 ± 1.2 | 33 ± 9 | 1.8 ± 0.2 | |

^a The conditions and the way the determinations were carried out are described in the Experimental Section. The errors shown were directly derived from the linear fitting using SigmaPlot. The k_{cat} and K_{M} listed correspond to the catalytic and Michaelis constant, respectively, for **1**.

^b Not determined. The K_{M} values in cyclohexane were much greater than the solubility of **1**; therefore, the individual kinetic constants could not be determined.

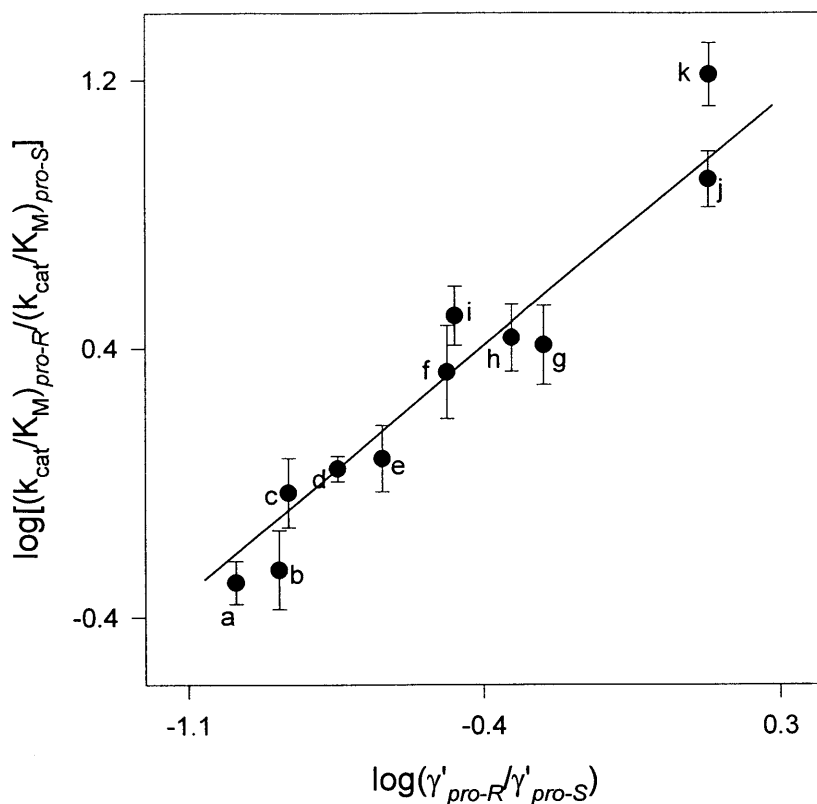


Figure 1. Dependence of the prochiral selectivity of crystalline chymotrypsin in the acylation of **1** (Scheme 1) in various organic solvents on the ratio of the thermodynamic activity coefficients of the desolvated portions of the substrate in the *pro-R* and *pro-S* transition states (equation 1).¹¹ Solvents: a—acetonitrile, b—propionitrile, c—methyl acetate, d—toluene, e—*para*-xylene, f—tetrahydrofuran, g—cyclohexane, h—dioxane, i—*tert*-butyl acetate, j—dibutyl ether, and k—diisopropyl ether. The straight line drawn, with the forced theoretically predicted slope of unity (eq. 1), has a correlation coefficient of 0.89. For conditions and methods, see the Experimental Section.

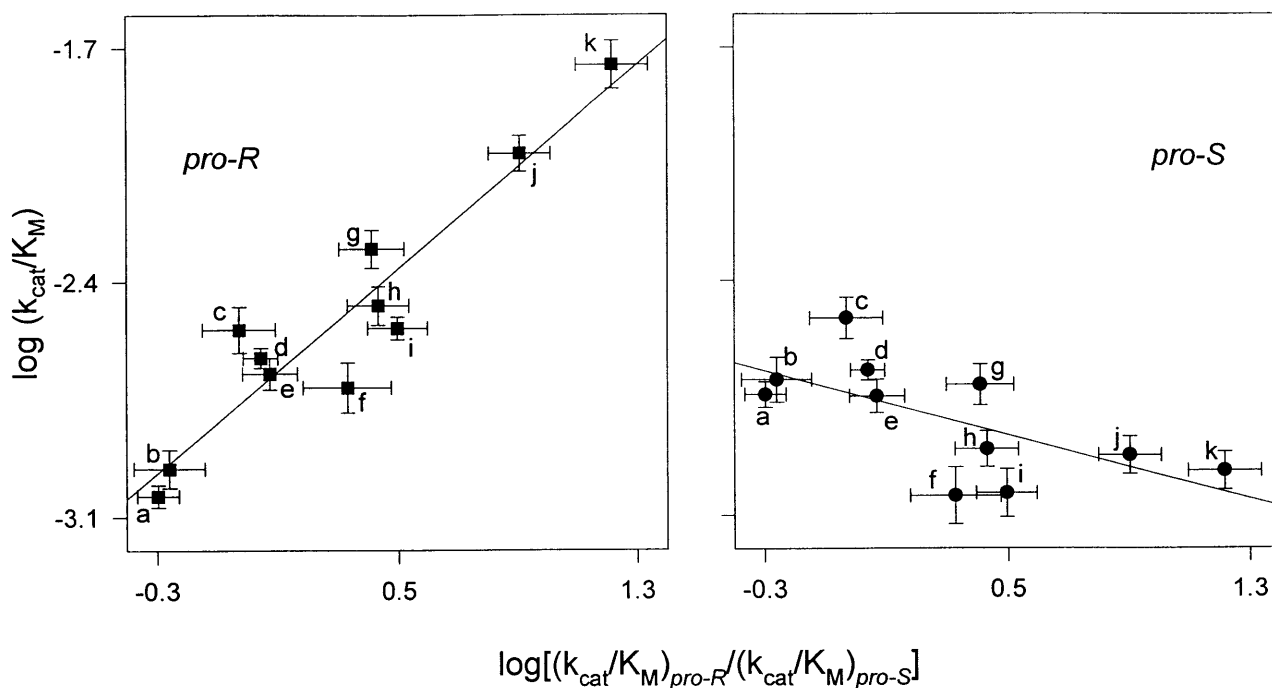


Figure 2. The $(k_{\text{cat}}/K_{\text{M}})_{\text{pro-R}}$ (left) and $(k_{\text{cat}}/K_{\text{M}})_{\text{pro-S}}$ (right) values plotted against the prochiral selectivity of crystalline chymotrypsin in the acylation of **1** (Scheme 1) in various organic solvents.¹¹ Solvents: see the legend to Fig. 1. The straight lines, drawn using linear regression, have slopes of 0.75 and -0.25 for the *pro-R* and *pro-S* stereochemical route, respectively. For conditions and methods, see the Experimental Section.

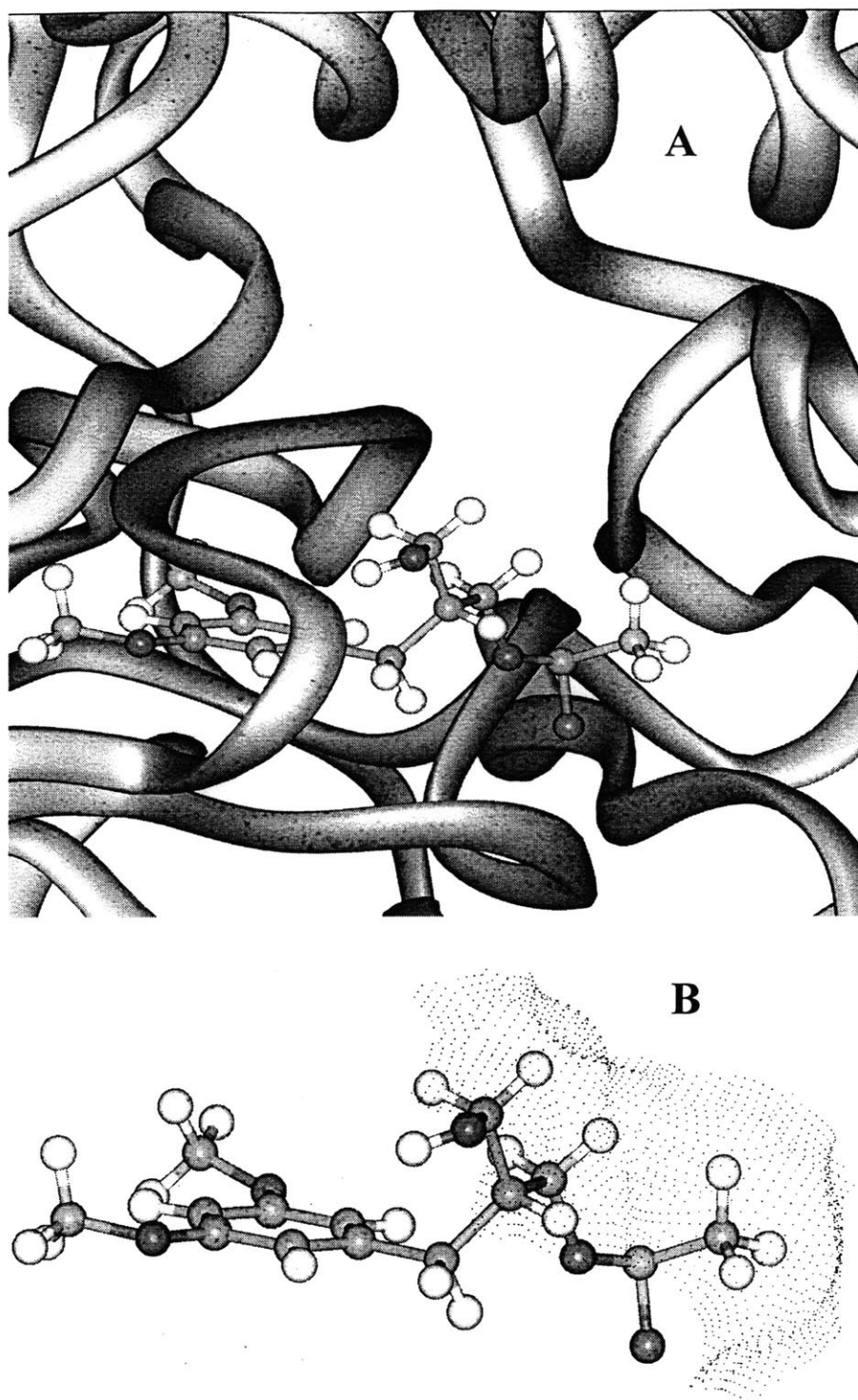


Figure 3. Conformation (A) and solvent-accessible surface area (B) of substrate 1 in the *pro-R* transition state with chymotrypsin. (A) The main chain of chymotrypsin in the active state regions is depicted as a ribbon diagram, and the substrate is represented by a ball-stick model. (B) The dots demarcate the solvent-accessible surfaces calculated using the Connolly method. See the Experimental Section for details.

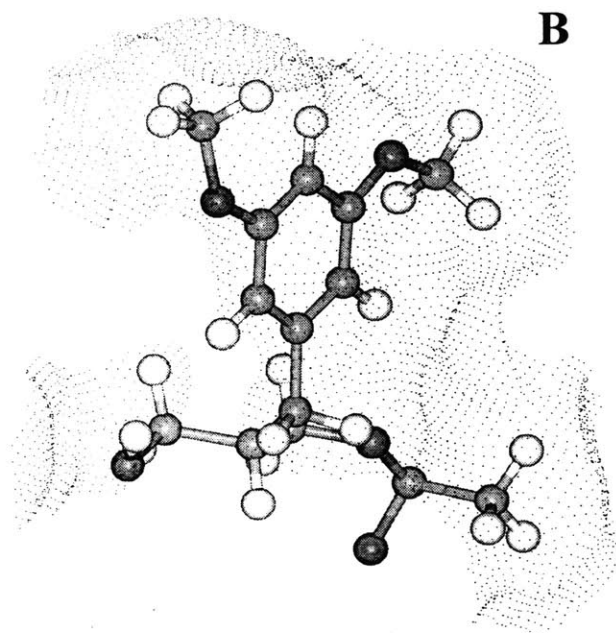
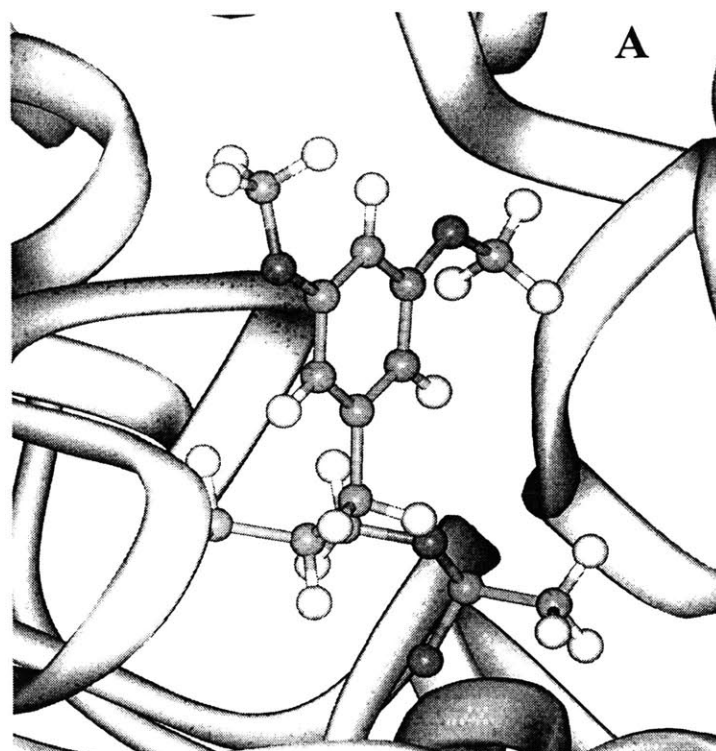


Figure 4. Conformation (A) and solvent-accessible surface area (B) of substrate **1** in the *pro-S* transition state with chymotrypsin. (A) The main chain of chymotrypsin in the active state region is depicted as a ribbon diagram, and the substrate is represented by a ball-stick model. (B) The dots demarcate the solvent-accessible surfaces calculated using the Connolly method. See the Experimental Section for details.

The next question was whether the solvent dependence of $(k_{\text{cat}}/K_{\text{M}})_{\text{pro-R}}$ primarily stems from that of k_{cat} , or K_{M} , or neither. To answer, we plotted the $(k_{\text{cat}}/K_{\text{M}})_{\text{pro-R}}$ values in various solvents against k_{cat} (Fig. 5A) and K_{M} (Fig. 5B) values in the same solvents. One can see that no discernible correlation exists for either parameter. This is presumably because both k_{cat} and K_{M} for enzymatic transesterifications in organic solvents, such as that in Scheme 1, are complex, multicomponent parameters.¹⁰ It is worth noting that a similar lack of correlation was also observed for the solvent dependence of the *pro-S* route (Figs. 5C and 5D).

In the bottom six solvents in Table 1, chymotrypsin's prochiral selectivity is low: neither stereochemical route is favored by more than 2-fold. In contrast, in the top two solvents, the *pro-R* pathway is preferred over the *pro-S* by some order of magnitude. In other words, such a change in the reaction medium converts the enzyme from an essentially nonselective to a very selective catalyst. A question arises whether this metamorphosis occurs at the expense of a reduced chymotryptic activity. To answer it, we plotted the prochiral selectivity in different solvents versus the sum of $k_{\text{cat}}/K_{\text{M}}$ values for *pro-R* and *pro-S* pathways in the same solvents (this sum was used as a measure of the overall enzymatic potency). The resultant graph¹¹ (Fig. 6) reveals not a hint of a systematic decline in enzymatic reactivity as prochiral selectivity undergoes a solvent-induced rise. In fact, the trend seems to be just the opposite, i.e., that the activity and selectivity ascend together. This phenomenon, if general, bodes well for the prospect of making enzymes both more selective and more active by optimizing the solvent.

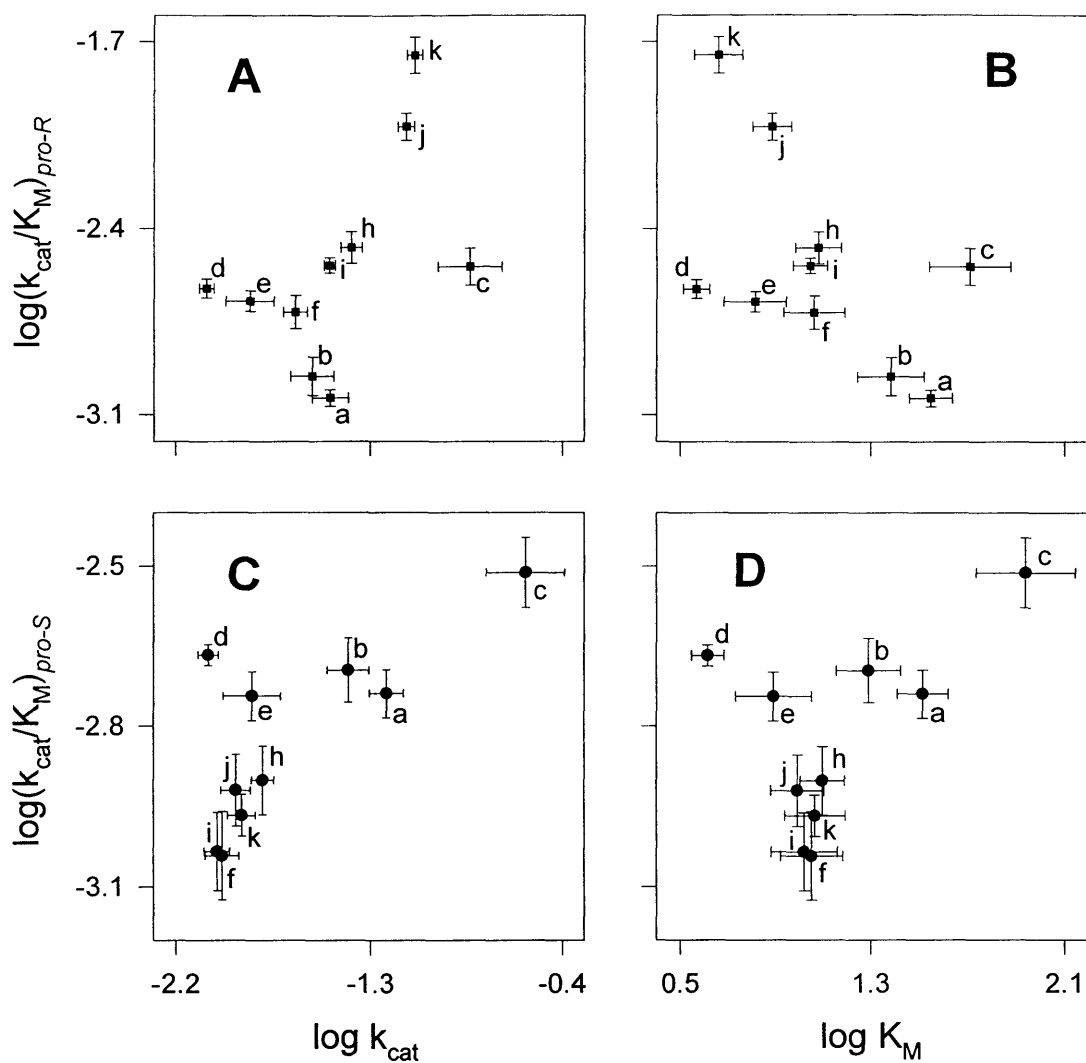


Figure 5. The $(k_{\text{cat}}/K_{\text{M}})_{\text{pro-R}}$ and $(k_{\text{cat}}/K_{\text{M}})_{\text{pro-S}}$ as a function of the individual k_{cat} and K_{M} values for the acylation of **1** (Scheme 1) catalyzed by crystalline chymotrypsin in various organic solvents.¹¹ Solvents: see the legend to Fig. 1, except that cyclohexane (g), where the individual k_{cat} and K_{M} values could not be determined, is missing. For conditions and methods, see the Experimental Section.

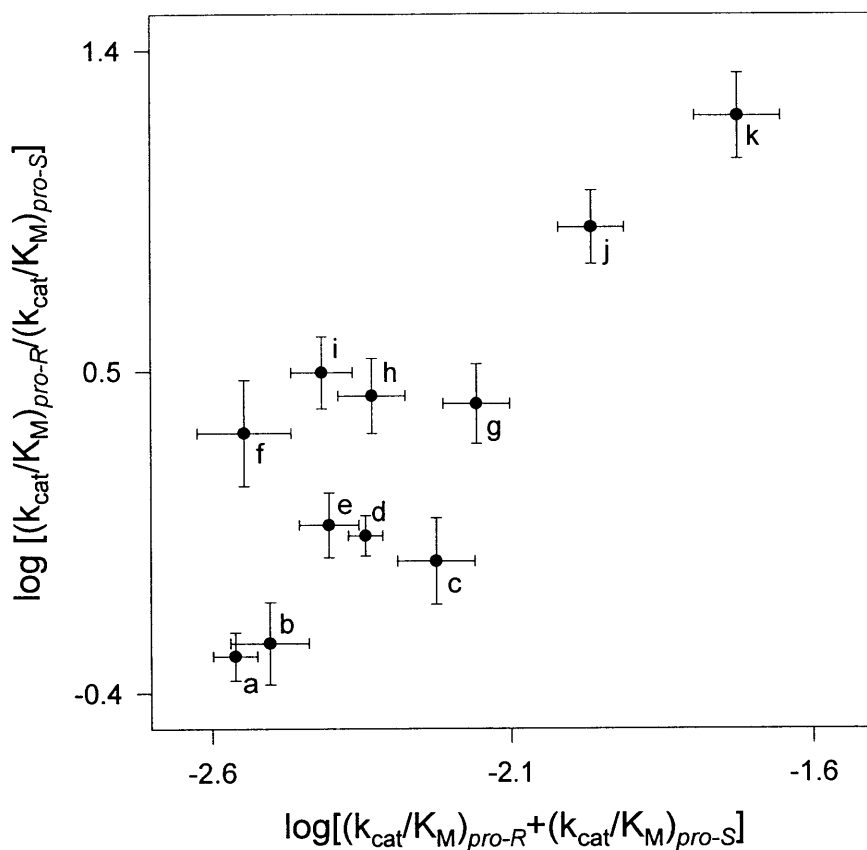


Figure 6. The prochiral selectivity of crystalline chymotrypsin in the acylation of **1** (Scheme 1) in various organic solvents plotted against the sum of the k_{cat}/K_M values for *pro-R* and *pro-S* stereochemical routes. For conditions and methods, see the Experimental Section.

C. EXPERIMENTAL SECTION

Materials. Bovine pancreatic α -chymotrypsin (EC 3.4.21.1), thrice crystallized (Type II), was purchased from Sigma Chemical Co. γ -Chymotrypsin crystals were obtained from the α -form of the enzyme following the method of Stoddard *et al.*¹² For use in organic solvents, the crystals were lightly cross-linked with glutaraldehyde and prepared for catalysis as described previously.⁵ Chemicals were from Aldrich Chemical Co. and were of analytical grade or purer. All organic solvents were purchased from commercial suppliers in the anhydrous state and were of the highest purity available. The prochiral diol **1** and its monoacetylated ester **2** were synthesized using the procedure described previously⁵ and verified by ¹H-NMR.

Kinetic Measurements. One milliliter of a solvent containing 100 mM vinyl acetate and various concentrations of **1** was added to 5 mg of cross-linked enzyme crystals. Then 0.2% (v/v) water was added to the suspension to enhance the rate of enzymatic transesterification.⁵ (In the presence of the dissolved substrates, this amount of added water was soluble in each of the solvents used.) The suspensions were shaken at 30 °C and 300 rpm. Periodically, a 5- μ L sample was withdrawn and assayed by chiral HPLC using a Chiralcel OD-H column (Chiral Technologies, Inc.) and a mobile phase consisting of 95:5 (v/v) hexane:2-propanol at a flow rate of 0.8 mL/min. The chemically synthesized racemic mixture of **2**, eluted with retention times of 29 and 32 min for the *R* and *S* enantiomer, respectively, was used to pre-calibrate the HPLC UV detector tuned to 220 nm.

Kinetic parameters (Table 1) of the chymotrypsin-catalyzed transesterification (Scheme 1) were measured by varying the concentration of the nucleophile, **1**, in the range from 1.6 to 100 mM, depending on the K_M value. Initial rate data were fitted to the Michaelis-Menten equation using the Lineweaver-Burk double reciprocal fit (SigmaPlot, Jandel Scientific). The linear

correlation coefficients, R^2 , obtained in various solvents were as follows (for the *pro-R* and *pro-S* stereochemical route, respectively): diisopropyl ether—0.92, 0.89; dibutyl ether—0.92, 0.95; *tert*-butyl acetate—0.85, 0.97; dioxane—0.93, 0.92; cyclohexane—0.91, 0.89; tetrahydrofuran—0.81, 0.85; *para*-xylene—0.93, 0.94; toluene—0.97, 0.98; methyl acetate—0.93, 0.91; propionitrile—0.88, 0.91; acetonitrile—0.96, 0.97.

Active Site Titration. The percentage of the catalytically competent chymotrypsin molecules in organic solvents (used to calculate $[E]_0$ in the Michaelis-Menten equation) was determined by titrating the active sites in the corresponding solvents with an irreversible serine protease inhibitor, phenylmethylsulfonyl fluoride (PMSF), as described previously.¹³ Cross-linked enzyme crystals (25 mg/mL) were placed in 2 mL of the solvent containing 1 mM PMSF, and the suspension was shaken at 30 °C and 300 rpm. The disappearance of PMSF, as well as any spontaneous hydrolysis product, were monitored by HPLC. Titration of thermoinactivated γ -chymotrypsin under identical conditions was used as the blank reference. Titration in three representative solvents of those listed in Table 1, diisopropyl ether, dioxane, and acetonitrile, done in quadruplicate to avoid random errors, yielded values statistically indistinguishable from each other: $22\pm 6\%$, $16\pm 4\%$, and $21\pm 7\%$, respectively. Given this fact, and that the titration requires a large amount of cross-linked enzyme crystals, the average value of these titration data, $20\pm 5\%$, was used in all k_{cat} and $k_{\text{cat}}/K_{\text{M}}$ calculations presented in Table 1.

Structural Modeling. Molecular models of the *pro-R* and *pro-S* transition states for the enzymatic transesterification in Scheme 1 were produced using the crystal structure of γ -chymotrypsin in hexane (Brookhaven data bank entry 1GMC).⁷ The tetrahedral intermediates in the deacylation step of the enzymatic reaction were selected as the models of the transition state.¹⁴ Such models were produced using the two-step procedure outlined below and described

in detail previously.⁵ First, potential binding modes of each enantiomeric product (*R* or *S* **2**) to the enzyme were generated by performing molecular dynamics simulations, followed by energy minimization. The carbonyl oxygen of the product was tethered to the oxyanion binding site using a harmonic potential with a force constant selected to allow widely different conformations to be explored, while preventing the product from diffusing too far from the enzyme. Second, each product binding mode thus identified was used as a template for creating an initial model of the tetrahedral intermediate. The lowest-energy conformer found thereafter using molecular dynamics simulations and energy minimization was selected as the model of the transition state (Figs. 3A and 4A), from which the solvent-accessible surface (Figs. 3B and 4B) was calculated by the method of Connolly¹⁵.

Activity Coefficient Calculation. All thermodynamic activity coefficients (γ' in equation (1)) were calculated using the UNIFAC method.^{16,5} All such calculations explicitly included the effects of 100 mM vinyl acetate and 0.2% (v/v) water.

D. REFERENCES AND NOTES

- (1) Wescott, C.R.; Klibanov, A.M. *Biochim. Biophys. Acta* **1994**, *1206*, 1-9. Carrea, G.; Ottolina, G.; Riva, S. *Trends Biotechnol.* **1995**, *13*, 63-70.
- (2) Koskinen, A.M.P.; Klibanov, A.M., Eds. *Enzymatic Reactions in Organic Media*; Blackie: London, 1996.
- (3) Poppe, L.; Novak, L. *Selective Biocatalysis*; VCH Publishers: New York, 1992. Wong, C.-H.; Whitesides, G.M. *Enzymes in Synthetic Organic Chemistry*; Pergamon: Oxford, 1994. Drauz, K.; Waldmann, H. *Enzyme Catalysis in Organic Synthesis*; VCH Publishers: New York, 1995. Faber, K. *Biotransformations in Organic Chemistry*; Springer-Verlag: Berlin, 1996.

(4) Hirose, Y., Kariya, K.; Sasaki, I.; Kurono, Y.; Ebiike, H.; Achiwa, K. *Tetrahedron Lett.* **1992**, *33*, 7157-7160. Terradas, F.; Teston-Henry, M.; Fitzpatrick, P.A.; Klibanov, A.M. *J. Am. Chem. Soc.* **1993**, *115*, 390-396. Faber, K.; Ottolina, G.; Riva, S. *Biocatalysis* **1993**, *8*, 91-132.

(5) Ke, T.; Wescott, C.R.; Klibanov, A.M. *J. Am. Chem. Soc.* **1996**, *118*, 3366-3374.

(6) Chen, C.-S.; Fujimoto, Y.; Girdaukas, G.; Sih, C.J. *J. Am. Chem. Soc.* **1982**, *104*, 7294-7299. Straathof, A.J.J.; Jongejan, J.A. *Enzyme Microb. Technol.* **1997**, *21*, 559-571.

(7) Yennawar, N.H.; Yennawar, H.P.; Farber, G.K. *Biochemistry* **1994**, *33*, 7326-7336. Yennawar, H.P.; Yennawar, N.H.; Farber, G.K. *J. Am. Chem. Soc.* **1995**, *117*, 577-585.

(8) Wescott, C.R.; Noritomi, H.; Klibanov, A.M. *J. Am. Chem. Soc.* **1996**, *118*, 10365-10370.

(9) Wescott, C.R.; Klibanov, A.M. *J. Am. Chem. Soc.* **1993**, *115*, 10362-10363.

(10) Chatterjee, S.; Russell, A.J. *Biotechnol. Bioeng.* **1992**, *40*, 1069-1077.

(11) Throughout this paper, we use double-logarithmic coordinates to give equal weight to all experimental points. Given a wide range in which the measured parameters vary (Table 1), linear coordinates would not afford such a possibility.

(12) Stoddard, B.L.; Bruhnke, J.; Porter, N.; Ringe, D.; Petsko, G.A. *Biochemistry* **1990**, *29*, 4871-4876.

(13) Schmitke, J.L.; Wescott, C.R.; Klibanov, A.M. *J. Am. Chem. Soc.* **1996**, *118*, 3360-3365.

(14) Warshel, A.; Naray-Szabo, G.; Sussman, F.; Hwang, J.-K. *Biochemistry* **1989**, *28*, 3629-3637.

(15) Connolly, M.L. *Science* **1983**, *221*, 709-712.

(16) Fredenslund, A.; Gmehling, J.; Rasmussen, P. *Vapor-Liquid Equilibria Using UNIFAC*; Elsevier: New York, 1977. Steen, S.-J.; Bärbel, K.; Gmehling, J.; Rasmussen, P. *Ind. Eng. Chem. Process Des. Dev.* **1979**, *18*, 714-722. Gmehling, J.; Rasmussen, P.; Fredenslund, A. *Ind. Eng. Chem. Process Des. Dev.* **1982**, *21*, 118-127. Macedo, E.A.; Weidlich, U.; Gmehling, J.; Rasmussen, P. *Ind. Eng. Chem. Process Des. Dev.* **1983**, *22*, 676-678. Tiegs, D.; Gmehling, J.; Rasmussen, P.; Fredenslund, A. *Ind. Eng. Chem. Process Des. Dev.* **1987**, *26*, 159-161. Hansen, H.K.; Rasmussen, P.; Schiller, M.; Gmehling, J. *Ind. Eng. Chem. Res.* **1991**, *30*, 2352-2355.

CHAPTER III. COMPUTATIONAL AND EXPERIMENTAL EXAMINATION OF THE EFFECT OF INORGANIC SALTS ON CHYMOTRYPTIC ENANTIOSELECTIVITY IN WATER

A. INTRODUCTION

Applications of enzymes as asymmetric catalysts continue to expand, particularly for the synthesis of chiral pharmaceuticals (Drauz and Waldmann, 1995; Faber, 1996; Zaks and Dodds, 1997). With this trend comes the ever-growing need to manipulate the enantioselectivity of an enzyme in order to optimize the stereochemical outcome of a desired chemical transformation. Since the promise of protein engineering is yet to be fulfilled, the means currently available to achieve this goal (Faber et al., 1993) are basically limited to temperature (Phillips, 1996) and the reaction medium. Concerning the latter, many studies (Jones and Mehes, 1979; Lam et al., 1986; Björkling et al., 1987; Lee et al., 1995; Hansen et al., 1995; Wolff et al., 1997) have explored addition of water-miscible organic cosolvents to alter enzymatic enantioselectivity. Surprisingly, no work has focussed on the effect of another obvious additive, inorganic salts, on enantioselectivity of enzymes (Faber et al., 1993). We have addressed this issue in the present investigation, with a special emphasis on mechanistic aspects.

Conducting enzymatic processes in neat organic solvents, i.e., nonaqueous enzymology (Koskinen and Klivanov, 1996), naturally leads to the question of the solvent dependence of enzymatic enantioselectivity. Indeed, it has been discovered that selectivity, including enantiomeric, of enzymes is greatly influenced by the solvent (Wescott and Klivanov, 1994; Carrea et al., 1995). Moreover, we have been able to almost quantitatively explain this phenomenon on the basis of the differential energetics of substrate enantiomers' desolvation in their enzyme-bound transition states in different solvents (Wescott et al., 1996). Herein we have

extended this thermodynamic analysis to aqueous solutions and, in particular, to those containing high salt concentrations.

B. MATERIALS AND METHODS

Materials

Bovine pancreatic α -chymotrypsin (EC 3.4.21.1), thrice crystallized and lyophilized, was purchased from Sigma Chemical Co. Chemicals were purchased from Aldrich Chemical Co. and were of analytical grade or better. Tropic acid methyl ester was synthesized using the procedure described by Wescott et al. (1996), and its structure was verified by $^1\text{H-NMR}$.

Kinetic Measurements

To 10 ml of an aqueous solution, containing 10 mM Tris·HCl, 10 mM racemic tropic acid methyl ester (substrate), and a 1.5 M inorganic salt (if any), α -chymotrypsin (5 mg/ml) was added at 30 °C, and the pH was adjusted to 7.2 to initiate the reaction. Periodically, a 0.8-ml aliquot was withdrawn, acidified by 0.2 ml of 3 M HCl, and extracted with 0.2 ml of ethyl acetate. After a brief centrifugation, 5 μl of the upper (ethyl acetate) layer was withdrawn and injected into a chiral HPLC column (see below) for analysis. For each enzymatic reaction studied, a blank reaction under identical condition but without enzyme was carried out, and the spontaneous hydrolysis rate for each enantiomer of the substrate was deducted from the overall initial rate to obtain the enzymatic initial rate. Because the hydrolysis leading to the *R* and *S* products takes place in the same reaction mixture and the substrate enantiomers compete for the same population of the free enzyme, the ratio of the enzymatic initial rates for the enantiomers equals $(k_{\text{cat}}/K_{\text{M}})_R / (k_{\text{cat}}/K_{\text{M}})_S$, i.e., the enantioselectivity *E* (Wescott and Klibanov, 1993a).

At least four time points were taken during the initial (below 20% of total) conversion for each enantiomer, and the error of measurements was estimated by linear regression.

Chiral HPLC separation of the product, tropic acid, was performed using a Chiralcel OD-H column (Chiral Technology) and a mobile phase consisting of 96:4:0.1 (v/v/v) hexane:2-propanol:trifluoroacetic acid. At a flow rate of 0.9 ml/min, the *R* and *S* enantiomers of tropic acid were separated with retention times of 23 and 29 min, respectively. They were quantified using UV absorbance at 250 nm.

Spectroscopic Studies

The intrinsic fluorescence emission of protein tryptophan residues was measured using a FluoroMax-2 spectrofluorometer (SPEX Industries) equipped with a temperature-controlled sample holder in which a quartz cell with a 10-mm path length was placed. The instrument was operated in the ratio-recording mode in order to correct for all fluctuations of the exciting light. The excitation wavelength was 295 nm, and emission spectra were recorded in the 300-400 nm range. The slit widths were 2 and 3 nm for excitation and emission beams, respectively.

Absorbance spectra were recorded in the 250-310 nm range using a Hitachi U-3110 spectrophotometer equipped with a temperature-controlled sample holder in which a quartz cell with a 10-mm path length was placed. The internal instrument software was used to obtain the second derivative of the absorbance spectra.

All spectral measurements were done at 30 °C, and the enzyme concentration was 0.03 and 0.16 mg/ml in fluorescence and absorbance measurements, respectively. The spectrum of the corresponding aqueous buffer solution was always subtracted from that in the presence of the enzyme.

Structural Modeling

Models of the tetrahedral reaction intermediates were adopted from our previous study (Wescott et al., 1996) using the crystal structure of γ -chymotrypsin (Brookhaven data bank entry 1GMC) (Yennawar et al., 1994). Since γ -chymotrypsin's active site structure is essentially identical to that of α -chymotrypsin (Steitz et al., 1969; Cohen et al., 1981), the models were applied to the hydrolysis of tropic acid methyl ester catalyzed by α -chymotrypsin in aqueous solution without modification. Because the transition state for the acylation of a serine protease is structurally similar to the corresponding tetrahedral intermediate (Warshel et al., 1989), the latter was used by us as the model. Such models were produced using the two-step procedure outlined below and described in detail previously (Wescott et al., 1996; Ke et al., 1996).

First, potential binding modes of each enantiomer of the substrate were generated by performing molecular dynamics simulations, followed by energy minimization. The carbonyl oxygen of the substrate was tethered to the oxyanion binding site using a harmonic potential with a force constant selected to allow widely different conformations to be explored, while preventing the substrate from diffusing too far from the enzyme. This substrate binding mode search is necessary because the covalently bound tetrahedral intermediate is sufficiently sterically constrained that molecular dynamics simulations do not sample highly different conformations separated by large energetic barriers. For the second step, each substrate binding mode thus identified was used as a template for creating an initial model of the tetrahedral intermediate. The low-energy conformation of each of these starting models was found using molecular dynamics simulations and energy minimization. The lowest-energy conformer of the tetrahedral intermediate was selected as the model of the transition state. The solvent-accessible surface areas were calculated by the method of Connolly (1983) for each group of the substrate, and the percentage of desolvation was calculated. The groups with percentage of desolvation

above 50% were approximated as completely desolvated; all others were considered completely solvated (Wescott et al., 1996). Only the desolvated portions of the substrate were taken into account (Ke et al., 1996; Wescott et al., 1996), and their activity coefficients were calculated using the UNIFAC method (see below).

Examination of the molecular models for the *R* and *S* transition states for the acylation of chymotrypsin by tropic acid methyl ester reveals distinct binding patterns for the enantiomers (Wescott et al., 1996). In the *R* transition state, the phenyl group of the substrate is buried in chymotrypsin's S1 binding pocket, while the hydroxyl group is oriented toward the solvent. In contrast, in the *S* transition state, the hydroxyl group is buried in the S1 binding pocket, whereas the phenyl group extends away from the enzyme toward the solvent. Thereafter, the percentage of desolvation for every group was calculated for both *R* and *S* transition state models. Using the 50% threshold rule mentioned above, 1 aryl C, 4 aryl CH, 1 carbonyl, and 1 methine were considered desolvated in the *R* transition state, while 1 hydroxyl, 1 aryl C, 3 aryl CH, 1 carbonyl, and 1 methine were considered desolvated in the *S* transition state.

Activity Coefficient Calculations

All thermodynamics activity coefficients (γ') were calculated using the UNIFAC group contribution method (Fredenslund et al., 1977). This method requires three types of parameters for each group in the system: the group's surface area, its volume, and empirically determined parameters which reflect the free energy of interaction between a given group and every other group in the system. In the calculation of γ' values with no salt added, all desolvated groups in *R* and *S* transition states were included in the model, and the original UNIFAC parameter set (Hansen et al., 1991) was used to allow direct comparison with the organic solvent values.

For the system with added 1.5 M inorganic salts, a modified UNIFAC parameter set had to be used (Archard et al., 1994) to take into account the salt effect on the activity coefficient of the desolvated portion of substrate. Since (i) some parameters of the desolvated groups shown above were missing in this parameter set, and (ii) the effect of common groups would approximately cancel out in the calculation of the γ' ratio, an additional approximation was made that only the desolvated groups different between the *R* and *S* transition states were included in the model (Wescott and Klibanov, 1993b). Therefore, only 1 aryl CH group was included for the *R* transition state model and 1 hydroxyl group for the *S* transition state model, while the common groups (1 aryl C, 3 aryl CH, 1 carbonyl, and 1 methine) were excluded. Under this approximation, the activity coefficient ratio γ'_R/γ'_S for water (no inorganic salts) was re-calculated using the modified UNIFAC parameter set (Archard et al., 1994). Although the absolute value of $(\gamma'_R/\gamma'_S)_{\text{H}_2\text{O}}$ (1.14) differed from the that obtained using the original UNIFAC parameter set (15.4), only the former value was used in the $(\gamma'_R/\gamma'_S)_{\text{salt}} / (\gamma'_R/\gamma'_S)_{\text{H}_2\text{O}}$ ratio to predict salt-induced changes in enantioselectivity; thus the discrepancy in the reference state (H_2O) should have no effect.

C. RESULTS AND DISCUSSION

Our thermodynamic rationale, mentioned in the Introduction, is based on the explicit assumption that the differences in the desolvation energetics of substrate enantiomers upon formation of their enzyme-bound transition states is the dominant factor in the solvent dependence of enzymatic enantioselectivity (Ke et al., 1996; Wescott et al., 1996). If so, our treatment predicts that enzymatic enantioselectivity *E* (the ratio of $k_{\text{cat}} / K_{\text{M}}$ values for the individual enantiomers (Chen et al., 1982; Straathof and Jongejan, 1997)) should be proportional

to the ratio of the thermodynamic activity coefficients γ' of the desolvated portions of the substrate enantiomers in the relevant transition states (Ke et al., 1996; Wescott et al., 1996):

$$\log E = \log(\gamma'_R / \gamma'_S) + \text{constant} \quad (1)$$

where the subscripts R and S refer to the corresponding enantiomers, and *constant* contains kinetics and thermodynamic terms in a separate, arbitrarily selected, reference reaction medium. The γ'_R/γ'_S ratio in a given solvent can be calculated, as described in the Methods, by (i) determining the desolvated portions of the substrate in the enzyme-bound R and S transition states using molecular modeling based on the crystal structure of the enzyme and (ii) then calculating the thermodynamic activity coefficients of these desolvated portions using the UNIFAC algorithm.

We experimentally examined the enantioselectivity of α -chymotrypsin in the hydrolysis of the methyl ester of tropic (3-hydroxy-2-phenylpropionic) acid, whose various esters are potent anticholinergics (Reynolds, 1982). Kinetic analysis of the enzymatic hydrolysis of the racemic ester in 10 mM aqueous Tris-HCl buffer, pH 7.2, at 30 °C, monitored by chiral HPLC, revealed that the R enantiomer was much more reactive than its S counterpart, with an E value of 31 ± 1 .

Previously, we investigated the enantioselectivity of the transesterification of tropic acid methyl ester with propanol catalyzed by crystalline chymotrypsin suspended in various organic solvents (Wescott et al., 1996). The E values obtained were plotted against the calculated γ'_R/γ'_S ratios, and a linear dependence with a slope of unity predicted by equation (1) indeed ensued. Now, we have expanded the list of solvents to include water, and the resultant broader correlation obtained is depicted in Figure 1. One can see that the aqueous enantioselectivity value (closed circle) fits in with the nonaqueous ones (open circles) with a good correlation coefficient of 0.95. In other words, equation (1) has now been validated, for the first time, for

aqueous, as well as nonaqueous, reaction media. Note that the linear correlation is observed over more than a 400-fold range of E values.

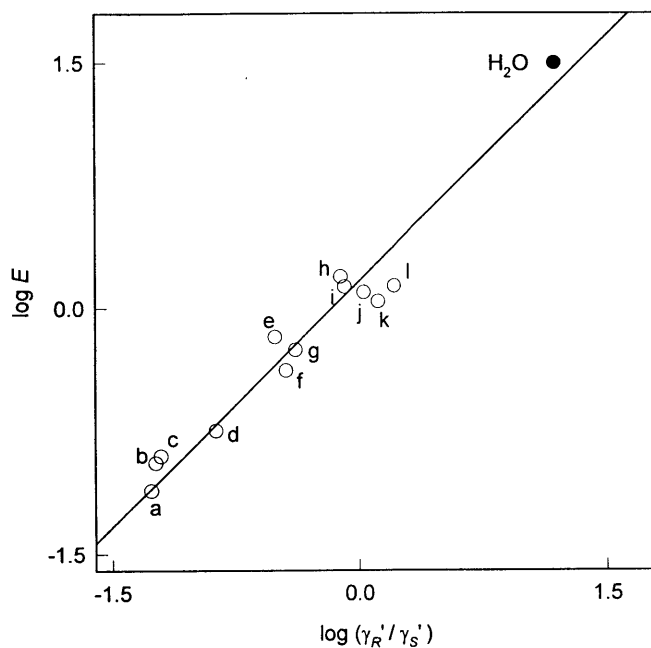


Figure 1. Dependence of enantioselectivity of α -chymotrypsin in the hydrolysis of tropic acid methyl ester in water (solid circle) and in the transesterification of this ester with propanol in various organic solvents (open circles; the data are adopted from Wescott et al., 1996) on the calculated γ' ratio. E is defined as $(k_{\text{cat}} / K_{\text{M}})_R / (k_{\text{cat}} / K_{\text{M}})_S$; γ' is the thermodynamic activity coefficient of the desolvated portion of the R or S enzyme-bound transition state. The slope of the line is forced to be unity, as required by equation (1); the resultant correlation coefficient is 0.95. The nonaqueous solvents were as follows: a — cyclohexane, b — octane, c — hexane, d — toluene, e — *tert*-butyl acetate, f — isopropyl acetate, g — tetrahydrofuran, h — acetone, i — dioxane, j — *tert*-amyl alcohol, k — *tert*-butyl alcohol and l — propanol.

The E values in Fig. 1 are also instructive in another respect. It is sometimes debated whether enzymes are more enantioselective in water or in organic solvents (e.g., see Chen and Sih, 1989). However, this question is a bit misplaced, because there is no such thing as enzymatic “enantioselectivity in organic solvents”, only that in a given organic solvent. For example, while in water chymotrypsin prefers the R over the S enantiomer of tropic acid methyl

ester by a factor of 31, in cyclohexane it prefers the *S* enantiomer over the *R* by a factor of 13 (Fig. 1). In other words, the enzyme is very enantioselective in both the aqueous and the organic solvent, albeit in the opposite manner. On the other hand, in such nonaqueous solvents as *tert*-butyl acetate and *tert*-butyl alcohol, chymotrypsin exhibits but a meager enantioselectivity with the same substrate (Fig. 1). Hence the correct view is that all different solvents, whether aqueous or nonaqueous, give rise to distinct enantioselectivities (and that difference between two organic solvents may be greater than between one of them and water).

Over the last decade, a methodology has been developed to calculate activity coefficients by UNIFAC not only in water but also in aqueous solutions of certain inorganic salts (Kikic et al., 1991; Achard et al., 1994). Therefore, one can test whether equation (1) is applicable to enzymatic enantioselectivities in such salt solutions, i.e., whether our thermodynamic model can account for salt effects on enantioselectivity. Subtracting equation (1) written for water from that written for an aqueous salt solution and making straightforward rearrangements, one obtains

$$\frac{E_{\text{salt}}}{E_{\text{H}_2\text{O}}} = \frac{(\gamma'_R/\gamma'_S)_{\text{salt}}}{(\gamma'_R/\gamma'_S)_{\text{H}_2\text{O}}} \quad (2)$$

where the subscripts refer to the medium, either water (slightly buffered) or salt (its aqueous solution), in which the given parameter is measured/calculated. If equation (2) is valid, then it follows that, as in different organic solvents, the distinct energetics of substrate desolvation are the principal factor by which the different salts influence enzymatic enantioselectivity in aqueous solution.

Table I. The calculated ratios of the thermodynamic activity coefficients (γ') for the desolvated portions of the *R* and *S* enantiomers of tropic acid methyl ester in their chymotrypsin-catalyzed hydrolysis transition states. Also presented are enantioselectivity ratios calculated from equation (2).^a

| Salt | γ'_R/γ'_S | $(\gamma'_R/\gamma'_S)_{\text{salt}} / (\gamma'_R/\gamma'_S)_{\text{H}_2\text{O}} = E_{\text{salt}} / E_{\text{H}_2\text{O}}$ |
|-----------------------------------|-----------------------|---|
| None | 1.14 | 1.00 |
| KBr | 1.05 | 0.921 |
| SrBr ₂ | 1.06 | 0.929 |
| KCl | 1.06 | 0.930 |
| SrCl ₂ | 1.07 | 0.939 |
| NaCl | 1.10 | 0.965 |
| NaBr | 1.10 | 0.965 |
| MgBr ₂ | 1.13 | 0.991 |
| NaF | 1.13 | 0.995 |
| KF | 1.14 | 1.00 |
| KNO ₃ | 1.14 | 1.00 |
| MgCl ₂ | 1.14 | 1.00 |
| NH ₄ Cl | 1.16 | 1.02 |
| NH ₄ Br | 1.16 | 1.02 |
| BaCl ₂ | 1.17 | 1.03 |
| BaBr ₂ | 1.17 | 1.03 |
| NaNO ₃ | 1.19 | 1.04 |
| LiCl | 1.19 | 1.04 |
| LiBr | 1.19 | 1.04 |
| CaBr ₂ | 1.19 | 1.04 |
| NH ₄ F | 1.20 | 1.05 |
| CaCl ₂ | 1.20 | 1.05 |
| Sr(NO ₃) ₂ | 1.22 | 1.07 |
| NH ₄ NO ₃ | 1.24 | 1.09 |

| | | |
|---|------|------|
| LiNO ₃ | 1.28 | 1.12 |
| Mg(NO ₃) ₂ | 1.33 | 1.17 |
| Ba(NO ₃) ₂ | 1.34 | 1.18 |
| K ₂ SO ₄ | 1.36 | 1.19 |
| Ca(NO ₃) ₂ | 1.39 | 1.22 |
| Na ₂ SO ₄ | 1.48 | 1.30 |
| MgSO ₄ | 1.53 | 1.34 |
| (NH ₄) ₂ SO ₄ | 1.59 | 1.39 |
| Li ₂ SO ₄ | 1.73 | 1.52 |

^a For details, see text. Note that those salts that are insoluble or only sparingly soluble in water have been excluded from the table because a 1.5 M solubility is unattainable for them.

Table I presents the γ'_R/γ'_S values calculated by us for the transition states of the chymotrypsin-catalyzed hydrolysis of tropic acid methyl ester in 1.5 M aqueous solutions of all salts for which the interaction parameters are available in the literature. Also listed are the calculated $(\gamma'_R/\gamma'_S)_{\text{salt}}/(\gamma'_R/\gamma'_S)_{\text{H}_2\text{O}}$ ratios, which equal the $E_{\text{salt}}/E_{\text{H}_2\text{O}}$ values for the enzymatic hydrolysis predicted by equation (2). Inspection of the table reveals that the salt-induced changes in enantioselectivity *due to the differential desolvation energetics* should be small, never exceeding some 50%.

In order to test these predictions experimentally, we selected one salt [(NH₄)₂SO₄] from the bottom of the Table I and another (KCl) from the top and measured chymotrypsin's enantioselectivity in their 1.5 M aqueous solutions. It is seen in Table II that the E value in KCl is indeed close to that in water. However, the E value in (NH₄)₂SO₄ was found to be almost 3 *times lower* than in water, while equation (2) predicts that it should be 39% *higher* than in water (Table I).

To ensure that the determined E value in the $(\text{NH}_4)_2\text{SO}_4$ solution is not an aberration, we measured the enantioselectivity in yet another salt solution, Na_2SO_4 , for which Table I predicts a 30% higher E than in water. Once again, the value obtained was very different both in the direction of the change and in its magnitude — some 3 fold lower than in water (Table II).

Table II. Enantioselectivity values E for chymotrypsin-catalyzed hydrolysis of tropic acid methyl ester in water and in 1.5 M aqueous solutions of several inorganic salts.^a

| Salt | E |
|------------------------------|------------|
| None | 31 ± 1 |
| $(\text{NH}_4)_2\text{SO}_4$ | 11 ± 1 |
| KCl | 26 ± 2 |
| Na_2SO_4 | 12 ± 1 |

^a For experimental conditions, see Methods. E is defined as $(k_{\text{cat}} / K_{\text{M}})_R / (k_{\text{cat}} / K_{\text{M}})_S$.

That equation (2) fails to correctly predict the E values in aqueous solutions of at least two salts indicates that the some 3-fold drop in chymotryptic enantioselectivity brought about by $(\text{NH}_4)_2\text{SO}_4$ and Na_2SO_4 must be due to a factor other than the energetics of substrate desolvation which thus, in contrast to Fig. 1, is not the main player with aqueous salt solutions (as it was not with water-miscible cosolvents (Luque et al., 1998)). The most likely candidate for such a factor appears to be a conformational change in the chymotrypsin molecule induced by a sulfate ion.

We tested this hypothesis by examining the fluorescence spectra of chymotrypsin dissolved in an aqueous buffer and in 1.5 M aqueous solutions of either $(\text{NH}_4)_2\text{SO}_4$ or KCl. One can see in Fig. 2A that there is no significant shift in the wavelength of maximal emittance among the three spectra, and, in fact, the fluorescence spectra in two salt solutions are nearly identical. We addressed the same issue using a different spectroscopy, UV absorbance, and, as

seen in Fig. 2B, once again, no significant spectral changes were observed. To increase the sensitivity, we also recorded second-derivative UV absorbance spectra (data not shown), and, as in case of other methods, no significant spectral changes were detected. Therefore we conclude that if $(\text{NH}_4)_2\text{SO}_4$ alters chymotryptic enantioselectivity (Table II) by changing the enzyme conformation, this change must be quite subtle (and thus not detectable by the spectroscopic techniques used by us). An alternative possibility is that the sulfate ion binds to the enzyme in the vicinity of its active site and unequally affects the energetics of the *R* and *S* transition states.

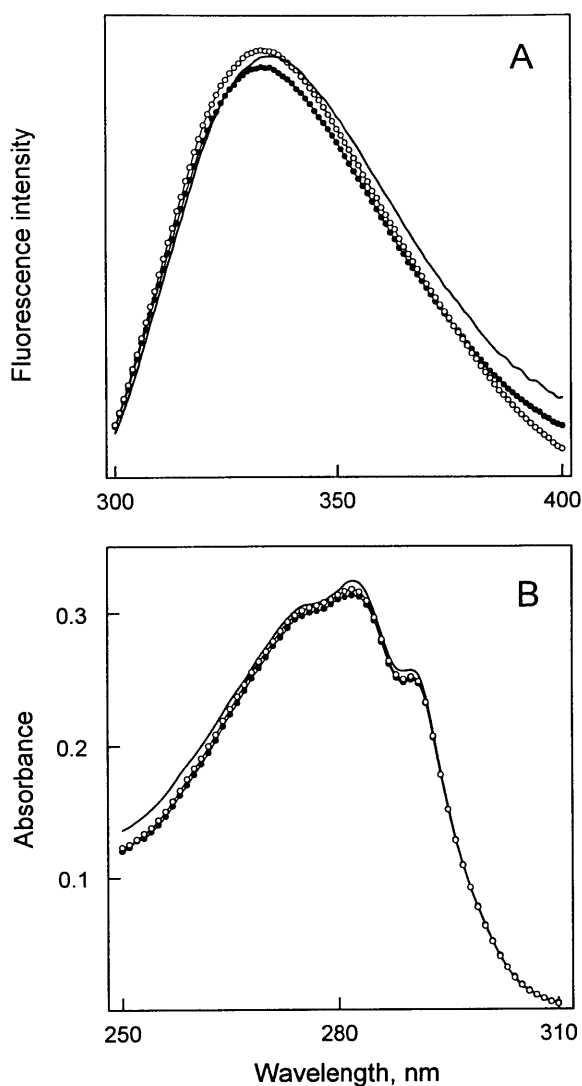


Figure 2. Fluorescence (A) and absorbance (B) spectra of α -chymotrypsin in: 10 mM Tris•HCl aqueous buffer, pH 7.2 (---), the same buffer containing 1.5 M KCl (-○-) or 1.5 M (NH₄)₂SO₄ (-●-). Fluorescence intensity is given in arbitrary units. The excitation wavelength for the fluorescence spectra was 295 nm. All measurements were done at 30 °C. Enzyme concentrations were 0.03 and 0.16 mg/ml for fluorescence and absorbance spectra, respectively. The spectrum of the blank buffer solution was always subtracted from that containing the enzyme. For other details, see Materials and Methods.

D. REFERENCES

- Achard, C., Dussap, C.G., Gros, J.B. 1994. Representation of vapour-liquid equilibria in water-alcohol-electrolyte mixtures with a modified UNIFAC group-contribution method. *Fluid Phase Equilibria* **98**: 71-89.
- Björkling, F., Boutelje, J., Hjalmarsson, M., Hult, K., Norin, T. 1987. Highly enantioselective route to *R*-proline derivative via enzyme catalyzed hydrolysis of *cis-N*-benzyl-2,5-bismethoxycarbonylpyrrolidine in an aqueous dimethylsulphoxide medium. *J. Chem. Soc., Chem. Commun.* 1041-1042.
- Carrea, G., Ottolina, G., Riva, S. 1995. Role of solvents in the control of enzyme selectivity in organic media. *Trends Biotechnol.* **13**: 63-70.
- Chen, C.-S., Fujimoto, Y., Girdaukas, G., Sih, C.J. 1982. Quantitative analyses of biochemical kinetic resolutions of enantiomers. *J. Am. Chem. Soc.* **104**: 7294-7299.
- Chen, C.-S., Sih, C.J. 1989. General aspects and optimization of enantioselective biocatalysis in organic solvents: the use of lipases. *Angew. Chem. Int. Ed. Engl.* **28**: 695-707.
- Cohen, G.H., Silverton, E.W., Davies, D.R. 1981. Refined crystal structure of γ -chymotrypsin at 1.9 Å resolution. *J. Mol. Biol.* **148**: 449-479.
- Connolly, M.L. 1983. Solvent-accessible surfaces of proteins and nucleic acids. *Science* **221**: 709-713.
- Drauz, K., Waldmann, H. 1995. *Enzyme Catalysis in Organic Synthesis*, VCH Publishers, New York.
- Faber, K. 1996. *Biotransformations in Organic Chemistry*, 2nd edition, Springer-Verlag, Berlin.
- Faber, K., Ottolina, G., Riva, S. 1993. Selectivity-enhancement of hydrolase reactions. *Biocatalysis* **8**: 91-132.

- Fredenslund, A, Gmehling, J., Rasmussen, P. 1977. Vapor-Liquid Equilibria Using UNIFAC, Elsevier, New York.
- Hansen, H.K., Rasmussen, P., Fredenslund, A., Schiller, M., Gmehling, J. 1991. Vapor-liquid equilibria by UNIFAC group contribution. 5. Revision and extension. *Ind. Eng. Chem. Res.* **31**: 2352-2355.
- Hansen, T.V., Waagen, V., Partali, V., Anthonsen, H.W., Anthonsen, T. 1995. Cosolvent enhancement of enantioselectivity in lipase-catalyzed hydrolysis of racemic esters. A process for production of homochiral C-3 building blocks using lipase B from *Candida antarctica*. *Tetrahedron: Asymmetry* **6**: 499-504.
- Jones, J.B., Mehes, M.M. 1979. Effects of organic cosolvents on enzyme stereospecificity. The enantiomeric specificity of α -chymotrypsin is reduced by high organic solvent concentrations. *Can. J. Chem.* **57**: 2245-2248.
- Ke, T., Wescott, C.R., Klibanov, A.M. 1996. Prediction of the solvent dependence of enzymatic prochiral selectivity by means of structure-based thermodynamic calculations. *J. Am. Chem. Soc.* **118**: 3366-3374.
- Kikic, I., Fermeglia, M., Rasmussen, P. 1991. UNIFAC prediction of vapor-liquid equilibria in mixed solvent-salt systems. *Chem. Eng. Sci.* **46**: 2775-2780.
- Koskinen, A.M.P., Klibanov, A.M., Eds. 1996. *Enzymatic Reactions in Organic Media*, Blakie, London.
- Lam, L.K.P., Hui, R.A.H.F., Jones, J.B. 1986. *Enzymes in organic synthesis.* 35. Stereoselective pig liver esterase catalyzed hydrolyses of 3-substituted glutarate diesters. Optimization of enantiomeric excess via reaction conditions control. *J. Org. Chem.* **51**: 2047-2050.

- Lee, W.L., Kim, K.-J., Kim, M.G., Lee, S.B. 1995. Enzymatic resolution of racemic ibuprofen esters: effects of organic cosolvents and temperature. *J. Ferment. Bioeng.* **80**: 613-615.
- Luque, S., Ke, T., Klibanov, A.M. 1998. On the role of transition-state substrate desolvation in enzymatic enantioselectivity in aqueous-organic mixtures. *Biocatalysis Biotrans.* **16**: in press.
- Phillips, R.S. 1996. Temperature modulation of the stereochemistry of enzymatic catalysis: prospects for exploitation. *Trends Biotechnol.* **14**: 13-16.
- Reynolds, J.E.F., Ed. 1982. *Martindale, the Extra Pharmacopoeia*, 2nd edition, Pharmaceutical Press, London, p. 304.
- Steitz, T.A., Henderson, R., Blow, D.M. 1969. Structure of crystalline α -chymotrypsin. III. Crystallographic studies of substrate and inhibitors bound to the active site of α -chymotrypsin. *J. Mol. Biol.* **46**: 337-348.
- Straathof, A.J.J., Jongejan, J.A. 1997. The enantiomeric ratio: origin, determination and prediction. *Enzyme Microb. Technol.* **21**: 559-571.
- Warshel, A., Naray-Szabo, G., Sussman, F., Hwang, J.-K. 1989. How do serine proteases really work? *Biochemistry* **28**: 3629-3637.
- Wescott, C.R., Klibanov, A.M. 1993a. Solvent variation inverts substrate specificity of an enzyme. *J. Am. Chem. Soc.* **115**: 1629-1631.
- Wescott, C.R., Klibanov, A.M. 1993b. Predicting the solvent dependence of enzymatic substrate specificity using semiempirical thermodynamic calculations. *J. Am. Chem. Soc.* **115**: 10362-10363.
- Wescott, C.R., Klibanov, A.M. 1994. The solvent dependence of enzyme specificity. *Biochim. Biophys. Acta* **1206**: 1-9.

- Wescott, C.R., Noritomi, H., Klibanov, A.M. 1996. Rational control of enzymatic enantioselectivity through solvation thermodynamics. *J. Am. Chem. Soc.* **118**: 10365-10370.
- Wolff, A., Straathof, A.J.J., Jongejan, J.A., Heijnen, J.J. 1997. Solvent induced change of enzyme enantioselectivity: rule or exception? *Biocatalysis Biotrans.* **15**: 175-184.
- Yennawar, N.H.; Yennawar, H.P., Farber, G.K. 1994. X-ray crystal structure of γ -chymotrypsin in hexane. *Biochemistry* **33**: 7326-7336.
- Zaks, A., Dodds, D.R. 1997. Application of biocatalysis and biotransformations to the synthesis of pharmaceuticals. *Drug Dev. Trends* **2**: 513-531.

CHAPTER IV. MOLECULAR-MODELING CALCULATIONS OF ENZYMATIC ENANTIOSELECTIVITY TAKING HYDRATION INTO ACCOUNT

A. INTRODUCTION

Exquisite enantioselectivity is among the most important properties of enzymes to chemists (Poppe and Novak, 1992; Sheldon, 1993). The ultimate goal in this regard would be the ability to tailor or design enzyme/solvent systems to catalyze any stereospecific chemical reaction at will. To assist in this ambitious endeavor, computer modeling approaches could give considerable guidance and insight. Indeed, attempts to use computations in this regard have been made by several research groups (DeTar, 1981a and b; Wipff *et al.*, 1983; Norin *et al.*, 1993). In all these studies, vacuum molecular mechanics were employed to calculate the energy difference between the *R* and *S* tetrahedral intermediates (mimicking the reaction transition states). This energy difference was subsequently equated to the activation free energy difference between the *R* and *S* enantiomers of the substrate (corresponding to enantioselectivity). For the substrates studied, at least a qualitative agreement was obtained between the calculated and experimental results.

Both the enzymatic reactions examined and others have been carried out in aqueous solution, and certainly *not* in vacuum. Hence since water plays an important role in enzyme catalysis (Rupley and Careri, 1991), including water in the simulation model would seem necessary for a realistic view of an enzymatic reaction. Unfortunately, computational means for doing so without the use of supercomputers until recently have been lacking.

During the past decade, the development and popularization of the continuum electrostatic approach to the treatment of protein solvation and electrostatic interactions have

provided both a useful tool and new insights (Davis and McCammon, 1990; Honig *et al.*, 1993; Honig and Nicholls, 1995; Gilson, 1995). With its point charges assigned to an analytical grid, the solute in this approach is described as a low-dielectric cavity in the solvent which is modeled as a dielectric continuum. The electrostatic potential at each grid point is obtained by solving the Poisson-Boltzmann equation, from which the total electrostatic free energy of the solute in the solvent is calculated. In the present work, we have combined the continuum electrostatic calculations with the vacuum molecular dynamics, and, for the first time, calculated the enantioselectivity of chymotrypsin for four chiral substrates in water instead of vacuum.

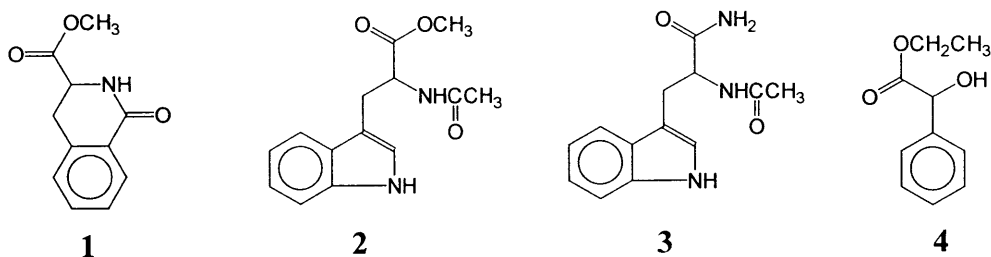
B. THEORY

The transition states for the acylation and deacylation of chymotrypsin by its substrates are thought to be structurally similar to the tetrahedral intermediates for the corresponding reactions (Warshel *et al.*, 1989). In this work, as in the previous studies (DeTar, 1981a and b; Wipff *et al.*, 1983; Norin *et al.*, 1993), the tetrahedral intermediate of the acylation step is used as the transition state model. The enantioselectivity of an enzymatic reaction which follows Michaelis-Menten kinetics can be quantitatively described either by the enantiomeric parameter E (which equals the $k_{\text{cat}}/K_{\text{M}}$ ratio for the enantiomers) (Chen *et al.*, 1982) or by the activation free energy difference between the R and S enantiomers of the chiral substrate, $\Delta\Delta G^\ddagger$. These two parameters are equally descriptive and related to each other as depicted in equation 1 (Norin *et al.*, 1993):

$$\Delta\Delta G^\ddagger = -RT \ln E \quad (1)$$

where $E = (k_{\text{cat}} / K_{\text{M}})_R / (k_{\text{cat}} / K_{\text{M}})_S$ and $\Delta\Delta G^\ddagger = \Delta G^\ddagger_R - \Delta G^\ddagger_S$.

Scheme 1.



Because water (as well as most other solvents) is achiral, the ground states of the two enantiomers have the same free energy. Moreover, the unbound form of the enzyme has the same free energy, whether it is to bind the *R* or the *S* enantiomer. Therefore, $\Delta\Delta G^\ddagger$ (enantioselectivity), can be equated to the total free energy difference between the *R* and *S* tetrahedral intermediates, ΔG_{R-S} :

$$\Delta\Delta G^\ddagger = \Delta G_{R-S} \quad (2)$$

We approximated this free energy difference in water as a sum over bonded and non-bonded interactions as follows:

$$\Delta G_{R-S}^{\text{water}} = \Delta E_{R-S}^{\text{covalent}} + \Delta E_{R-S}^{\text{vdW}} + \Delta G_{R-S}^{\text{elec}} + \Delta G_{R-S}^{\text{non-polar}} \quad (3)$$

$\Delta E_{R-S}^{\text{covalent}}$ is the difference in the bonded energy terms and $\Delta E_{R-S}^{\text{vdW}}$ is the difference in the van-der-Waals energy for molecular mechanics energy minimized structures of the two intermediates. $\Delta G_{R-S}^{\text{elec}}$ is the electrostatic contribution in continuum solvent consisting of Coulombic and reaction field contribution and computed from finite-difference solutions to the Poisson-Boltzmann equation (Honig *et al.*, 1993; Honig and Nichols, 1995). Note that the effect of hydrogen bonding, as well as of polar and charge interactions, are collectively described in the continuum electrostatic term ($\Delta G_{R-S}^{\text{elec}}$) in equation 3. $\Delta G_{R-S}^{\text{non-polar}}$ is computed from the solvent

accessible surface area difference between the *R* and *S* enzyme-bound tetrahedral intermediate (Friedman and Honig, 1995). The energy minimized structures were determined using molecular dynamics *in vacuum* (Ke *et al.*, 1996). Ab initio calculations were performed to assign point charges (Singh and Kollman, 1984) to the atoms of the model transition-state complex (Figure 1). These procedures are described in detail below.

(i) Point charge assignment. A model tetrahedral complex of each substrate was built using the Insight II program from Biosym, Inc., where OCH₃ was used as an analog of the side chain of chymotrypsin's Ser195 (Figure 1). For both the *R* and *S* tetrahedral complexes, molecular dynamics were carried out in vacuum at 500 °K for 5 ps using the AMBER forcefield (Weiner *et al.*, 1984, 1986). Every 1 ps, one sample structure was saved and minimized to a maximum gradient of 0.001 kcal/(mol·Å). Eventually, 10 conformations of the *R* and *S* tetrahedral complexes were saved as the input to the ab initio calculations. The total -1 charge was assigned to each tetrahedral complex since they include an oxyanion. For each conformation, a restricted Hartree-Fock (RHF) calculation using the STO-3G basis set (Frisch *et al.*, 1996) was used to optimize the geometry. Then, the molecular electrostatic potential (ESP) fitting method was used to fit all-atom point charge distributions to the electrostatic potential (Singh and Kollman, 1984). Although the ESP method gives more realistic charge distributions than other methods, such as the Mulliken population, the point charge is dependent on the conformation of the substrate (Singh and Kollman, 1984). Consequently, we assigned the atomic point charges the average values calculated from the aforementioned 10 conformations.

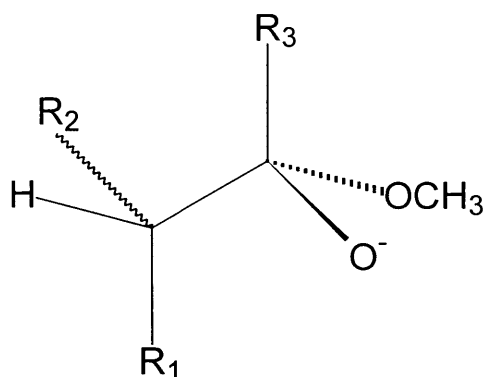


Figure 1. The structure of the model substrate tetrahedral complex used in the atomic point charge assignment. The side chain (OCH_2) of α -chymotrypsin's Ser 195 is approximated by OCH_3 (see the Theory section). The notations used in the figure for different groups are: R_1 - side chain group in the substrate, R_2 - polar group in the substrate, R_3 - acyl group in the tetrahedral intermediate.

(ii) Conformational search. After the point charges of the substrate were assigned, a conformational search for the enzyme-substrate tetrahedral intermediate was performed using a similar method (Ke *et al.*, 1996) with some modifications. First, the AMBER forcefield was used instead of the CVFF forcefield because the former is consistent with the point charge assignment for the substrate complex using ab initio calculations (Weiner *et al.*, 1984). The distance-dependent dielectric constant ϵ was used as with a proportionality coefficient of 4 to be consistent with the later internal dielectric constant used in the continuum solvation model (*i.e.*, $\epsilon = 4r$, where r is the interatomic distance in \AA). A cutoff distance of 24 \AA was used for both the electrostatic and van-der-Waals terms to save computer time. For the enzyme, the default AMBER charge assignment (Biosym, 1994) was used, while the atomic point charges derived from the foregoing ab initio calculations were used for the substrate tetrahedral complex. In addition, in the molecular dynamics calculations of the tetrahedral intermediate, all the residues within 5 \AA of the substrate molecule were allowed to move with a 2.5 kcal/mol $\cdot\text{\AA}$ harmonic potential tethered from their original positions, while the rest of the enzyme atoms were fixed

(Norin *et al.*, 1993). The crystal structure of α -chymotrypsin (Blevins and Tulinsky, 1985) (Brookhaven Protein Data Bank entry 5CHA) was used instead of γ -chymotrypsin because all the experimental enantioselectivity data were for the α form of the enzyme. The resulting energy-minimized conformations were used in the following continuum electrostatic calculations (Smith and Honig, 1994).

(iii) Continuum electrostatic calculations. The electrostatic free energy contribution in water was computed as a sum of two contributions, each calculated using a variety of schemes:

$$G_{R \text{ or } S}^{\text{elec}} = G_{R \text{ or } S}^{\text{elec,coul}}(\epsilon_i) + G_{R \text{ or } S}^{\text{elec,rf}}(\epsilon_i, \epsilon_o) \quad (4)$$

where ϵ_i and ϵ_o represent the internal and external dielectric constants, respectively. The first, Coulombic term was computed with no non-bonded cutoff but either with or without the non-bonded exclusion inherent in the AMBER force field as implemented in the Discover program (Biosym, 1994). The second, reaction-field term was computed as either

$$G_{R \text{ or } S}^{\text{elec,rf}} = G_{R \text{ or } S}^{\text{elec,total}}(\epsilon_i, \epsilon_o) - G_{R \text{ or } S}^{\text{elec,total}}(\epsilon_i, \epsilon_i) \quad (5)$$

or

$$G_{R \text{ or } S}^{\text{elec,rf}} = G_{R \text{ or } S}^{\text{elec,total}}(\epsilon_i, \epsilon_o) - G_{R \text{ or } S}^{\text{elec,total}}(\epsilon_i, 1) \quad (6)$$

where $\Delta G_{R \text{ or } S}^{\text{elec,total}}(x,y)$ represents the total electrostatic energy computed by Delphi (including grid-energy contributions) with internal dielectric x and external dielectric y . The difference calculations above used the same grid placement to facilitate cancellation of the grid energy.

Because the variations produced similar $\Delta G_{R \text{ or } S}^{\text{elec,rf}}$ values, only the results using the full Coulombic energy and equation 5 are reported here.

For all the calculations, ϵ_i was set at 4 and ϵ_o to 80. The default AMBER charges were used, except for the substrate for which the ab initio fit point charges were used (Norin *et al.*,

1993). The ionic strength was set to 200 mM according to the experimental conditions used in the literature (Hein and Niemann, 1962) for the calculation of $G_{R \text{ or } S}^{\text{elec, total}}(\epsilon_i, \epsilon_o)$, while it was set to 0 mM for the calculation of $G_{R \text{ or } S}^{\text{elec, total}}(\epsilon_i, \epsilon_i \text{ or } 1)$ (Gilson and Honig, 1988). AMBER radius set (Weiner *et al.*, 1986) was used for all the continuum electrostatic calculations.

As part of further analysis, the electrostatic desolvation free energy (Hendsch and Tidor, 1994) of the substrate **4** was calculated as follows: (a) The electrostatic free energy of **4** in the tetrahedral intermediate with α -chymotrypsin was calculated. All the atoms of the enzyme were assigned to zero charges, which meant that the enzyme was treated as a "dielectric blob" surrounding the substrate. (b) Using the same grid and coordinates as in (a), the electrostatic free energy of **4** in aqueous solution without enzyme was calculated. (c) The difference between the values obtained in (a) and (b) was equated to the electrostatic desolvation free energy of the substrate. All the parameter settings were the same as before.

(iv) Non-polar contributions. The solvent-accessible surface areas (Connolly, 1983) of the *R* and *S* tetrahedral intermediates were calculated to take into account the non-polar contributions ($\Delta G_{\text{np}}^{\text{water}}$). All the residues within 10 Å around the substrate molecule were included in this calculation. Since we were only interested in the free energy *difference* between the *R* and *S* tetrahedral intermediates, only the *difference* in their solvent-accessible areas (ΔArea) was used in the calculation of the nonpolar contributions:

$$\Delta G_{R-S}^{\text{non-polar}} = \gamma_{\text{water/alkane}} \cdot \Delta \text{Area} \quad (7)$$

where $\gamma_{\text{water/alkane}}$ is the interfacial surface tension coefficient between water and an alkane with the assigned value as 0.058 kcal/(mol·Å²) (Friedman and Honig, 1995).

(v) **Combination of energy components.** Finally, we added $\Delta E_{R-S}^{\text{covalent}}$, $\Delta E_{R-S}^{\text{vdW}}$, $\Delta G_{R-S}^{\text{elec}}$, and $\Delta G_{R-S}^{\text{non-polar}}$ for the *R* and *S* enantiomers to obtain ΔG_{R-S} in water (Honig *et al.*, 1993; Friedman and Honig, 1995). The latter parameter represents the calculated enantioselectivity (equation 2), which can be directly compared with the experimentally determined value.

C. RESULTS AND DISCUSSION

The objective of this work was to develop a computational methodology for the calculation of enzymatic enantioselectivity taking hydration into account. While in the previous studies (DeTar, 1981a and b; Wipff *et al.*, 1983; Norin *et al.*, 1993) calculations of enzymatic enantioselectivity had been carried out for vacuum as the reaction medium (obviously, not a realistic one), we herein took into account the effect of the actual reaction medium, water.

The approach described in the foregoing section should be applicable to any milieu in which enzyme-substrate interactions take place. In particular, they should be valid for vacuum. Therefore, as a first test of our methodology, we applied it to calculate the vacuum enantioselectivity of α -chymotrypsin with four different chiral substrates for which (a) experimental data on enantioselectivity were available from the literature, and (b) vacuum molecular mechanics had been previously used (DeTar, 1981a and b; Wipff *et al.*, 1983; Norin *et al.*, 1993) to calculate the enantioselectivity using less accurate than herein atomic point charge assignments for the substrate (see above).

Table I. Comparison of experimentally determined enantioselectivities in the α -chymotrypsin-catalyzed hydrolyses of **1** through **4** with simulation results in vacuum and in aqueous solution^a

| Substrate | Experimental $\Delta\Delta G^\ddagger$ (kcal/mol) | Calculated | | Calculated $\Delta\Delta G^\ddagger$ in water (kcal/mol) |
|-----------|--|--|-----------|---|
| | | $\Delta\Delta G^\ddagger$ in vacuum (kcal/mol) | | |
| | | literature | this work | |
| 1 | -4.9 ^b | -5.2 ^c | -4.4 | -4.5 |
| | | -4.1 ^f | | |
| 2 | > 7 ^c | 7.4 ^e | 6.3 | 5.3 |
| | | 4.2 ^f | | |
| 3 | > 7 ^c | 9.3 ^g | 8.0 | 8.7 |
| 4 | 0.1 ^d | 0.1 ^f | 1.2 | 0.1 |

^a Experimental $\Delta\Delta G^\ddagger$ values are defined by equation 2. The data in the last column are calculated herein.

^b Hein and Niemann, 1962.

^c Huang and Niemann, 1951.

^d Cohen *et al.*, 1966.

^e DeTar, 1981a and b.

^f Norin *et al.*, 1993.

^g Wipff *et al.*, 1983.

Table I depicts the calculated $\Delta\Delta G^\ddagger$ (enantioselectivity) values for substrates **1** through **4**, both taken from the literature and obtained by us, as well as the experimentally determined values. One can see that in all but one instance, our calculated $\Delta\Delta G^\ddagger$ values are within 1.3 kcal/mol of those calculated by others. Inclusion of the experimental values in this comparison is quite revealing. For substrate **1**, our calculated value of $\Delta\Delta G^\ddagger$ of -4.4 kcal/mol is within 0.5

kcal/mol from the actual enantioselectivity, as compared to 0.3 kcal/mol of DeTar (1981b). On the other hand, our value is 0.3 kcal/mol closer to the actual enantioselectivity than that of Norin *et al.* (1993). For substrate **2**, our calculation result is inferior to that of DeTar (1981b) but superior to that of Norin *et al.* (1993). For substrate **3**, both our calculated $\Delta\Delta G^\ddagger$ value and that of Wipff *et al.* (1983) are equally consistent with the experimental range of $\Delta\Delta G^\ddagger > 7$ kcal/mol. Finally, for substrate **4** our calculated enantioselectivity value is farther away from the actual one than that of Norin *et al.* (1993).

Overall, inspection of Table I shows that out of six literature values of calculated enantioselectivities for substrates **1** through **4**, two are superior to ours, two are inferior, one is similar, and in one case no judgment can be made. Thus for the vacuum situation, the predictive power of our methodology is comparable to those elaborated by others. Since our methodology, as mentioned earlier, affords more accurate atomic point charge assignments, we conclude that the contribution of this improvement to the last term in equation 3, and hence to enantioselectivity, is minor. It is also worth noting that there is no systematic trend in the discrepancies between our predicted enantioselectivity values and those determined experimentally: sometimes ours are higher, and sometimes lower (Table I).

Next, we performed enantioselectivity calculations which took hydration into account. The results obtained (the last column of Table I) were surprising in that they turned out to be similar to those in vacuum. The $\Delta\Delta G^\ddagger$ values in vacuum and in water for each of the substrates were found to be within 1.1 kcal/mol (Table I), corresponding to the *E* values within an order of magnitude from one another. In comparison with the experimental data, the calculations in water vs. those in vacuum afforded an improvement for substrate **4**, about the same accuracy for

substrate **1**, an inferior predictive ability for substrate **2**, and an uncertain outcome for substrate **3**.

Conceptually, the calculations in water differ from those in vacuum in two respects. First, the electrostatic contribution to the activation free energy, ΔG^\ddagger , of the interactions between the solvent (water) and the solute (enzyme-substrate tetrahedral intermediate) is taken into account (Honig *et al.*, 1993). Second, the non-polar contribution of the solvent-solute interactions to the ΔG^\ddagger is taken into account (Friedman *et al.*, 1995). Note that these two contributions involve only the desolvated portions of the tetrahedral intermediates (Ke *et al.*, 1996; Wescott *et al.*, 1996). Therefore, a possible explanation for the observed lack of the solvent effect (Table I) is that both the *R* and *S* tetrahedral intermediates of the substrate are desolvated to the same extent (*i.e.*, these two contributions are the same for the *R* and *S* enantiomers). Since the enantioselectivity is only related to the free energy *difference* between the *R* and *S* tetrahedral intermediates, including the solvent should have no effect on the $\Delta\Delta G^\ddagger$ which equals $\Delta G_R^\ddagger - \Delta G_S^\ddagger$.

In order to test this explanation, we calculated the extents of desolvation of different groups in the *R* and *S* tetrahedral intermediates of the substrate (Table II). All groups of the enzyme (*R* vs. *S*) are desolvated to the same extent (within 12% difference in percentage of desolvation). For substrates **1** through **3**, the percentage of desolvation of the R_1 , R_2 , and R_3 groups (Figure 1) were indeed within 11% between the *R* and *S* tetrahedral intermediates (Table II). In contrast, for substrate **4**, while the desolvations of the side-chain (R_1) and acyl (R_3) groups in the *R* and *S* tetrahedral intermediates also differ by less than 10%, that of the R_2 group, a hydroxyl, differs greatly: 34% and 100%, respectively (Table II). Since hydroxyl group is polar, the dehydration free energy of the *S* enantiomer should be higher than that of its *R* counterpart.

And yet, this does not make an appreciable contribution to the calculated enantioselectivity in water compared to that in vacuum.

Table II. Extent of group (Figure 1) desolvation of substrates **1** through **4** in their tetrahedral intermediates with α -chymotrypsin^a

| Substrate | Percentage of desolvation, % | | | | | |
|-----------|------------------------------|----------------|----------------|----------------|----------------|----------------|
| | <i>R</i> | | | <i>S</i> | | |
| | R ₁ | R ₂ | R ₃ | R ₁ | R ₂ | R ₃ |
| 1 | 93 | - | 20 | 90 | - | 22 |
| 2 | 93 | 14 | 28 | 93 | 25 | 25 |
| 3 | 86 | 17 | 30 | 91 | 24 | 39 |
| 4 | 100 | 34 | 27 | 95 | 100 | 17 |

^a For R₁, R₂, and R₃, see the legend to Figure 1. The percentage of desolvation is calculated using the same method as in Ke *et al.* (1996).

In order to rationalize this observation, we examined the values of the aforementioned two contributions to ΔG^\ddagger for substrate **4**. First, the electrostatic dehydration free energies (Hendsch and Tidor, 1994) of the substrate (including the hydroxyl group) in both the *R* and *S* tetrahedral intermediates were calculated using the three-step procedure outlined in the Theory section: The energy values thus obtained were 5.7 and 6.9 kcal/mol for the *R* and *S* enantiomers of **4**, respectively. Therefore, while the electrostatic dehydration free energy for the *S* enantiomer is indeed higher than for the *R*, the difference, 1.2 kcal/mol, is relatively small and well within the range of discrepancies between the calculated and experimentally observed $\Delta\Delta G^\ddagger$ values (Table I). Second, the non-polar contribution (ΔG_{np}^{water}) was found to be quite low, 0.4 kcal/mol. This can be due to a small size of the hydroxyl group which would make its contribution to the difference in the solvent-accessible area ($\Delta Area$ in equation 7) insignificant.

We thus conclude that taking the solvent into account would make a significant contribution to the calculated $\Delta\Delta G^\ddagger$ value only when the substrate has groups more “impactful” (Wescott *et al.*, 1996) than a hydroxyl, *e.g.* a charged group. Such a group would also have to exhibit a large difference in the percentage of desolvation between the *R* and *S* tetrahedral intermediates.

In closing, in this work, we introduced a new, more realistic than the heretofore available model to simulate enzymatic enantioselectivity in aqueous solution. A reasonable agreement was obtained in most cases between the calculated enantioselectivities and the experimentally determined values. Surprisingly, for the four substrates examined, the vacuum simulation yielded the results comparable with those obtained by means of continuum hydration. This is because either the *R* and *S* tetrahedral intermediates were desolvated to the same extent or although a group did exhibit a large difference in desolvation for the *R* and *S* enantiomers, it was not impactful enough to make a significant difference on $\Delta\Delta G^\ddagger$. We are currently applying the methodology developed herein to calculate enzyme stereoselectivity in organic solvents.

E. REFERENCES

- Biosym. 1994. Discover user guide (Version 2.9.5 & 94.0). Biosym Technologies, Inc.
- Blevins, R.A., Tulinsky, A. 1985. The refinement and the structure of the dimer of α -chymotrypsin at 1.67 Å resolution. *J. Biol. Chem.* **260**: 4264-4269.
- Chen, C.-S., Fujimoto, Y., Girdaukas, G., Sih, C.J. 1982. Quantitative analyses of biochemical kinetic resolutions of enantiomers. *J. Am. Chem. Soc.* **104**: 7294-7299.
- Cohen, S.G., Neuwirt, Z., Weinstein, S.Y. 1966. Stereospecificity in hydrolysis by α -chymotrypsin of esters of α - α -disubstituted acetic and β - β -disubstituted propionic acids. *J. Am. Chem. Soc.* **88**: 5315-5319.
- Connolly, M.L. 1983. Solvent accessible surfaces of proteins and nucleic acids. *Science* **221**: 709-712.
- Davis, M.E., McCammon, J.A. 1990. Electrostatics in biomolecular structure and dynamics. *Chem. Rev.* **90**: 509-521.
- DeTar, D.F. 1981a. Computation of peptide-protein interactions. Catalysis by chymotrypsin: prediction of relative substrate reactivities. *J. Am. Chem. Soc.* **103**: 107-110.
- DeTar, D.F. 1981b. Computation of enzyme-substrate specificity. *Biochemistry* **20**: 1730-1743.
- Fersht, A. 1985. Enzyme structure and mechanism. Freeman, New York.
- Friedman, R.A., Honig, B. 1995. A free energy analysis of nucleic acid base stacking in aqueous solution. *Biophys. J.* **69**: 1528-1535.
- Frisch, M.J., Frisch, A.E., Foresman, J.B. 1996. Gaussian 94 user's reference (Revision D.1 and higher). Gaussian, Inc., Pittsburgh.

- Gilson, M.K. 1995. Theory of electrostatic interactions in macromolecules. *Cur. Opin. Struct. Biol.* **5**: 216-223.
- Gilson, M.K., Honig, B. 1988. Calculation of the total electrostatic energy of a macromolecular system: solvation energies, binding energies, and conformational analysis. *Proteins* **4**: 7-18.
- Gilson, M.K., Sharp, K.A., Honig, B.H. 1987. Calculating the electrostatic potential of molecules in solution: method and error assessment. *J. Comp. Chem.* **9**: 327-335.
- Hein, G.E., Niemann, C. 1962. Steric course and specificity of α -chymotrypsin-catalyzed reactions. *J. Am. Chem. Soc.* **84**: 4487-4494.
- Hendsch, Z.S., Tidor, B. 1994. Do salt bridges stabilize proteins? A continuum electrostatic analysis. *Protein Sci.* **3**: 211-226.
- Honig, B., Nicholls, A. 1995. Classical electrostatics in biology and chemistry. *Science* **268**: 1144-1149.
- Honig, B., Sharp, K., Yang, A.S., 1993. Macroscopic models of aqueous solutions: biological and chemical applications. *J. Phys. Chem.* **97**: 1101-1109.
- Huang, H.T., Niemann, C. 1951. The evaluation of the enzyme-inhibitor dissociation constant of α -chymotrypsin and acetyl-D-tryptophan methyl ester. *J. Am. Chem. Soc.* **73**: 3228-3231.
- Ke, T., Wescott, C.R., Klibanov, A.M. 1996. Prediction of the solvent dependence of enzymatic prochiral selectivity by means of structure-based thermodynamic calculations. *J. Am. Chem. Soc.* **118**: 3366-3374.
- Norin, M., Hult, K., Mattson, A., Norin, T. 1993. Molecular modeling of chymotrypsin-substrate interactions: calculation of enantioselectivity. *Biocatalysis* **7**: 131-147.

- Poppe, L., Novak, L. 1992. Selective biocatalysis. VCH Publishers, New York.
- Rupley, J.A., Careri, G. 1991. Protein hydration and function. *Adv. Protein Chem.* **41**: 37-172.
- Sheldon, R.A. 1993. Chirrotechnology: industrial synthesis of optically active compounds. M. Dekker, New York.
- Singh, U.C., Kollman, P.A. 1984. An approach to computing charges for molecules. *J. Comp. Chem.* **5**: 129-145.
- Smith, K.C., Honig, B. 1994. Evaluation of the conformational free energies of loops in proteins. *Proteins* **18**: 119-132.
- Warshel, A., Naray-Szabo, G., Sussman, F., Hwang, J.-K. 1989. How do serine proteases really work? *Biochemistry* **28**: 3629-3637.
- Weiner, S.J., Kollman, P.A., Case, D.A., Singh, U.C., Ghio, C., Alagona, G., Profeta, S., Jr., Weiner, P. 1984. A new force field for molecular mechanical simulation of nucleic acids and proteins. *J. Am. Chem. Soc.* **106**: 765-784.
- Weiner, S.J., Kollman, P.A., Nguyen, D.T., Case, D.A. 1986. An all atom forcefield for simulations of proteins and nucleic acids. *J. Comp. Chem.* **7**: 230-252.
- Wescott, C.R., Noritomi, H., Klibanov, A.M. 1996. Rational control of enzymatic enantioselectivity through solvation thermodynamics. *J. Am. Chem. Soc.* **118**: 10365-10370.
- Wipff, G., Dearing, A., Weiner, P.K., Blaney, J.M., Kollman, P.A. 1983. Molecular mechanics studies of enzyme-substrate interactions: the interaction of L- and D- *N*-acetyltryptophanamide with α -chymotrypsin. *J. Am. Chem. Soc.* **105**: 997-1005.

CHAPTER V. ON ENZYMATIC ACTIVITY IN ORGANIC SOLVENTS AS A FUNCTION OF ENZYME HISTORY

A. INTRODUCTION

A basic, extensively verified tenet of enzymology is that the catalytic behavior of an enzyme dissolved in water is independent of the enzyme's history (otherwise biochemical studies done in different laboratories would not be reproducible). This lack of "memory" is due to the conformational mobility, "breathing", of enzymes in aqueous solution (Rupley and Careri, 1991; Gregory, 1995) which leads to the acquisition of the native, thermodynamically favored structure regardless of the prior history. For example, although enzymes and other proteins denature upon lyophilization, and the extent of this process depends on experimental conditions, all such reversibly denatured conformations spontaneously revert back to the same native one upon redissolution in water (Griebenow and Klibanov, 1995).

The situation is different in organic solvents where, due to the absence of the "molecular lubricant" water (Rupley and Careri, 1991), enzymes are conformationally rigid. Indeed, this conformational rigidity prevents enzymes from unfolding and consequently inactivating when placed in anhydrous solvents (Klibanov, 1989 and 1997). The same phenomenon is responsible for the molecular memory of enzymes in organic solvents (Klibanov, 1995) whereby the enzymatic activity and selectivity in such media are affected by substrate analogs, inhibitors, and lyoprotectants co-lyophilized with the enzyme (Russell and Klibanov, 1989; Stahl et al., 1991; Dabulis and Klibanov, 1993; Khmel'nitsky et al., 1994; Noritomi et al., 1995; Rich and Dordick, 1997).

Enzymes "remember" their history in organic solvents because they are kinetically

trapped in their previous conformations. In the present study, we have examined how and why the extent of this kinetic trapping depends on the solvent.

B. MATERIALS AND METHODS

Materials

Subtilisin Carlsberg (serine protease from *Bacillus licheniformis*, EC 3.4.21.14) with a specific activity of 14 units/mg and bovine pancreatic α -chymotrypsin (EC 3.4.21.1) with a specific activity of 52 units/mg were purchased from Sigma Chemical Co. N-Acetyl-L-phenylalanine ethyl ester (NAPEE) and phenyl acetate were from Aldrich Chemical Co. All solvents used in this work were purchased from commercial suppliers in the anhydrous state and were of analytical grade or purer.

Enzyme Preparation

Subtilisin and chymotrypsin were dissolved in 20 mM potassium phosphate buffer at a 5 mg/ml concentration (Zaks and Klibanov, 1988). The pH of the enzyme solution was adjusted to 7.8 at 0 °C prior to a 24-hour lyophilization in a Labconco freeze-drier (-50 °C, 5-10 μ m of Hg). The final enzyme concentration in the lyophilized powder was 60% by weight (the remaining 40% was the buffer salt).

The lyophilized enzyme powder was processed via two alternative routes prior to kinetic measurements (Fig. 1). In route 1, it was suspended in an organic solvent containing 1% (v/v) water and 20 mM NAPEE. In route 2, the enzyme powder was redissolved in deionized water at 0 °C, and the resultant (pH 7.8) aqueous solution was quickly (within 1 min) diluted 100-fold with an organic solvent containing 20 mM NAPEE. In both cases, the final water content in the system was 1% (v/v). After a 20-s sonication, 1 M propanol was added to initiate the enzymatic

transesterification at 30 °C. Note that no appreciable autolysis occurs in route 2 at 60 mg/ml enzyme concentrations under the conditions used. This conclusion follows from the observation that the rates of enzymatic hydrolysis of NAPEE in water catalyzed by chymotrypsin or subtilisin that had gone through a 60 mg/ml solution were within 10% from those obtained with the enzyme that had been dissolved at only 5 mg/ml.

The final enzyme concentration in a suspension, the same for both preparations depicted in Fig. 1, was 0.60 mg/ml (corresponding to 1.0 mg/ml of the lyophilized powder) except for the following cases: subtilisin in *tert*-amyl alcohol (0.12 mg/ml), *tert*-butanol (0.30 mg/ml), acetone (0.06 mg/ml), and propanol (0.06 mg/ml); chymotrypsin in propanol (0.06 mg/ml). In experiments where 0.1% rather than 1% water in the solvent was desired, 60 mg/ml enzyme solutions were diluted 1,000 fold instead of 100 fold.

The enzymatic glycerolysis of phenyl acetate was examined in glycerol (Xu et al., 1997) instead of the propanolysis of NAPEE used in all other solvents because the latter ester is sparingly soluble in glycerol and because glycerol (the solvent) acts as a nucleophile itself in a transesterification. The enzyme preparation was the same as above with the final enzyme concentration from both routes of 0.025 mg/ml.

Kinetic Measurements

The initial rates of the enzymatic transesterification of NAPEE were followed by gas chromatography (HP-5890 with a 10-m HP-5 silica gel capillary column, 5% phenyl/95% methyl silicone gum coating). The flame ionization detector response was calibrated by use of a standard solution of N-acetyl-L-phenylalanine propyl ester. It was shown previously (Zaks and Klibanov, 1988; Wescott and Klibanov, 1993) that this enzymatic transesterification is not compromised by diffusional limitations. The NAPEE assay could not be used in glycerol (see

above), and therefore another transesterification, glycerolysis of phenyl acetate, was used instead (Xu et al., 1997). The reaction product (phenol) was followed by HPLC using a Waters Symmetry C₁₈ reverse-phase column (3.9 x 150 mm); the mobile phase used was 65:35 (v/v) water (containing 0.1% CF₃COOH):acetonitrile with a flow rate of 0.5 ml/min. Phenol was extracted prior to the measurements as described by Xu et al. (1997); the UV detector at 274 nm was precalibrated by a standard solution of phenol using the same procedure. In both cases, at least 4-5 points within a 10% conversion were taken, and the initial rates were calculated using linear regression.

C. RESULTS AND DISCUSSION

The experimental strategy designed by us for this study was to prepare a given suspension of an enzyme in an organic solvent (usually containing 1% (v/v) water for the reasons explained below) via two dissimilar routes (Fig.1). In the first, an enzyme lyophilized from an aqueous solution was directly suspended in a hydrous solvent. In the second mode, the enzyme was precipitated from its aqueous solution by addition of the anhydrous solvent to produce the same 99% solvent/1% water mixture. The enzymatic activities were then measured in the nonaqueous system and compared with each other. If the situation is under thermodynamic control, the same activity should ensue for the identical enzyme content regardless of how, whether via the first or second route, a given enzyme suspension was prepared. In contrast, different enzymatic activities would reveal that they are under kinetic control. To ensure the generality of our observations, a number of organic solvents and two enzymes were employed in this investigation.

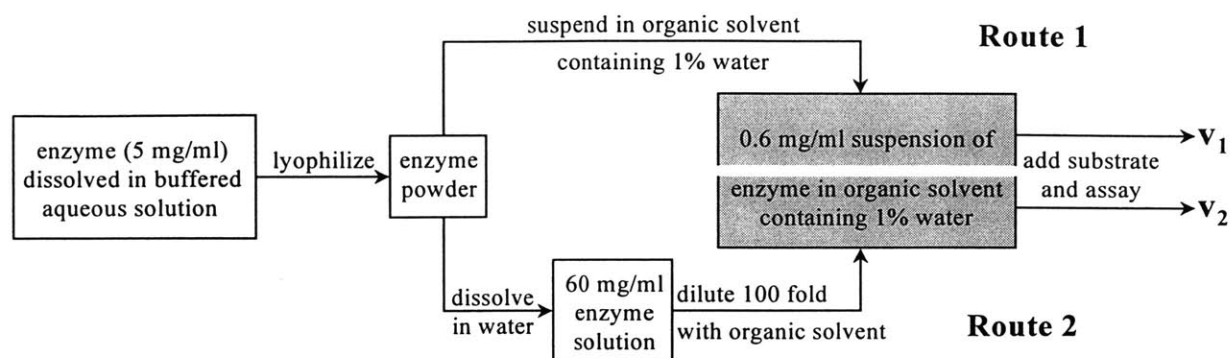


Figure 1. Schematic depiction of two alternative ways to prepare the same enzyme suspension in an organic solvent containing 1% water. See test for details.

Tables I and II show the catalytic activities of the proteases α -chymotrypsin and subtilisin Carlsberg, respectively, in a number of organic solvents containing 1% water. One can see that in most cases enzymatic reactions rates (v_1 and v_2) corresponding to the aforementioned two modes of enzyme preparations (Fig. 1) are not the same, i.e., their ratio in a majority of solvents is distinct from unity. For example, the chymotrypsin activity is *tert*-amyl alcohol is almost an order of magnitude higher when the enzyme was prepared via route 2 rather than route 1 (Table I).

Table I. Initial rates of the propanolysis of N-acetyl-L-phenylalanine ethyl ester in different organic solvents catalyzed by chymotrypsin prepared by two different methods (Fig. 1)^a

| solvent | v_1 $\mu\text{mol}\cdot\text{hr}^{-1}\cdot(\text{mg enzyme})^{-1}$ | v_2 | v_2 / v_1 ^c |
|---------------------------------|---|--------|--------------------------|
| <i>tert</i> -amyl alcohol | 0.065 | 0.60 | 9.4 |
| <i>tert</i> -butanol | 0.033 | 0.30 | 9.1 |
| 3-pentanol | 0.067 | 0.57 | 8.6 |
| ethyl acetate | 0.065 | 0.48 | 7.4 |
| dioxane | 0.010 | 0.067 | 6.7 |
| propanol | 2.5 | 14 | 5.5 |
| acetone | 0.38 | 1.8 | 4.8 |
| tetrahydrofuran | 0.053 | 0.14 | 2.6 |
| acetonitrile | 0.055 | 0.13 | 2.4 |
| pyridine | 0.0023 | 0.0047 | 2.0 |
| methyl <i>tert</i> -butyl ether | 3.3 | 3.4 | 1.1 |
| glycerol ^b | 2.1 | 2.3 | 1.1 |

^a For experimental conditions, see Materials and Methods. Note that, as discussed in Methods, no appreciable autolysis of the enzyme was observed in route 2 despite a high (60 mg/ml) enzyme concentration in water encountered in the course of the experiment.

^b In this solvent, (i) another enzymatic transesterification, glycerolysis of phenyl acetate, was used (see Methods); and (ii) in contrast to all the others used herein, the enzyme was soluble under the conditions used.

^c A typical error in the determinations of this ratio did not exceed 15%.

Table II. Initial rates of the propanolysis of N-acetyl-L-phenylalanine ethyl ester in different organic solvents catalyzed by subtilisin prepared by two different methods (Fig. 1)^a

| solvent | v_1 | v_2 | v_2 / v_1 ^c |
|---------------------------------|--|-------|--------------------------|
| | $\mu\text{mol}\cdot\text{hr}^{-1}\cdot(\text{mg enzyme})^{-1}$ | | |
| dioxane | 0.021 | 0.073 | 3.5 |
| tetrahydrofuran | 0.18 | 0.57 | 3.2 |
| acetonitrile | 0.28 | 0.38 | 1.4 |
| pyridine | 3.0 | 4.3 | 1.4 |
| methyl <i>tert</i> -butyl ether | 0.15 | 0.18 | 1.3 |
| propanol | 27 | 32 | 1.2 |
| 3-pentanol | 0.23 | 0.25 | 1.1 |
| acetone | 20 | 22 | 1.1 |
| <i>tert</i> -amyl alcohol | 13 | 13 | 1.0 |
| ethyl acetate | 0.020 | 0.020 | 1.0 |
| glycerol ^b | 50 | 51 | 1.0 |
| <i>tert</i> -butanol | 4.6 | 4.3 | 0.91 |
| dimethylformamide | 0.13 | 0.078 | 0.59 |

^a See footnote a to Table I.

^b See footnote b to Table I.

^c See footnote c to Table I.

In addition to indicating that the catalytic performance of both chymotrypsin and subtilisin in most organic solvents containing 1% water is kinetically controlled, i.e., dependent on how the enzyme was prepared, inspection of the tables affords other important conclusions. First, it is seen that for a given enzyme the extent of this kinetic control strongly varies with the solvent. For instance, for chymotrypsin, while the v_2/v_1 ratio in the three alcohols at the top of Table I is approximately nine, it is essentially one in methyl *tert*-butyl ether and glycerol. Second, the dependence of catalytic activity on enzyme history is not the same for the two

enzymes; namely, it is far more pronounced for chymotrypsin than for subtilisin. Third, in nearly all cases (Tables I and II), route 2 results in a higher activity than route 1, i.e., $v_2 > v_1$.

We propose the following mechanistic hypothesis to explain the data in the tables. In aqueous solution, at any point in time the vast majority of enzyme molecules are in the native, catalytically active conformation because it is energetically favored. Upon lyophilization, the enzyme undergoes reversible denaturation brought about by dehydration (Griebenow and Klibanov, 1995). Consequently, the lyophilized enzyme is comprised of various non-native conformations, as well as of some residual native one (which is no longer most stable and is in the minority). Due to the structural rigidity of the dehydrated enzyme, in contrast to the situation in aqueous solution, there is no free interconversion among different conformations in the lyophilized enzyme. When the latter is placed in an organic solvent, it becomes more mobile than in the dry state, albeit not nearly as much so as in water (which is a particularly potent molecular lubricant and, consequently, facilitator of conformational mobility (Rupley and Careri, 1991)). As a result, kinetic barriers separating various conformations in the lyophilized enzyme diminish giving rise to interconversions among some (but, generally speaking, not all) conformations; the degrees of the diminution and interconversions should depend on the solvent. (Note that in different solvents the free energies associated with various enzyme conformations, including native, should be distinct as well.) Finally, when an aqueous solution of an enzyme is diluted 100-fold with an organic solvent, the enzyme is again denatured due to dehydration. The resultant suspension consists of various denatured conformations and a small portion of the native one. As in the previous case, the interconversions among denatured and native conformations are hindered due to kinetic trapping.

This hypothesis can rationalize the data in Tables I and II as follows. Since there is no

free interconversion among different conformations in an enzyme however it is suspended in a 99% organic solvent, the catalytic activity (reflecting the fraction of the native conformation) should depend on how the suspension was obtained. Moreover, one would expect that route 2 (Fig. 1) would result in a higher retention of the native conformation than route 1, i.e., $v_2 > v_1$. This is because if enzyme denaturation is caused by dehydration, the greater the degree of dehydration, the greater the extent of denaturation. Hence a dry lyophilized enzyme should be more denatured than the enzyme suspension obtained by the solvent precipitation since it is exposed to a medium (vacuum/air) containing no water (in the latter case, the medium, organic solvent, contains 1% water). Even the subsequent placement of the lyophilized enzyme in an organic solvent containing 1% water may not restore the native conformation due to the lack of free structural interconversions.

In terms of our model, it is easy to understand why v_2/v_1 varies with the organic solvent used, for the heights of kinetic barriers separating the native conformation from denatured ones must depend on the solvent. In some solvents (e.g., *tert*-amyl alcohol for chymotrypsin, Table I), the barriers are presumably high, while in others (e.g., methyl *tert*-butyl ether for chymotrypsin) they are apparently low enough to allow some recovery of the native conformations lost upon lyophilization-induced excessive dehydration. Also, our model readily explains why chymotrypsin and subtilisin do not have the same solvent dependence of v_2/v_1 : the heights of the kinetic barriers, as well as their lowering by organic solvents, should be enzyme-specific.

The foregoing mechanistic hypothesis affords several predictions that could be tested experimentally. The first group of such predictions deals with the effect of the molecular lubricant water. One would expect that as the water content in the solvent and hence conformational flexibility is increased, the enzyme memory will diminish (as was observed for

imprinted proteins (Braco et al., 1990)) and, consequently, for a given enzyme in a given solvent the value of v_2/v_1 will drop. We tested this with chymotrypsin in *tert*-amyl alcohol by examining the dependence of the rate ratio on the water content in the solvent. The data shown in Fig. 2A indeed confirm this prediction: as the water content is raised from the original 1% to 6%, the v_2/v_1 ratio drops almost 3-fold. The water mimic formamide (Kitaguchi and Klibanov, 1989) exhibits a similar role (Fig. 2B).

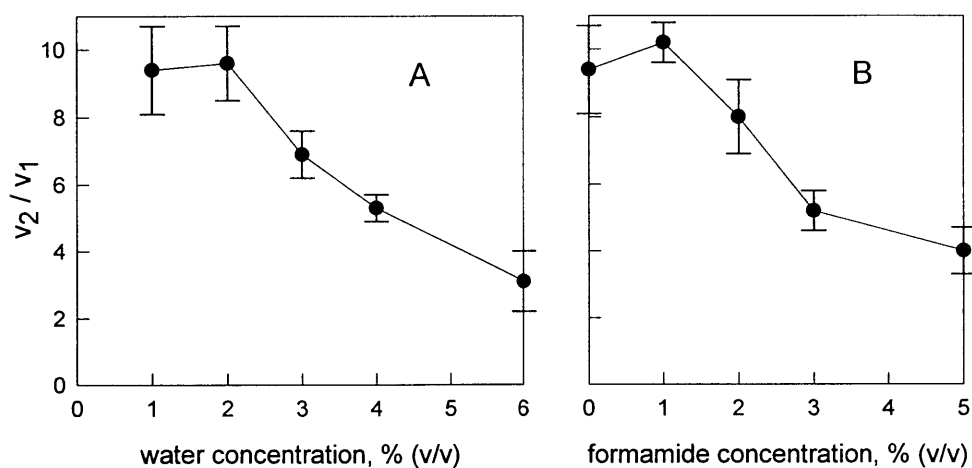


Figure 2. The effect of water (A) and formamide (B) content on α -chymotrypsin's memory (as reflected by v_2/v_1 , see Fig. 1) in *tert*-amyl alcohol. Experimental conditions: 0.6 mg/ml chymotrypsin, 20 mM N-acetyl-L-phenylalanine ethyl ester, 1 M propanol, 30 °C; for other details, see Materials and Methods. In the case of B, the solvent always contained 1% (v/v) water. The error bars correspond to the standard deviations of the initial rate ratios for four independent experiments.

Conversely, one would expect that if the water content of an organic solvent is below the standard 1%, then the values of v_2/v_1 should be higher than in Tables I and II because the enzyme should be more rigid. To this end, we lowered the final water content to 0.1%. Since this requires a 1000-fold dilution of enzymes in aqueous solution and consequently results in very low (0.06 mg/ml) enzyme concentrations, only in a few instances could the enzymatic

reaction rates be reliably measured. All of them unequivocally confirmed our prediction. For chymotrypsin in *tert*-amyl alcohol, the v_2/v_1 ratio jumped from 9.4 in 1% water (Table I) to 17 in 0.1% water. For subtilisin in acetone and *tert*-amyl alcohol, the v_2/v_1 ratio more than quadrupled from 1.1 and 1.0 in 1% water (Table II) to 4.6 and 4.8, respectively, in 0.1% water.

The second group of predictions stemming from our mechanistic hypothesis involves the role of the starting conformational state of the enzyme. One would expect that the more severely denatured (i.e., more remote from the native structure) the enzyme is in route 1 (Fig. 1), the higher will be the v_2/v_1 ratio in a given solvent. Our recent FTIR study (Griebenow and Klibanov, 1997) revealed a greater enzyme denaturation in dimethylsulfoxide (DMSO) compared to the lyophilized state. Therefore, we modified the experimental protocol depicted in Fig. 1. In route 1, a lyophilized enzyme was dissolved in pure DMSO, followed by a 100-fold dilution with an organic solvent containing 1% water. In route 2, an aqueous solution of the enzyme was diluted 100-fold with the solvent containing 1% DMSO. When this protocol was implemented with chymotrypsin and acetone, the resultant v_2/v_1 ratio was found to exceed 250 (was too large to be accurately measured).

The same experiment could not be carried out with subtilisin which undergoes a rapid irreversible (in contrast to chymotrypsin's reversible) denaturation in DMSO (Almarsson and Klibanov, 1996). Thus in route 1 we instead dissolved subtilisin in an equivolume mixture of DMSO and another denaturing solution, 8 M aqueous urea (no irreversible denaturation was observed in this mixture). The resultant v_2/v_1 ratio in *tert*-amyl alcohol (containing 1% water, 0.5% DMSO, and 0.5% 8M aqueous urea), as predicted, was much higher than in Table II, namely, 8.1 vs. 1.0. That in both the chymotrypsin/DMSO and subtilisin/DMSO/urea systems enzyme denaturation was found to be reversible is equivalent to the absence of enzyme memory

in aqueous solution (where the reversibility was tested). Thus, once again, enzymes remember their prior history only in organic solvents, and the harsher the history, the more vivid the memory.

In closing, this work constitutes a further step toward the mechanistic understanding of the phenomenon of enzyme memory in nonaqueous media.

D. REFERENCES

- Almarsson, Ö., Klivanov, A.M. 1996. Remarkable activation of enzymes in nonaqueous media by denaturing organic cosolvents. *Biotechnol. Bioeng.* **49**: 87-92.
- Braco, L., Dabulis, K., Klivanov, A.M. 1990. Design of novel receptors by molecular imprinting of proteins. *Proc. Natl. Acad. Sci. USA* **87**: 274-277.
- Dabulis, K., Klivanov, A.M. 1993. Dramatic enhancement of enzymatic activity in organic solvents by lyoprotectants. *Biotechnol. Bioeng.* **41**: 566-571.
- Gregory, R.B., Ed. 1995. *Protein-Solvent Interactions*, M. Dekker, New York.
- Griebenow, K., Klivanov, A.M. 1995. Lyophilization-induced reversible changes in the secondary structure of proteins. *Proc. Natl. Acad. Sci. USA* **92**: 10969-10976.
- Khmelnitsky, Y.L., Welch, S.H., Clark, D.S., Dordick, J.S. 1994. Salts dramatically enhance activity of enzymes suspended in organic solvents. *J. Am. Chem. Soc.* **116**: 2647-2648.
- Kitaguchi, H., Klivanov, A.M. 1989. Enzymatic peptide synthesis via segment condensation in the presence of water mimics. *J. Am. Chem. Soc.* **111**: 9272-9273.
- Klivanov, A.M. 1989. Enzymatic catalysis in anhydrous organic solvents. *Trends Biochem. Sci.* **14**: 141-144.
- Klivanov, A.M. 1995. Enzyme memory - What is remembered and why? *Nature* **374**: 596.

- Klibanov, A.M. 1997. Why are enzymes less active in organic solvents than in water? *Trends Biotechnol.* **15**: 97-101.
- Noritomi, H., Almarsson, Ö., Barletta, G.L., Klibanov, A.M. 1996. The influence of the mode of enzyme preparation on enzymatic enantioselectivity in organic solvents and its temperature dependence. *Biotechnol. Bioeng.* **51**: 95-98.
- Rich, J.O., Dordick, J.S. 1997. Controlling subtilisin activity and selectivity in organic media by imprinting with nucleophilic substrates. *J. Am. Chem. Soc.* **119**: 3245-3252.
- Rupley, J.A., Careri, G. 1991. Protein hydration and function. *Adv. Protein Chem.* **41**: 37-172.
- Russell, A.J., Klibanov, A.M. 1988. Inhibitor-induced enzyme activation in organic solvents. *J. Biol. Chem.* **263**: 11624-11626
- Stahl, M., Jeppsson-Wistrand, U., Mansson, M.-O., Mosbach, K. 1991. Induced stereoselectivity and substrate selectivity of bio-imprinted α -chymotrypsin in anhydrous organic media. *J. Am. Chem. Soc.* **113**: 9366-9368.
- Wescott, C.R., Klibanov, A.M. 1993. Solvent variation inverts substrate specificity of an enzyme. *J. Am. Chem. Soc.* **115**: 1629-1631.
- Xu, K., Griebenow, K., Klibanov, A.M. 1997. Correlation between catalytic activity and secondary structure of subtilisin dissolved in organic solvents. *Biotechnol. Bioeng.*, in press.
- Zaks, A., Klibanov, A.M. 1988. Enzymatic catalysis in nonaqueous solvents. *J. Biol. Chem.* **263**: 3194-3201.

CHAPTER VI. MARKEDLY ENHANCING ENZYMATIC ENANTIOSELECTIVITY IN ORGANIC SOLVENTS BY FORMING SUBSTRATE SALTS

INTRODUCTION

Spurred by the ever-growing demand for enantiopure pharmaceuticals, as well as for crop protection and other specialty chemicals, the use of enzymes as asymmetric practical catalysts continues to rapidly expand.¹ One of the major obstacle to this expansion is that an enzyme from a given source is often insufficiently enantioselective with a particular (e.g., commercially valuable) substrate, thus leading to its incomplete enzymatic resolution and a poor e.e. of the resultant product.² A traditional remedy for this problem is to screen other (usually microbial) sources of the enzyme in the hope of finding a more enantioselective one.³ This empirical and laborious approach is unappealing to organic chemists, and therefore alternative strategies have been sought. Among such means^{2,4} identified to manipulate enzymatic enantioselectivity, temperature⁵ and, in the case of nonaqueous enzymology⁶, solvent⁷, are notable for their broad applicability.

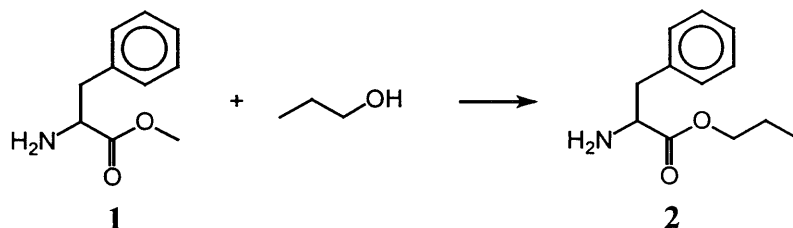
The realization that enzymes can function in organic solvents and the current widespread use of this phenomenon⁶ have offered novel opportunities for improving enzymatic enantioselectivity. For example, in addition to the aforementioned solvent control of enzyme enantioselectivity,⁷ the latter also has been found to be a function of enzyme history.⁸ In this study, we propose a new strategy for increasing the enantioselectivity of enzymes in organic solvents. It is based on the idea that discrimination between the two substrate enantiomers by a given enzyme can be enhanced by temporarily enlarging the substrate via salt formation. A bulky counter-ion of the substrate will exacerbate the steric hindrance encountered by the less

reactive (and hence more sterically constrained) enantiomer in the enzyme-bound transition state, thus increasing the enantioselectivity E^9 and, in turn, product e.e. Following the enzymatic resolution and enzyme removal, the reaction mixture is simply treated with a strong acid or base to dissociate the salt and recover the free substrate and product.

RESULTS AND DISCUSSION

Our overall goal is to discover and exploit new, facile approaches to enhancing the enantioselectivity of a given enzyme toward a given substrate. In doing so, as mentioned in the Introduction, we take advantage of the opportunities stemming from conducting enzymatic resolutions in organic solvents instead of water.

Scheme 1



When one substrate enantiomer is preferred by an enzyme over the other, it means that the Gibbs free energy of the former's enzyme-bound transition state G^\ddagger is lower than that of the latter. In the simplest case, this difference in the free energies is due to greater encumbrances suffered by the less reactive enantiomer in the enzyme active site. In this instance, complexing the substrate with a bulky agent should exaggerate the steric difficulties experienced by the less reactive enantiomer (presumably to a larger extent than for the more reactive one), raise its G^\ddagger even further, and thus increase enantioselectivity. In the present work, we explored and

validated this rationale by forming salts between substrates and suitable Brønsted-Lowry acids or bases. In contrast to a covalent modification of the substrate which permanently converts it to an altered compound (different from the synthetic target), a salt, while stable in organic solvents, is readily decomposed by addition of an acid or base to regenerate the free reactants.

The first asymmetric transformation examined by us herein was enzymatic transesterification of phenylalanine methyl ester (**1**) depicted in Scheme 1. We employed cross-linked crystalline enzyme as catalyst¹⁰ because their structure in organic solvents has been shown to be essentially native¹¹ (unlike that of lyophilized enzymes¹²), and it was our intention in this study to perform structure-based computer modeling of enzyme-bound transition states of chiral substrates such as **1**.

Of the four cross-linked crystalline enzymes tested by us as catalysts of the transesterification of **1** to **2** in anhydrous acetonitrile, namely bovine pancreatic α -chymotrypsin, subtilisin Carlsberg, and lipases from *Candida rugosa* and *Pseudomonas cepacia*,¹³ the protease were too enantioselective ($E > 50$) to be accurately assayed, and the third one was unreactive. On the other hand, the crystalline *P. cepacia* lipase was found to be both reasonably reactive and enantioselective not only in acetonitrile but also in other solvents, both organic and aqueous, with E values varying from 5 to 30 (first line in Table 1).

The E value of 5.7 observed in acetonitrile (Table 1), while clearly reflecting the enzyme's preference for the *S* enantiomer of **1**, would be insufficient for an efficient resolution of the racemate. Therefore we attempted to improve it by using the rationale outlined above. Specifically, a salt was formed between the amine group of **1** and the carboxyl group of a common organic acid, benzoic acid.¹⁴ This salt was then subjected to the enzymatic transesterification (Scheme 1) in acetonitrile under the same conditions as the free **1**. While the

reactivity of the more reactive, *S* enantiomer upon salt formation with benzoic acid decreased by less than a third, that of the *R* enantiomer dropped precipitously, thereby resulting in more than a 4-fold rise in the *E* (Table 1).

Table 1. Enantioselectivity of crystalline *Pseudomonas cepacia* lipase toward **1** and its salts with various carboxylic acids in the transesterification reaction depicted in Scheme 1 in different anhydrous solvents and in the hydrolysis reaction in water.^a

| substrate | <i>E</i> (<i>S</i> / <i>R</i>) | | | | |
|--|----------------------------------|---------------------|------------------------------|-------------------------|---------------------|
| | acetonitrile | THF | methyl <i>t</i> -butyl ether | <i>t</i> -butyl acetate | water |
| 1 | 5.7 ± 1.0 | 10 ± 1 | 9.4 ± 1.2 | 20 ± 2 | 28 ± 2 |
| 1 • chloroacetic acid | 4.8 ± 1.1 ^b | | | | |
| 1 • benzoic acid | 24 ± 1 ^b | | | | 27 ± 2 ^b |
| 1 • 3,4,5-trimethoxycinnamic acid | 38 ± 2 ^b | 40 ± 2 ^b | 37 ± 3 ^b | > 50 ^{b,c} | 28 ± 1 ^b |

^a The conditions for the transesterification reaction were: 40 mM ester substrate, 200 mM propanol, 10 mg/mL of cross-linked crystalline lipase, shaking at 30 °C and 300 rpm. For the hydrolysis reaction (the last column) the conditions were: 10 mM aqueous phosphate buffer (pH 7.0), 10 mM ester substrate, 0.2 mg/mL enzyme, shaking at 4°C and 300 rpm. Under these conditions, no appreciable reaction was detected without enzyme in any of the solvents. The enantioselectivity *E*, defined as $(k_{cat}/K_M)_S/(k_{cat}/K_M)_R$, was measured by means of chiral HPLC using Chiralcel OD-H (transesterifications) or Crownpak CR-(+) (hydrolysis) columns. The *E* values presented are the mean values obtained from at least three independent measurements, with the standard deviations indicated. The salts were obtained by mixing **1** and the corresponding acid in water (pH 7.0), followed by extraction with ethyl acetate, rotary evaporation of the solvent, and subsequent redissolution in one of the solvents listed in the table. For other experimental conditions, see Methods.

^b The initial reaction rate for the faster (*S*) enantiomer of **1** were reduced due to salt formation as follows: by 40%, 32% and 46% in acetonitrile for the salts given in the table order; by 53%, 43% and 50% for the 3,4,5-trimethoxycinnamic acid salt in tetrahydrofuran, methyl *tert*-butyl ether and *tert*-butyl acetate, respectively. There was no appreciable rate reduction in water.

^c Estimated based on the detection limit of our chiral HPLC technique.

It was interesting to examine how the E value of a **1** salt depends on the size of the Brønsted-Lowry acid. To this end, we selected on carboxylic acid smaller (chloroacetic), and another larger (3,4,5-trimethoxycinnamic), than benzoic. The data presented in the first column of Table 1 show that the bulkier the counter-ion, the greater the reactivity of the resultant **1** salt. The highest enantioselectivity, $E = 38$, was observed with the salt of 3,4,5-trimethoxycinnamic acid whose S enantiomer was still more than half as reactive as **1**'s, while the reactivity of the R enantiomer plummeted almost 12 fold compared to that of the free base.

In order to obtain further insights into why *P. cepacia* lipase is more enantioselective toward **1**'s salts than toward the free base (Table 1), we employed the means of molecular modeling involving molecular dynamics, energy minimization, and Van-der-Waals surface calculations.¹⁵ The structure of the enzyme-bound transition state of **1** in the propanolysis reaction depicted in Scheme 1, approximated by the corresponding tetrahedral intermediate (see Methods), was built from the recently published crystal structure of the enzyme¹⁶. Figure 1 shows such transition-state structures for the S and R enantiomers of **1** (A and B, respectively). The dotted surfaces are parts of the substrate transition states that overlap with the enzyme. Figs. 1C and 1D show such structures deduced for the enantiomers of the salt of **1** and 3,4,5-trimethoxycinnamic acid (the darkened fragment). One can see that the counter-ion in

the *R* transition state (Fig. 1D) has a substantially greater surface overlap with the enzyme (i.e., greater steric hindrances) than the *S* enantiomer.

Table 2. Comparison of the experimentally determined enantioselectivities of crystalline *P. cepacia* lipase toward **1** and its salts with molecular modeling data. The *E* values are for the transesterification depicted in Scheme 1 in anhydrous acetonitrile. The molecular modeling (Fig. 1) data include the areas of the Van-der-Waals surfaces of the substrate transition states that overlap with those of the enzyme, as well as the difference in that parameter between the *R* and *S* enantiomers.^a

| substrate | <i>E</i> (<i>S</i> / <i>R</i>) | area of surface overlap (ASO), ^b Å ² | | |
|--|----------------------------------|---|----------|------------|
| | | <i>S</i> | <i>R</i> | <i>R-S</i> |
| 1 | 5.7 ± 1.0 | 40.1 | 45.4 | 5.3 |
| 1 • chloroacetic acid | 4.8 ± 1.1 | 45.6 | 51.4 | 5.8 |
| 1 • benzoic acid | 24 ± 1 | 50.9 | 63.7 | 12.8 |
| 1 • 3,4,5-trimethoxycinnamic acid | 38 ± 2 | 63.7 | 78.1 | 14.4 |

^a For *E* determinations, see the first column of Table 1. The ASO values were calculated using the following protocol: i) molecular models of the transition state of the enzyme-bound substrate was constructed for both **1** and its salts; ii) using the models, ASO for each enantiomer of the substrate was derived from the difference in Van-der-Waals surface between its unbound and enzyme-bound states. For details, see Methods.

^b In addition of ASO, we also calculated $\Delta\Delta G^\ddagger$ between the *S* and *R* transition state models. In the order of the above table, $\Delta\Delta G^\ddagger$ (calculated) values (in kcal/mol) were as follows: -0.36, -0.10, -1.37, -1.24. Comparing with the following experimental $\Delta\Delta G^\ddagger$ (in kcal/mol) derived from *E* values listed in the table: -1.05, -0.94, -1.91, -2.18, $\Delta\Delta G^\ddagger$ (calculated) only gave a qualitative agreement with the overall trend of the change in $\Delta\Delta G^\ddagger$ (experimental). In addition, there was a systematic shift in all the calculated value that can not be explained. Therefore, we only adopt the ASO as our means to explain the effect of salt formation on enzyme enantioselectivity.

Similar molecular models were generated for the other salts depicted in Table 1, and the calculated areas of the surface overlap (ASO) for both free **1** and its salts are presented in Table

2. These data confirm quantitatively that there is a correlation between lipase's enantioselectivity and the difference in the ASO between the two enantiomers (the last column of Table 2).

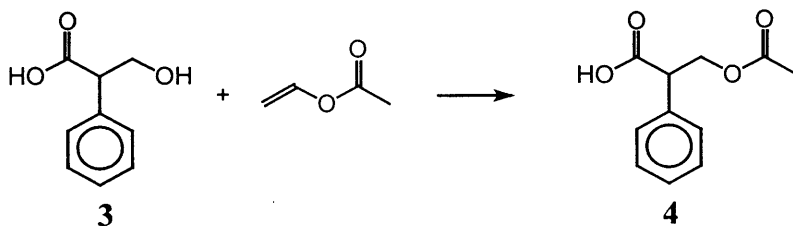
In order to ensure that the observed enhancement of lipase's enantioselectivity toward **1** due to salt formation is not limited to acetonitrile as a reaction medium, we examined this effect in several other anhydrous solvents. It is seen in Table 1 that 3,4,5-trimethoxycinnamic acid, which afforded the greatest *E* enhancement in acetonitrile, also increases several-fold the enzymatic enantioselectivity in tetrahydrofuran, methyl *tert*-butyl ether, and *tert*-butyl acetate. In contrast, there is *no* enantioselectivity enhancement in water (the last column in Table 1), presumably because the salts dissociate in aqueous solution, and hence the chemical species reacting with the enzyme is protonated **1** regardless of whether its initial form is the free base or a salt (such a dissociation should not occur in organic solvents).

While we used crystalline *P. cepacia* lipase to catalyze the transesterification of **1** (to know the enzyme structure and thus be able to carry out molecular modeling depicted in Fig. 1), lyophilized enzymes are still most frequently used as catalyst in organic solvents.⁶ Upon lyophilization, the enzyme structure usually (reversibly) changes,¹² giving rise to altered enantioselectivity when assayed in organic solvents (in water the reversibly denatured conformation reverts back to the native one). We found herein that the enantioselectivity of lyophilized lipase in the reaction shown in Scheme 1 in acetonitrile is 3.2 ± 0.9 , i.e., significantly lower than that of its crystalline counterpart. However, this *E* value can be improved to 7.8 ± 1.1 by forming a salt of **1** with 3,4,5-trimethoxycinnamic acid.

It is worth mentioning that all the salts of **1** listed in Table 1 were preformed in water, extracted with ethyl acetate, and then dissolved in one of the solvents following rotary evaporation of the ethyl acetate (see Methods for details). Alternatively, a salt can be prepared

directly in the solvent of interest by mixing the substrate and a desired acid, followed by a 15-min refluxing. The more expedient procedure gave the same result, in terms of both the structure of the salt formed (as elucidated by FTIR) and the enhanced *E* value obtained (36 ± 2 vs. 38 ± 2).

Scheme 2



It was essential to ascertain the generality of the proposed approach to enhancing enzymatic enantioselectivity with respect to the substrate. To this end, we selected another one, tropic acid (3), the *S* enantiomer whose many derivatives are potent anti-cholinergic drugs.¹⁷ In addition to being structurally distinct from 1, 3 would act as a Brønsted-Lowry acid (instead of a base) in the salt formation and was employed as a nucleophile (instead of an acyl donor) in an enzymatic transesterification (Scheme 2).

Table 3. Enantioselectivity of crystalline *Pseudomonas cepacia* lipase toward **3** and its salts with various bases in the transesterification reaction depicted in Scheme 2 in different anhydrous solvents.^a

| substrate | <i>E</i> (<i>R/S</i>) | | |
|-------------------------------|-------------------------|------------------------|------------------------|
| | acetonitrile | tetrahydrofuran | toluene |
| 3 | 1.1 ± 0.1 | 1.0 ± 0.2 | 1.6 ± 0.1 |
| 3 • tetrabutylammonium | 2.4 ± 0.2 ^b | | |
| 3 • tribenzylamine | 3.5 ± 0.3 ^b | | |
| 3 • 3,5-lutidine | 3.8 ± 0.3 ^b | | |
| 3 • isoquinoline | 4.2 ± 0.4 ^b | | |
| 3 • 4-phenylpyridine | 5.8 ± 0.4 ^b | | |
| 3 • 1-adamantanamine | 5.9 ± 0.4 ^b | | |
| 3 • quinuclidine | 7.0 ± 0.6 ^b | 7.6 ± 0.5 ^b | 6.2 ± 0.5 ^b |

^a The conditions for the transesterification reaction were: 40 mM ester substrate, 200 mM vinyl acetate, 2 mg/mL of cross-linked crystalline lipase, shaking at 30 °C and 300 rpm. Under these conditions, no appreciable reaction was detected without enzyme in any of the solvents. The enantioselectivity *E*, defined as $(k_{cat}/K_M)_R/(k_{cat}/K_M)_S$, was measured by means of chiral HPLC Chiralcel OD-H column. The *E* values presented are the mean values obtained from at least two independent measurements, with the errors indicated. The salts were obtained by mixing **3** and the corresponding equal molar of base in acetonitrile, followed by a 15-min reflux, rotary evaporation of the solvent, and subsequent redissolution in one of the solvents listed in the table. For other experimental conditions, see Methods.

^b The initial reaction rate for the faster (*R*) enantiomer of **3** were reduced due to salt formation as follows: by 72%, 83%, 23%, 34%, 41%, 43% and 35% in acetonitrile for the salts given in the table order; by 33% and 39% for the quinuclidine salt in tetrahydrofuran and toluene, respectively.

P. cepacia lipase exhibited no appreciable enantioselectivity in the acylation of **3** with vinyl acetate in acetonitrile ($E = 1.1 \pm 0.1$, Table 3).¹⁸ We endeavored to make the enzyme enantioselective toward **3** by using the substrate's carboxyl group to form salts with tertiary and quaternary amines. The data obtained for seven such amines of diverse structures are presented in the first column of Table 3. One can see that while all of them induce lipase to prefer that *R*

enantiomer of the substrate, the magnitude of the effect is strongly influenced by the nature of the base. Bulky but flexible tetrabutylammonium and tribenzylamine afford only modest E values (2.4 and 3.5, respectively). Among structurally rigid amines, the enantioselectivity enhancement grows with size to reach 7.0 for quinuclidine which is quite impressive given essentially no enantiopreference of the enzyme for free **3**.

Table 4. Comparison of the experimentally determined enantioselectivities of crystalline *P. cepacia* lipase toward **3** and its salts with molecular modeling data. The E values are for the transesterification depicted in Scheme 2 in anhydrous acetonitrile. The molecular modeling (Fig. 2) data include the areas of the Van-der-Waals surfaces of the substrate transition states that overlap with those of the enzyme, as well as the difference in that parameter between the R and S enantiomers.^a

| substrate | E (R/S) | area of surface overlap (ASO), Å ² | | |
|-------------------------------|---------------|---|------|-------|
| | | R | S | $S-R$ |
| 3 | 1.1 ± 0.1 | 42.3 | 42.9 | 0.6 |
| 3 • tetrabutylammonium | 2.4 ± 0.2 | 70.1 | 73.1 | 3.0 |
| 3 • tribenzylamine | 3.5 ± 0.3 | 76.2 | 79.6 | 3.4 |
| 3 • 3,5-lutidine | 3.8 ± 0.3 | 54.5 | 61.4 | 6.9 |
| 3 • isoquinoline | 4.2 ± 0.4 | 53.2 | 60.8 | 7.5 |
| 3 • 4-phenylpyridine | 5.8 ± 0.4 | 55.6 | 63.5 | 7.9 |
| 3 • 1-adamantanamine | 5.9 ± 0.4 | 58.4 | 66.2 | 7.8 |
| 3 • quinuclidine | 7.0 ± 0.6 | 57.6 | 67.0 | 9.3 |

^a For E determinations, see the first column of Table 3. See footnotes to Table 2 and Methods for more details.

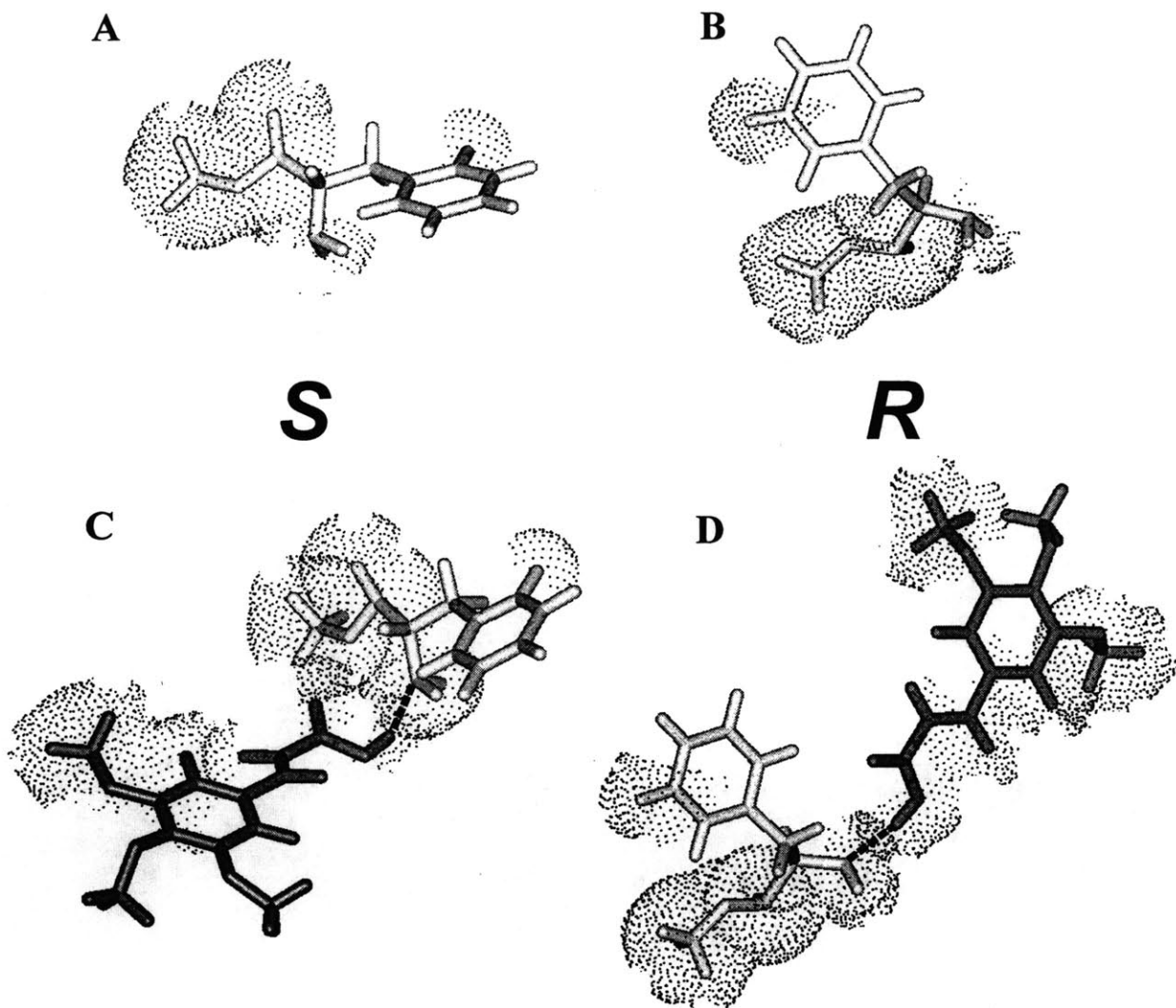
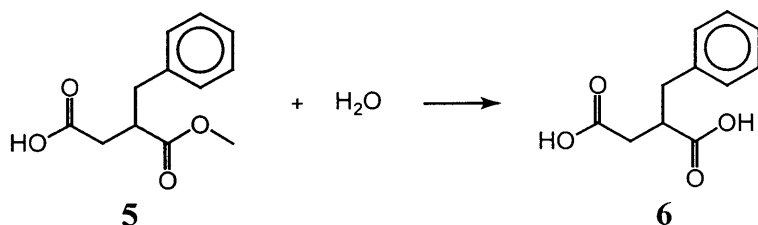


Figure 1. Molecular models of the enzyme-bound transition state of *S*-1 (A), *R*-1 (B), as well as of their 3,4,5-trimethoxycinnamic acid salts (C and D, respectively). The transition states, approximated by the relevant tetrahedral intermediates, corresponding to the acylation phase of the transesterification reaction depicted in Scheme 1 catalyzed by *Pseudomonas cepacia* lipase. The molecular models were built on the basis of the X-ray crystal structure of the lipase using molecular dynamics, energy minimization, and Van-der-Waals surface calculations, as described in the Methods. Only the substrate portions of the transition states are shown for clarity; the position of the enzyme (not shown) is identically fixed in all four instances (A through D). The dots correspond to the Van-der-Waals surfaces of the substrate transition states that overlap with those of the enzyme. In C and D, the darkened structures represent the 3,4,5-trimethoxycinnamic counter-ion of the salt, and the dashed lines represent the putative salt bridge between the counterion and 1.

As with **1** (Fig. 1), molecular modeling was employed to rationalize these observations. One can see in Figure 2 (A and B) and in the first line of Table 4 that the lipase-bound *R* and *S* transition states of **3** have very similar area of surface overlap, which is evidently responsible for the lack of enantioselectivity. The situation is conspicuously different with the quinuclidine salts, where the counter-ion in the more reactive *R* enantiomer (Fig. 2C) is enveloped with far fewer dots than the *S* one (Fig. 2D); the quantitative ASO data (the last line in Table 4) support these visual impressions. In addition, for all the salts examined there is a clear correlation between the observed *E* and ΔASO ($\text{ASO}_R - \text{ASO}_S$) (the first and last columns, respectively in Table 4) — The greater the steric hindrances suffered disproportionately by the less reactive (*S*) enantiomer, the greater the enzymatic enantioselectivity.

As in the case of **1**, the enhancement of enantioselectivity brought about salt formation of **3** was manifested in various solvents: in tetrahydrofuran the *E* rose from 1.0 to 7.6 and in toluene from 1.6 to 6.2 upon transition from free **3** to its quinuclidine salt (Table 3). The results obtained for **3** with different modes of salt formation and with lyophilized (rather than crystalline) *P. cepacia* lipase were also qualitatively similar to those with **1**. The quinuclidine salt of **3** prepared in water, followed by extraction (rather than by direct mixing in the nonaqueous solvent, followed by refluxing, as in Table 3) gave the *E* value of 6.8 ± 0.7 in acetonitrile. Likewise, the enantioselectivity of the lyophilized lipase in that solvent rose from 1.3 ± 0.1 for the free substrate to 4.8 ± 0.4 for its quinuclidine salt.

Scheme 3



To verify the generality of our strategy further, we next extended its scope not only to another, dissimilar substrate but also to a distinct type of a reaction catalyzed by a different enzyme. Specifically, we examine the hydrolysis (instead of transesterification) of 2-benzylsuccinic acid 1-monomethyl ester (**5**) catalyzed by the crystalline protease subtilisin Carlsberg (instead of *P. cepacia* lipase) as shown in Scheme 3. The enantioselectivity in this reaction carried out in *tert*-amyl alcohol containing 1% water (for the hydrolysis) was 1.5 (Table 5), i.e., subtilisin exhibited a slight preference for *S*-**5**.

Six tertiary amine were selected, either from Table 3 or new, as salt-forming bases with the carboxyl group of **5** and hence as potential enantioselectivity-enhancing agents. The data obtained, presented in Table 5, reveal that all of them indeed raise subtilisin's enantioselectivity, with, e.g., 4-(4-chlorobenzoyl)pyridine exerting more than a 5-fold effect. Note that the order of the amines in terms of their enantioselectivity enhancement in Table 5 is distinct from that in Table 3: for example, quinuclidine which was the most potent agent with **3**, is in the bottom half with **5**. Molecular modeling (Figure 3) proved instructive in explaining this trend. As can be seen in Table 6, the order of the ascending *E* values is unmistakably dictated by the order of the increasing Δ ASO values.

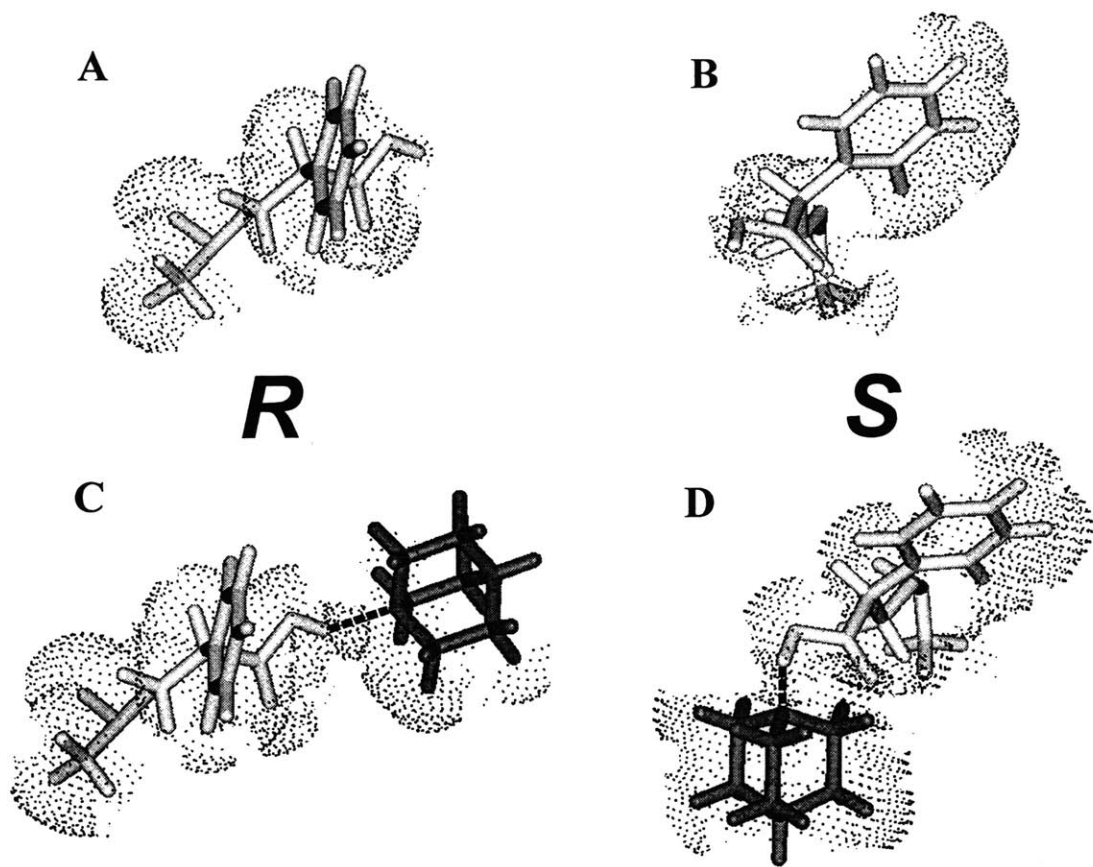


Figure 2. Molecular models of the enzyme-bound transition states of *R*-2 (A), *S*-2 (B), as well as of their quinuclidine salts (C and D, respectively). The transition states correspond to the deacylation phase of the transesterification reaction depicted in Scheme 2 catalyzed by *P. cepacia* lipase. For other details, see the legend to Fig. 1 (with quinuclidine being the counter-ion).

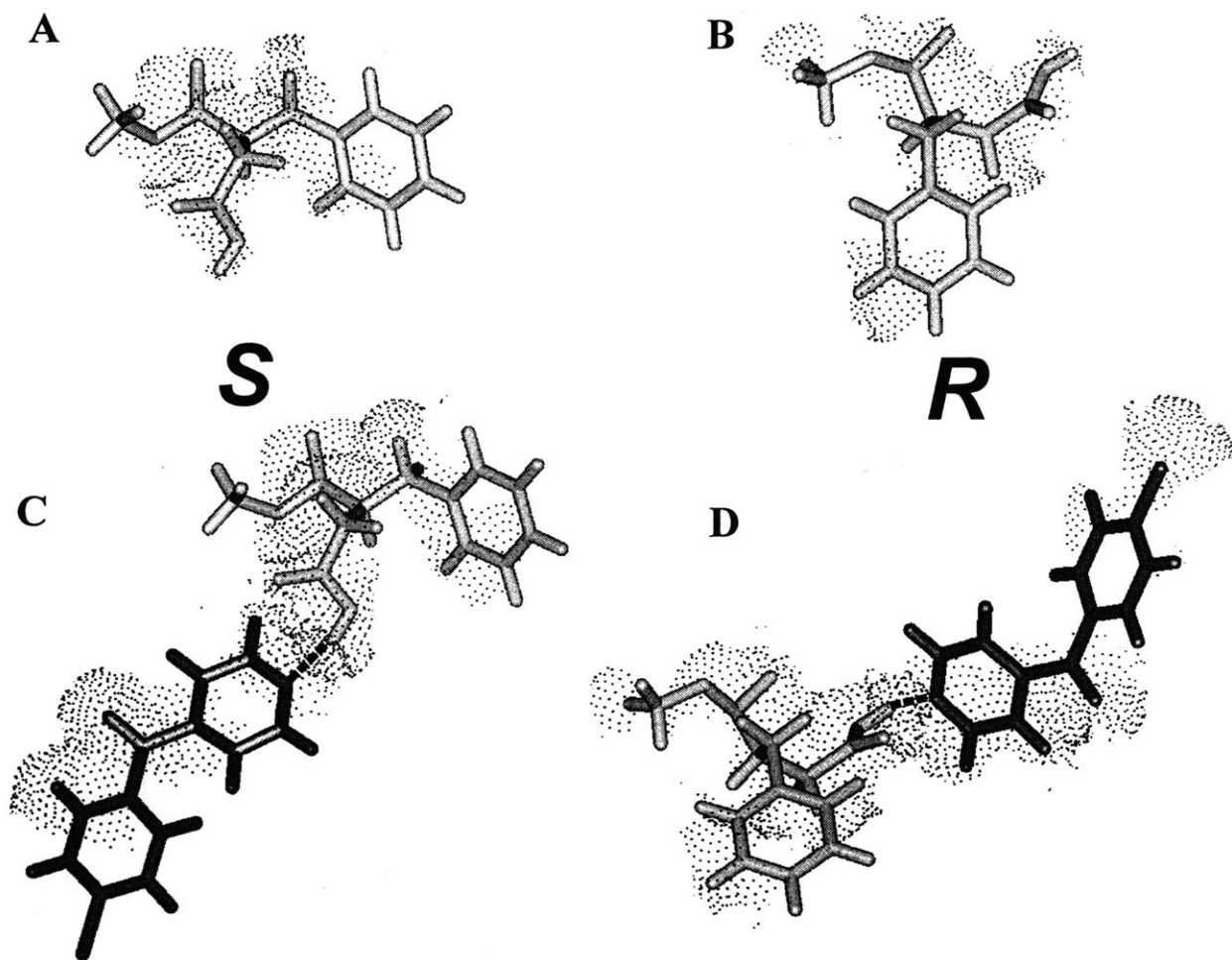


Figure 3. Molecular models of the enzyme-bound transition states of the *S*-3 (A), *R*-3 (B), as well as of their 4-(4-chlorobenzoyl)pyridine salts (C and D, respectively). The transition states correspond to the acylation phase of the hydrolysis reaction depicted in Scheme 3 catalyzed by the protease subtilisin Carlsberg. For other details, see the legend to Fig. 1 (with 4-(4-chlorobenzoyl)pyridine being the counter-ion).

Table 5. Enantioselectivity of crystalline subtilisin Carlsberg toward **5** and its salts with various bases in the hydrolysis reaction depicted in Scheme 3 in different organic solvents containing 1% water and in water.^a

| substrate | <i>E</i> (<i>S/R</i>) | | | | | |
|--|-------------------------|------------------------------|------------------------|------------------------|------------------------|------------------------|
| | <i>t</i> -amyl alcohol | methyl <i>t</i> -butyl ether | acetonitrile | <i>t</i> -butanol | 2-propanol | water |
| 5 | 1.5 ± 0.1 | 2.0 ± 0.1 | 1.8 ± 0.1 | 2.0 ± 0.2 | 2.1 ± 0.2 | 9.8 ± 0.9 |
| 5 • 3,5-lutidine | 2.8 ± 0.2 ^b | | | | | |
| 5 • isoquinoline | 3.1 ± 0.3 ^b | | | | | |
| 5 • quinuclidine | 3.6 ± 0.3 ^b | | | | | |
| 5 • 1-adamantanamine | 4.3 ± 0.4 ^b | | | | | |
| 5 • 4-phenylpyridine | 6.9 ± 0.5 ^b | 5.9 ± 0.4 ^b | 7.3 ± 0.6 ^b | | | |
| 5 • 4-(4-chlorobenzoyl)pyridine | 8.1 ± 0.6 ^b | 7.0 ± 0.5 ^b | 7.8 ± 0.5 ^b | 8.4 ± 0.7 ^b | 6.5 ± 0.5 ^b | 9.6 ± 0.6 ^b |

^a The conditions for the hydrolysis reaction in organic solvents were: 40 mM ester substrate, 1% (v/v, 556 mM) water, 10 mg/mL of cross-linked crystalline lipase, shaking at 30 °C and 300 rpm. For the hydrolysis reaction in water (the last column), the conditions were: 10 mM aqueous phosphate buffer (pH 7.0), 10 mM ester substrate, 0.4 mg/mL enzyme, shaking at 4 °C and 300 rpm. Under these conditions, no appreciable reaction was detected without enzyme in any of the solvents. The enantioselectivity *E*, defined as $(k_{cat}/K_M)_S/(k_{cat}/K_M)_R$, was measured by means of chiral HPLC Chiralcel OD-H column. The *E* values presented are the mean values obtained from at least three independent measurements, with the standard deviations indicated. The salts were obtained by mixing **5** and the corresponding equal molar base in acetonitrile, followed by a 15-min reflux, rotary evaporation of the solvent, and subsequent redissolution in one of the solvents listed in the table. For other experimental conditions, see Methods.

^b The initial reaction rate for the faster (*S*) enantiomer of **5** were reduced due to salt formation as follows: by 32%, 41%, 28%, 34%, 41% and 55% in *tert*-amyl alcohol for the salts given in the table order; by 33% and 39% for the 4-phenylpyridine salt in methyl *tert*-butyl ether and acetonitrile, respectively; by 53%, 45%, 60% and 61% for the 4-(4-chlorobenzoyl)pyridine salt in methyl *t*-butyl ether, acetonitrile, *t*-butanol and 2-propanol, respectively. There is no detectable rate reduction in water.

Table 6. Comparison of the experimentally determined enantioselectivities of crystalline subtilisin Carlsberg toward **5** and its salts with molecular modeling data. The *E* values are for the hydrolysis depicted in Scheme 3 in *tert*-amyl alcohol containing 1% water. The molecular modeling (Fig. 3) data include the areas of the Van-der-Waals surfaces of the substrate transition states that overlap with those of the enzyme, as well as the difference in that parameter between the *R* and *S* enantiomers.^a

| substrate | <i>E</i> (<i>S</i> / <i>R</i>) | area of surface overlap (ASO), Å ² | | |
|--|----------------------------------|---|----------|---------------------|
| | | <i>S</i> | <i>R</i> | <i>R</i> - <i>S</i> |
| 5 | 1.5 ± 0.1 | 27.0 | 27.9 | 0.9 |
| 5 • 3,5-lutidine | 2.8 ± 0.2 | 34.3 | 36.8 | 2.5 |
| 5 • isoquinoline | 3.1 ± 0.3 | 40.1 | 43.1 | 3.0 |
| 5 • quinuclidine | 3.6 ± 0.3 | 36.3 | 40.6 | 4.3 |
| 5 • 1-adamantanamine | 4.3 ± 0.4 | 39.8 | 44.2 | 4.4 |
| 5 • 4-phenylpyridine | 6.9 ± 0.5 | 42.5 | 47.4 | 4.9 |
| 5 • 4-(4-chlorobenzoyl)pyridine | 8.1 ± 0.6 | 45.3 | 50.7 | 5.4 |

^a For *E* determinations, see the first column of Table 5. For more details, see footnotes to Table 2 and Methods.

Inspection of Table 5 reveals that, as with **1** and **3**, salts of **5** are better enantiodiscriminated enzymatically than the free substrate in a variety of organic solvents (all containing 1% water). On the other hand, as with **1** (Table 1), in water the enzymatic enantioselectivity against even the 4-(4-chlorobenzoyl)-pyridine salt was the same as that against the free **5**.

The observed enzymatic enantioselectivity against a given substrate salt was once again, independent of how the latter was prepared — whether via direct mixing in a solvent, followed by refluxing (Table 5) or via formation in water followed by extraction. Likewise, the enantioselectivity of lyophilized subtilisin toward **5** in *tert*-amyl alcohol was also raised by

forming the salt with 4-(4-chlorobenzoyl)pyridine (from 1.7 ± 0.1 to 5.2 ± 0.4), although to a lesser extent than in the case of the crystalline enzyme (Table 5).

To illustrate the synthetic utility of our enantioselectivity enhancement strategy, we carried out preparative resolution of racemic **3** catalyzed by *P. cepacia* lipase. When the free acid was enzymatically acetylated (Scheme 2) in acetonitrile¹⁹, the e.e. value of the acetyl-**3** obtained after a 35% conversion was an insignificant 6%. However, when the resolution was conducted with the quinuclidine salt of **3** under otherwise the same conditions, the e.e. of the resultant acetyl-**3** was a much more impressive 65%.

In closing, in the study we propose a new approach to making a given enzyme more enantioselective in organic solvents toward a given substrate with no covalent alteration of either by converting the latter into a readily reversible salt. This approach was validated using several structurally diverse substrates, salt-forming Brønsted-Lowry acids and bases, and solvents, as well as different enzymes and reactions catalyzed by them. The results suggest that, at least for the instances examined, the steric hindrances suffered by the less reactive substrate enantiomer in the enzyme-bound transition state are the predominant reason for enzymatic enantiodiscrimination; when these hindrances are exacerbated further by enlarging the substrate due to salt formation, the enantioselectivity rises. Molecular modeling of *R* and *S* enzyme-bound transition states, for both the free substrates and their various salts, reveals a surprisingly good correlation in each substrate series between experimentally determined *E* values and the calculated differential area of surface overlap (ASO for the less reactive enantiomer minus that for the more reactive one). The proposed enantioselectivity enhancement strategy is effective in organic solvents but *not* in water (where the salts evidently dissociate thus reverting the free substrate). Thus the present work points to novel synthetic opportunities afforded by

nonaqueous (as opposed to aqueous) enzymatic catalysis. In addition to the salt formation explored herein, these presumably may also include other reversible complexes stable in organic solvents but not in water.

MATERIALS AND METHODS

Chemicals and Solvents

Most of the chemicals and solvents were purchased from Aldrich Chemical Co. and Sigma Co. except that (*R*) and (*S*)-**5** were from Chirotech Technology Ltd., (\pm)-**6** was from Narchem Corp. The organic solvents were of the highest purity available from that vendor (analytical grade or better) and were dried prior to use by shaking with Linde's 3-Å molecular sieves.

(\pm)-**1** was prepared by dissolving 1.0 g of (\pm)-phenylalanine methyl ester hydrochloride in 40 mL of deionized water and adjusting pH to 10.0. The resulting solution was extracted by 50 mL of ethyl acetate thrice then dried over MgSO₄. Rotary evaporation of the dried product solution resulted 0.74 g of (\pm)-**1** (90% of theoretical yield). (*R*)-**1** was prepared in the same way to determine the eluting sequence of the enantiomers for chiral HPLC. Using a mobile phase of 99% hexane /1% isopropanol/0.1% diethylamine (v/v/v) with a flow rate of 0.80 mL/min and a Chiralcel OD-H column, (*R*) and (*S*)-**1** was separated with retention times of 34.4 and 38.6 min, respectively.

(\pm)-**2** was synthesized from (\pm)-phenylalanine using the existing protocol.²⁰ 200 mg of (\pm)-phenylalanine was refluxed for 2 hours in 20 mL anhydrous propanol, along with the purge of dried HCl (gas). The resulting reaction mixture was concentrated *in vacuo*, and cooling, and the crystals are filtered off and recrystallised from propanol (yield of 130 mg, 60% of theoretical

yield). ¹H-NMR (CDCl₃) δ 7.37 (5H, m), δ 4.20 (1H, m), δ 3.84 (2H, t, J = 7.2 Hz), δ 3.30 (1H, dd, J = 6.2, 11.5 Hz), δ 3.19 (1H, dd, J = 4.6, 11.4 Hz), δ 1.64 (2H, m), δ 7.3 (3H, t, J = 7.7 Hz).

In order to determine the eluting sequence of the enantiomers, (*R*)-**2** was synthesized in the same way except using (*R*)-phenylalanine as starting material. Using a mobile phase of 99% hexane/1% isopropanol/0.1% diethylamine (v/v/v) with a flow rate of 0.80 mL/min and a Chiralcel OD-H column, (*R*) and (*S*)-**2** was separated with retention times of 23.2 and 25.6 min, respectively.

(*R*)-**3** was prepared using the procedure described by McKenzie and Wood.²¹ (±)-**3** was recrystallised three times with equal molar of quinine in ethanol, and the resulting **3** was of 96% of e.e. determined by chiral HPLC. Using a mobile phase of 96% hexane/4% isopropanol/0.1% trifluoroacetic acid with a flow rate of 0.50 mL/min and a Chiralcel OD-H column, (*R*) and (*S*)-**3** was separated with retention times of 40.7 and 46.0 min, respectively.

(±)-**4** was synthesized from (±)-**3** using the published procedure.²² 250 mg of tropic acid (**3**) was dissolved in 20 mL of dried THF, and 200 mg of acetyl chloride was added dropwise under 4 °C. The resulting reaction mixture was stirred under room temperature overnight and quenched by addition of 20 mL of water. After three times of extraction using ethyl acetate, the product was dried over MgSO₄, concentrated by rotary evaporation and purified by flash column chromatography (yield of 213mg (±)-**4**, 68% of theoretical yield). ¹H-NMR (CDCl₃) δ 7.32 (5H, s), δ 4.57 (dd, 1H, J=9.5, 10.9 Hz), δ 4.34 (dd, 1H, J=9.5, 10.9 Hz), δ 3.95 (dd, 1H, J=5.5, 9.5 Hz), δ 2.03 (s, 3H). (*R*)-**4** was prepared using the identical method from (*R*)-**3** in order to determine the HPLC eluting sequence of **4**. Using a mobile phase of 96% hexane/4% isopropanol/0.1% trifluoroacetic acid (v/v/v) with a flow rate of 0.50 mL/min and a Chiralcel OD-H column, (*R*) and (*S*)-**4** was separated with retention times of 22.6 and 20.5 min, respectively.

(*R*)-4 was also prepared enzymatically from (\pm)-3 • quinuclidine salt (prepared by the refluxing method, see the Salt Preparation Section below for details) using the methodology developed herein. 330 mg of (\pm)-3 • quinuclidine (1.20 mmol) and 520 mg of vinyl acetate (6 mmol) were dissolved in 30 ml of acetonitrile, followed by addition of 60 mg of CLECs of lipase *Pseudomonas Cepacia*. Under 30 °C, the reaction mixture was shaken at 300-rpm and followed by chiral HPLC. Once the overall conversion reached 35% (12.1 hrs), the reaction was stopped by filtration of the enzyme, and concentrated using rotary evaporation. The resultant was redissolved in small amount of chromatography mobile phase (60% ethyl acetate/40% hexane/0.1% trifluoroacetic acid) to break the salt pair, purified using flash column chromatography and yield 75 mg of (*R*)-4 (30% of theoretical yield, and 65% e.e. determined by chiral HPLC). ¹H-NMR (CDCl₃) was as follows: δ 7.34 (5H, s), δ 4.60 (dd, 1H, J=9.5, 11.1 Hz), δ 4.37 (dd, 1H, J=9.4, 11.0 Hz), δ 3.95 (dd, 1H, J=5.5, 9.5 Hz), δ 2.06 (s, 3H). Using the same procedure, the acetylation of 3 was also carried out in 8.4 hrs, which yielded 78 mg of (*R*)-4 (32% of theoretical yield, and 6% ee determined by chiral HPLC). ¹H-NMR (CDCl₃) was as follows: δ 7.21 (5H, s), δ 4.61 (dd, 1H, J=9.9, 11.4 Hz), δ 4.31 (dd, 1H, J=9.3, 11.8 Hz), δ 3.90 (dd, 1H, J=5.7, 9.2 Hz), δ 2.01 (s, 3H).

Using a mobile phase of 97.5% hexane/2.5% isopropanol/0.1% trifluoroacetic acid (v/v/v) with a flow rate of 0.80 mL/min and a Chiralcel OD-H column, (*R*)-5, (*S*)-5, (*R*)-6 and (*S*)-6 were separated with retention times of 27.4, 32.3, 40.7 and 54.5 min, respectively.

Enzymes

Cross-linked enzyme crystals (CLECs) of lipase *Pseudomonas Cepacia*, lipase *Candida Rugosa* and subtilisin Carlsberg were kind gifts from Altus Co. γ -Chymotrypsin CLECs were

prepared using the previous procedure.¹⁵ Prior to use, enzyme crystals were filtrated, washed twice with dry acetonitrile, then twice with the corresponding solvent.

Lyophilized enzyme powder was prepared as follows: 5 mg/mL of enzyme was dissolved in 20 mM potassium phosphate buffer under 4 °C, then the solution was frozen using liquid nitrogen and lyophilized for 48 hrs. Prior to freeze, the pH of enzyme solution was adjusted to 7.0 and 7.8, for lipase *Pseudomonas Cepacia* and subtilisin Carlsberg, respectively.

Kinetic Measurement

In the transesterification of **1** in anhydrous organic solvents with propanol, 10 mg/mL of enzyme, 40 mM of racemic **1**, and 200 mM of propanol was used, while for the hydrolysis of **1** in 10 mM aqueous phosphate buffer (pH 7.0), 10 mM of racemic **1** and 0.2 mg/mL of enzyme was used. For the esterification of **2** with vinyl acetate, 2 mg/mL of enzyme, 40 mM of racemic **3**, 200 mM of vinyl acetate was used. In the hydrolysis of **5** in organic solvents, 10 mg/mL of enzyme, 40 mM of racemic **5** and 1 % (v/v, 556 mM) of deionized water was added, while for the hydrolysis of **5** in aqueous phosphate buffer (pH 7.8, 10 mM), 0.4 mg/mL of enzyme and 40 mM of racemic **5** was used. All kinetic experiments in organic solvent were carried under 30 °C and 300 rpm, while the hydrolysis reactions in water were carried under 4 °C and 300 rpm. In all cases, the corresponding blank reaction was monitored under identical condition without the enzyme and no appreciable reaction rate was detected.

Periodically, a 25- μ L sample was withdrawn and assayed by chiral HPLC with a UV detector tuned to 258 nm. A Chiralcel OD-H column was used for most of the separations except a Crownpak CR-(+) was used for the separation of *R*- and *S*- phenylalanine. In all initial rate measurements, the product conversion never exceeded 15%. Because the transesterifications or hydrolyses which lead to the *R* and *S* products take place in the same

reaction mixture and the substrate enantiomers compete for the same population of free enzyme, the ratio of initial velocities of the reaction is equal to $(k_{\text{cat}}/K_{\text{M}})_R/(k_{\text{cat}}/K_{\text{M}})_S$.²³ The measurement was carried at least twice and the typical deviation did not exceed 15 %.

FTIR Measurement

The salt bridge formation between substrates and corresponding acids or bases was verified by FTIR measurement.²⁴ Under identical condition, the FTIR spectrum of the salt, the substrate and the salt-forming agent was recorded. It was found that upon the formation of salt, the peak at around 1740 cm^{-1} of the participating carboxylic group typically disappeared completely or substantially decreased by 2 to 3 folds in absorbance.²⁴ This can be explained as the disruption of C=O bond by forming a hydrogen bond network (C—O—H—N).²⁴ In case of pyridine derivative as salt forming agents (some entries in Table 3 and 5), a small peak around 1640 cm^{-1} was also found, which can be assigned as aromatic N—H stretching.^{24c,e}

The FT-IR measurement was carried out in a Nicolet Magna-IR System 550 optical bench as described previously.¹² Samples were prepared in acetonitrile solution under the same conditions as in corresponding kinetic measurements. For substrate **5**, *tert*-amyl alcohol solutions were also measured and resulted in identical spectra as in acetonitrile. 100- μm spacers were used in all measurements, and blank solutions of solvents were used as background.

Salt Preparation

Typically intermolecular salts were prepared as follows: 50 mM of substrate and salt forming agent was dissolved in acetonitrile, followed by reflux for 15 min. Then the resulting solution was cooled, concentrated by rotary evaporation, vacuumed overnight and used directly without further preparation.

Certain salts were also formed in an alternative way using extraction method as comparison to the typical preparation method. For example, 50 mM of **1** was desolved in deionized water, and pH was adjusted to 7.0 by addition of saturated solution of 3,4,5-trimethoxycinnamic acid (salt forming agent for **1**). The resulting solution was extracted by equal volume of ethyl acetate thrice. The extractant was collected, dried over MgSO₄, and concentrated *in vacuo* overnight. The similar preparations were carried for the salt pairs of **1** with benzoic acid, **1** with chloroacetic acid, **3** with quinuclidine, and **5** with 4-phenylpyridine. In all the subsequent FTIR and kinetic experiments, the salts prepared using this method gave identical results as the salts prepared using the typical reflux method.

Structural Modeling

Molecular models were produced using the crystal structures of lipase *Pseudomonas Cepacia* (Brookhaven entry 2LIP)¹⁶ and subtilisin Carlsberg in acetonitrile (Brookhaven entry 1SCB)¹¹. Because the transition state for the acylation and deacylation is structurally similarly to the corresponding tetrahedral intermediate for the reaction, transitions states were modeled as the tetrahedral intermediates for the reactions.²⁵ Such models were produced using the two-step procedure described previously¹⁵ with minor modification. First, potential binding modes of each enantiomer of the substrate were generated by performing molecular dynamic simulations, followed by energy minimization. The carbonyl oxygen of the potential with a force constant selected to allow widely different conformations to be explored, while preventing the substrate from diffusing too far from the enzyme. This substrate binding mode search is necessary because the covalently bound tetrahedral intermediate is sufficiently sterically constrained that molecular dynamics simulations do not sample highly different conformations separated by large energetic barriers. For the second step, each substrate-binding mode thus identified was used as

a template for creating an initial model of the tetrahedral intermediate. The low-energy conformation of each of these starting models was found using molecular dynamics simulations and energy minimizations. The lowest-energy conformer of the tetrahedral intermediate was selected as the model of the transition state. In case of modeling salt complex of substrate, the salt forming group (amine group or carboxylic group) in salt forming agent was tethered to the vicinity of substrate using a harmonic potential ($50 \text{ kcal/mol}\cdot\text{\AA}^2$). A perfect geometry of hydrogen bond (distance of hydrogen to acceptor atom as 2.0 \AA , and hydrogen bond angle of 180°) was used as starting position.²⁶ The complex underwent the same two-step procedure, the final lowest-energy conformer was selected as the model of the transition state.

The area of surface overlap (ASO) was calculated as follows: i) using the final conformation of transition state model, the Van-der-Waals surface of substrate, salt forming agent without enzyme-bound was calculated individually using Connolly's method²⁷ with a probe size of 0 \AA ; ii) with enzyme bound, the surface area of the salt complex was calculated again under otherwise identical condition; iii) the area of surface overlap (Table 2, 4 and 6) was derived as the difference between the sum of free substrate and salt forming agent (step i) and final salt complex when there is enzyme around (step ii). This parameter is used as an indicator for visualizing the steric hindrance of enzyme-substrate interaction (similar to the number of close contacts used previously²⁸).

REFERENCES AND FOOTNOTES

-
- (1) Sheldon, R.A. *Chirotechnology: Industrial Synthesis of Optically Active Compounds*; M. Dekker: New York, 1993. Wong, C.-H.; Whitesides, G.M. *Enzymes in Synthetic Organic Chemistry*; Pergamon Press: Oxford, 1994. Drauz, K.; Waldmann, H. *Enzyme Catalysis in*

-
- Organic Synthesis*; 2nd edn.; Springer-Verlag: Berlin, 1996. Zaks, A.; Dodds, D.R. *Drug Dev. Trends* **1997**, *2*, 513-531.
- (2) Faber, K.; Ottolina, G.; Riva, S. *Biocatalysis* **1993**, *8*, 91-132.
- (3) Roberts, S.M.; Turner, N.J.; Willetts, A.J.; Turner, M.K. *Introduction to Biocatalysis Using Enzymes and Microorganisms*; Cambridge University Press: New York, 1995.
- (4) Chen, C.-S.; Sih, C.J. *Angew. Chem. Ind. Ed. Engl.* **1989**, *28*, 695-707. Hult, K.; Norin, T. *Pure Appl. Chem.* **1992**, *64*, 1129-1134.
- (5) Phillips, R.S. *Trends Biotechnol.* **1996**, *14*, 13-16.
- (6) Koskinen, A.M.P.; Klivanov, A.M., Eds. *Enzymatic Reactions in Organic Media*; Blackie: London, 1996.
- (7) Wescott, C.R.; Klivanov, A.M. *Biochim. Biophys. Acta* **1994**, *1206*, 1-9. Carrea, G.; Ottolina, G.; Riva, S. *Trends Biotechnol.* **1995**, *13*, 63-70. Wescott, C.R.; Noritomi, H.; Klivanov, A.M. *J. Am. Chem. Soc.* **1996**, *118*, 10365-10370.
- (8) Stahl, M.; Jeppsson-Wistrand, U.; Mansson, M.-O.; Mosbach, K. *J. Am. Chem. Soc.* **1991**, *113*, 9366-9368. Noritomi, H.; Almarsson, Ö.; Barletta, G.L.; Klivanov, A.M. *Biotechnol. Bioeng.* **1996**, *51*, 95-98. Ke, T.; Klivanov, A.M. *Biotechnol. Bioeng.* **1998**, *57*, 746-750.
- (9) Chen, C.-S.; Fujimoto, Y.; Girdaukas, G.; Sih, C.J. *J. Am. Chem. Soc.* **1982**, *104*, 7294-7299. Straathof, A.J.J.; Jongejan, J.A. *Enzyme Microb. Technol.* **1997**, *21*, 559-571.
- (10) Margolin, A.L. *Trends Biotechnol.* **1996**, *18*, 223-230.
- (11) Fitzpatrick, P.A.; Steinmetz, A.C.U.; Ringe, D.; Klivanov, A.M. *Proc. Natl. Acad. Sci. USA* **1993**, *90*, 8653-8657. Fitzpatrick, P.A.; Ringe, D.; Klivanov, A.M. *Biochem. Biophys. Res. Commun.* **1994**, *198*, 675-681. Schmitke, J.L.; Stern, L.J.; Klivanov, A.M. *Proc. Natl.*

Acad., Sci. USA **1997**, *94*, 4250-4255. Schmitke, J.L.; Stern, L.J.; Klivanov, A.M. *Proc.*

Natl. Acad. Sci. USA **1998**, *95*, 12918-12923.

(12) Griebenow, K.; Klivanov, A.M. *Proc. Natl. Acad. Sci. USA* **1995**, *92*, 10969-10976.

(13) Chymotrypsin was crystallized and cross-linked by us as described previously.¹⁵ The other three cross-linked crystalline enzymes, commercially available from Altus Biologics, Inc., were generously donated by that company.

(14) The structure of all Brønsted-Lowry salts examined in this work was confirmed by FTIR spectroscopy, as described in Methods.

(15) Ke, T.; Wescott, C.R.; Klivanov, A.M. *J. Am. Chem.Soc.* **1996**, *118*, 3366-3374. Ke, T.; Klivanov, A.M. **1998**, *120*, 4259-4263.

(16) Schrag, J.D.; Li, Y.; Cygler, M.; Lang, D.; Burgdorf, T.; Hecht, H.-J.; Schmid, R.; Schomburg, D.; Rydel, T.J.; Oliver, J.D.; Strickland, L.C.; Dunaway, C.M.; Larson, S.B.; Day, J.; McPherson, A. *Structure*, **1997**, *5*, 187-202.

(17) These include atropine, hyoscyamine, and scopolamine (Reynolds, J.E.F., Ed. *Martindale, the Extra Pharmacopoeia*, 28th ed.; Pharmaceutical Press: London, 1982; p. 304.

(18) Subtilisin and *C. rugosa* lipase were found to be catalytically inactive in this reaction, while chymotrypsin was both active and very enantioselective ($E = 12.2 \pm 0.2$).

(19) In 30 mL of anhydrous acetonitrile, 1.2 mmol of *R,S*-3 (its quinuclidine salt) and 6 mmol of vinyl acetate were dissolved. The enzymatic reaction was initiated by adding 60 mg of crystalline *P. cepacia* lipase. The reaction mixture was shaken at 300 rpm and 30 °C for 8.3 hr (free substrate) or 12.1 hr (substrate salt). Then the enzyme was removed by filtration, and the remaining was worked up by rotary evaporation, redissolution in a 60% ethyl acetate/40%

hexane/0.1% trifluoroacetic acid (which also decompose the salt), and using this solvent as a mobile phase in silica gel flash column chromatography (see Methods for details).

- (20) Vanderhaeghe, H. *J. Pharm. Pharmacol.* **1954**, *6*, 57-59.
- (21) McKenzie, A.; Wood, J.K. *J. Chem. Soc.* **1919**, 828-834.
- (22) Wolffenstein, M. *Chem. Ber.* **1908**, *41*, 730-736. Schmidt, R. *J. Pharm. Sci.* **1968**, *57*, 443-452.
- (23) Wescott, C.R.; Klibanov, A.M. *J. Am. Chem. Soc.* **1993**, *115*, 1629-1631.
- (24) (a) Barrow, G.M.; Yerger, E.A. *J. Am. Chem. Soc.* **1954**, *76*, 5211-5216. (b) Yerger, E.A.; Barrow, G.M.; *J. Am. Chem. Soc.* **1955**, *77*, 4474-4478. (c) Barrow, G.M. *J. Am. Chem. Soc.* **1956**, *78*, 5802-5814. (d) Yerger, E.A.; Barrow, G.M.; *J. Am. Chem. Soc.* **1955**, *77*, 6206-6207. (e) Johnson, S.L.; Rumon, K.A. *J. Phy. Chem.* **1965**, *69*, 74-85.
- (25) Warshel, A.; Naray-Szabo, G.; Sussman, F.; Hwang, J.-K. *Biochemistry* **1989**, *28*, 3629-3635.
- (26) (a) Donohue, J. *J. Am. Chem. Soc.* **1951**, *56*, 502-520. (b) Fuller, W. *J. Am. Chem. Soc.* **1959**, *63*, 1705-1713.
- (27) Connolly, M.L. *Science*, **1983**, *221*, 709-715.
- (28) Fitzpatrick, P.A.; Ringe, D.; Klibanov, A.M. *Biotech. Bioeng.* **1992**, *40*, 735-740.

BIOGRAPHICAL NOTE

Education

MASSACHUSETTS INSTITUTE OF TECHNOLOGY Cambridge, MA
Ph.D. Nov 1998

Thesis title: "Mechanistic studies of enzyme stereo-selectivity in non-aqueous environment"

Advisor: Professor A.M. Klivanov

Business related courses taken in Sloan School of Management include Marketing Management, Finance Theory

UNIVERSITY OF SCIENCE AND TECHNOLOGY OF CHINA Hefei, P.R.China
B.Sc. July 1993

Chemistry and polymer science major

Thesis title: "Synthesis and characterization of series of polyester-typed liquid crystal materials"

Advisor: Professors R.K. Bai and C.Y. Pan

Excellent student award of the university, 1989-93. GPA 3.9/4.0

Experiences

Lab of Enzyme Technology, MIT Cambridge, MA
Graduate research assistant Jan 1994 to Nov 1998

Use molecular modeling techniques combined with various chemical and biochemical methods to study the mechanism of enzyme stereoselectivity

Lab Safety Officer Jan 1998 to Nov 1998

Ensured that the lab was in compliance with federal and state laws

Great Eastern Technology, Inc. Woburn, MA
Consulting associate Aug 1996 to Sep 1996

Trained a group from Beijing Statistics Bureau in UNIX system administration and graphics design of web page

Functional Polymer Lab, USTC Hefei, P.R. China
Research assistant May 1992 to June 1993

Synthesized and characterized a series of polyester-typed liquid crystal materials with their potential usage in LCD

Skills

- Experienced in various molecular modeling techniques including: molecular dynamics, continuum electrostatic calculation, Monte Carlo simulation, protein homology modeling and ab initio calculation
- Installed and maintained software packages including: InsightII/Discover, Delphi, Macromodel, Midas, Gaussian94, Gamess, VMD/NAMD
- Familiar with UNIX (Linux, IRIX), DOS/Windows operation systems. Experienced in system administration for more than 2 years
- Programming languages: C/C++, Fortran, Perl, HTML, BASIC

- Familiar with GC and HPLC for chiral and non-chiral separation
- Acquaint with protein purification, stabilization and assay methods with specialty in enzyme preparation (including crystallization)
- Experienced in organic synthesis including asymmetric reaction, determination of absolute configuration, polymer synthesis, purification and characterization

Publications

"Prediction of the solvent dependence of enzymatic prochiral selectivity by means of structure-based thermodynamic calculations"

T. Ke, C.R. Wescott, A.M. Klibanov
J. Am. Chem. Soc. **1996**, *118*, 3366-3374

"Molecular modeling of the enzymatic enantioselectivity taking hydration into account"

T. Ke, B. Tidor, A.M. Klibanov
Biotechnol. Bioeng. **1998**, *57*, 741-745

"On the enzymatic activity in organic solvents as a function of enzyme history"

T. Ke, A.M. Klibanov
Biotechnol. Bioeng. **1998**, *57*, 746-750

"Insights into the Solvent Dependence of Chymotryptic Prochiral Selectivity"

T. Ke, A.M. Klibanov
J. Am. Chem. Soc. **1998**, *120*, 4259-4263

"On the role of transition-state substrate desolvation in enzymatic enantioselectivity in aqueous-organic mixtures"

S. Luque, T. Ke, A.M. Klibanov
Biocatalysis Biotransformation **1998**, *16*, 233-248

"Computational and experimental examination of the effect of inorganic salts on chymotryptic enantioselectivity in water"

T. Ke, R.V. Rariy, J.L. Schmitke, A.M. Klibanov
Biocatalysis Biotransformation **1998**, *in press*

"Markedly Enhancing Enzymatic Enantioselectivity in Organic Solvents by Forming Substrate Salts"

T. Ke, A.M. Klibanov
J. Am. Chem. Soc. **1998**, *submitted*

Leadership & Activities

Special Class for Gifted Young (SCGY), entering class of 1989, USTC. Vice-president, SCGY Student Association, 1990-92. Captain, Departmental Table Tennis Team, 91-92.